Iron Chelators Improve the Pathophysiology of β-Thalassemia *In Vitro* and *In Vivo*

Natasha Szuber

Department of Physiology

McGill University, Montreal

August 2004

A thesis submitted to McGill University in partial fulfilment of the requirements of the degree of Master of Science

Canada

Abstract

Thalassemia is a blood disorder requiring lifelong transfusions for survival. Erythrocytes accumulate toxic iron at their membranes, triggering an oxidative cascade that leads to their premature destruction. We hypothesized that removing this proximate iron compartment as a primary treatment using novel iron chelators, could prevent hastened red cell removal and clinically alleviate the need for transfusion. Novel, highly cell permeable iron chelators, pyridoxal isonicotinoyl hydrazone (PIH) and pyridoxal *ortho*-chlorobenzoyl hydrazone (*o*-108) were compared to the present mainstay, desferrioxamine (DFO) and deferiprone (L1), *in vitro* and *in vivo*. Treatment of human model β-thalassemic erythrocytes with chelators resulted in significant depletion of membrane-associated iron and reduced oxidative stress as indicated by a decrease in methemoglobin levels. When administered to β-thalassemic mice, iron chelators mobilized erythrocyte membrane iron, reduced cellular oxidation, and prolonged erythrocyte survival. Consistently, these mice showed improved hematological abnormalities. A beneficial effect as early as the erythroid precursor stage was also determined by normalized proportions of mature versus immature reticulocytes. Remarkably, all four chelators reduced iron accumulation in target organs. Most importantly, *o*-108 revealed superior activity, decreasing iron in liver and spleen by ~5-fold and ~2-fold, respectively, compared to DFO. Our study demonstrates that iron chelators ameliorate thalassemia in a human and murine model, and validates their primary use as an alternative to transfusion therapy.

Résumé

La thalassémie est une hémoglobinopathie héréditaire nécessitant de fréquentes transfusions sanguines pour assurer la survie du patient. La thalassémie et les transfusions sanguines causent une accumulation de fer toxique dans les érythrocytes et déclenchent une cascade oxydative menant à leur destruction prématurée. Nous avons émis l'hypothèse que l'utilisation de chélateurs de fer *comme traitement de premier choix* pourrait réduire ou éliminer le fer dans les globules rouges et ainsi augmenter leur durée de vie. D'un point de vue clinique, le besoin de transfusions serait réduit sinon écarté. Deux nouveaux chélateurs de fer, l'hydrazone d'isonicotinoyl de pyridoxal (PIH) et l'hydrazone *ortho*-chlorobenzoyl de pyridoxal (*o*-108), hautement perméables dans les cellules ont été comparés aux chélateurs de fer actuels, la desferrioxamine (DFO) et la deferiprone (L1), *in vitro* et *in vivo*. Le traitement des érythrocytes β-thalassémique humains *in vitro* par les nouveaux chélateurs de fer a causé une diminution significative du fer associé à la membrane et une diminution du niveau de méthémoglobine montrant ainsi qu'ils protègent aussi contre l'oxydation cellulaire. *In vivo*, le traitement de souris β-thalassémiques par ces nouveaux chélateurs de fer a mobilisé le fer des membranes érythrocytaires, atténué l'oxydation des érythrocytes et prolongé leur demi-vie. Ces souris ont toutes démontrées une amélioration de leurs paramètres hématologiques. De plus, un effet bénéfique inattendu de ces chélateurs a été observé au cours de la maturation érythroïde par la présence de proportions presque normales de réticulocytes matures et immatures. Des analyses histopathologiques ont montrées que les quatre chélateurs ont réduit l'accumulation de fer dans les organes cibles. Toutefois, le chélateur *o*-108 s'est révélé supérieur à la DFO, diminuant davantage le fer dans le foie et la rate par ~5 fois et ~2 fois, respectivement. Notre étude démontre que les chélateurs de fer améliorent substantiellement le phénotype thalassémique chez les modèles humain et murin, et soutient ainsi leur utilisation comme traitement de premier choix au lieu de la thérapie transfusionnelle.

Acknowledgements

Many thanks to Dr. Andrea Romero of the Concordia Chemistry Department for mass spectrometry analysis, Dr. Mark Scott for his insights on *in vitro* studies, Dr. Lorraine Chalifour for instruction of surgical technique, Dr. Martin Loignon for instruction of FACS, and to the LDI and IRCM Animal Care staff for teaching and reinforcing humane care of animals. Thanks to Billy Joel's Greatest Hits Vol. 2 for providing the soundtrack in the mouse house.

My deepest gratitude to Dr. Joan Buss, Shan Soe-Lin, and Alex Sheftel for their continual assistance throughout the project and for their support, both on a scientific and human level. Support for Dr. J. Buss came from the Thalassemia Foundation of Canada, whose funding made this project possible. I also thank my colleagues in the lab - Carlos, Lidia, Marc, and Guangjun - for fostering a refreshing learning environment and for taking the time to listen, teach, and challenge. Sincere thanks to the members of my graduate committee, Dr. T. Chang, Dr. W. Lapp, Dr. J. Orlowski, and Dr. J. F. Prchal, for graciously giving of their time and expertise.

I am greatly indebted to Dr. Marie Trudel for her exceptional generosity, her sound advice, and her strength of spirit. Dr. Trudel kindly donated the animals and taught the techniques necessary to carry out the *in vivo* experiments. Dr. Trudel's team at the IRCM - Hady, Hugues, Patricia and Mariette - were also extremely helpful throughout the course of the *in vivo* studies.

A very special thank you to "Dearest" Dr. Prem Ponka for what developed into a journey that surpassed all my expectations. Thank you for your guidance, patience, inspiration, infectious curiosity, and your giant heart – and most especially, for always encouraging personal development in equal measure with scientific growth.

Finally, infinite gratitude to Mom, Dad, Maria and Liv for their love and unconditional support, the most fundamental gifts of all.

Table of Contents

List of Tables

List of Figures

General: Thalassemia

Figure 1- Pathways Involved in Membrane Damage and Shortened RBC Lifespan in β-Thalassemia

Figure 2- Clinical Consequences of α-Chain Accumulation in β-Thalassemia

β-Thalassemia: Models (*In Vitro* and *In Vivo*)

Figure 3- Preparation of Human Model β-Thalassemic Erythrocytes

Figure 4- Generation of a β-Thalassemic Mouse Population

Preparation of Model β-Thalassemic Erythrocytes

Figure 5- Standard and Experimental ESI-Mass Spectra of Human α-Hemoglobin

Figure 6- Sequential Spectrophotometric Scans of Normal Human Hemolysate

Figure 7- Initial and Final (Post-20 h Incubation) Scans of Purified α-Hemoglobin

Figure 8- Encapsulation of Purified α-Hemoglobin Chains into Human Erythrocytes

Effects of Iron Chelators on Model β-Thalassemic Erythrocytes

Figure 9- Effects of Iron Chelators on Membrane-Associated Non-Heme Iron and Iron-Mediated Hemoglobin Oxidation in Human Control and Model β-Thalassemic RBC

Generation of Mouse Models of β-Thalassemia

Figure 10- Glucose Phosphate Isomerase (Gpi) Phenotyping of Recipient Mice 4, 7, and 10 Weeks Following Murine β-Thalassemic Bone Marrow Transplant

Effects of Iron Chelators on Murine β-Thalassemic Erythrocytes and Tissues

Abbreviations

o-108: pyridoxal *ortho*-chlorobenzoyl hydrazone

AU: absorbance units

Biotin-X-NHS: biotinamidocaproate *N*-hydroxysuccinimide ester or biotin

BM: bone marrow

BMT: bone marrow transplant

BSA: bovine serum albumin

C57BL/6J^{GPI-1a} or $^{GPI-1b}$: mice expressing "a" or "b" form of glucose phosphate isomerase-1 enzyme

CO: carbon monoxide

CO-Hb: carbon monoxide-treated hemoglobin

d: days(s)

ddH$_2$O: double distilled water

Da: dalton

Dex: dextran

DFO: desferrioxamine or desferal or deferoxamine

DMF: dimethyl formamide

DMT1: divalent metal transporter 1

EDTA: ethylene diamine tetraacetic acid

ESI-MS: electrospray ionization mass spectrometry

FACS: fluorescence-associated cell sorting

Fe: iron

Ferrozine: 3-(2-pyridyl)-5,6-bis(4-phenylsulfonicacid)-1,2,4-triazine

FITC: fluorescein isothiocyanate

FITC-Avidin: fluorescein isothiocyanate-conjugated avidin

FITC-Dex: fluorescein isothiocyanate-conjugated dextran

Gpi: glucose phosphate isomerase

[³H]-NEM: ³H-N-ethyl malemide

Hb: hemoglobin

Hbb^{tm1Tow}/Hbb^s: designated abbreviation for hemizygous β-globin knockout mice

HBED: *N,N*-bis(2-hydroxybenzyl)ethylenediamine-*N,N*-diacetic acid

HBSS: Hank's Balanced Salt Solution

Hct: hematocrit

HES-DFO: hydroxyethyl starch derivative of desferrioxamine (high molecular weight)

h: hour(s)

H RETIC: high staining-intensity, designating most immature reticulocytes

IgG: immunoglobulin G

IMDM: Iscove's Modified Dulbelco's Medium

IRE: iron-responsive element(s)

IRP: iron regulatory protein(s)

L1: 1,2-dimethyl-3-hydroxypyridin-4-ones or deferiprone

LIP: labile iron pool

L RETIC: low staining-intensity, designating most mature reticulocytes

MCH: mean cell hemoglobin

MCHC: mean cell hemoglobin concentration

MCV: mean cell volume, mature RBC index

MCVr: mean cell volume, reticulocyte index

MDA: malondialdehyde

min: minute(s)

M RETIC: medium staining-intensity, designating intermediate maturation of reticulocytes

mRNA: messenger RNA

MS: mass spectrometry

MTT: 3-(4,5-dimethylthiazol-2-yl)-2,5-diphenyltetrazolium bromide

MW: molecular weight(s)

NADP: nicotinamide adenine dinucleotide phosphate

Nramp2: natural resistance associated macrophage protein 2

NTBI: non-transferrin bound iron

OD: optical density

pRBC: packed red blood cell(s)

PBS: phosphate-buffered saline

PE: phosphatidylethanolamine

PIH: pyridoxal isonicotinoyl hydrazone

PMB: parahydroxymercuribenzoate

PMS: phenazine methosulfate

PS: phosphatidylserine

PUFA: polyunsaturated fatty acid(s)

RBC: red blood cell(s)

SH: sulfhydryl

SD: standard deviation

$t_{1/2}$: half-life

Introduction

1.1. Iron Metabolism

Iron (Fe) is a precious metal essential for life. Serving multiple functions in biological systems, iron is especially valued for its role in oxygen transport as a key constituent of the molecule hemoglobin (Hb). However, because of iron's potential to catalyze the formation of damaging reactive oxygen species, careful orchestration of its acquisition, transport, and storage is absolutely required in order to maintain body iron homeostasis and minimize iron toxicity. A series of specialized molecules and mechanisms have evolved to this end and will be discussed briefly in this section.

The iron cycle may be envisioned as beginning, arbitrarily, in the small intestine, at its site of absorption from the diet. This is a critical control point, since humans have a limited capacity to excrete iron; therefore, steady body iron levels are achieved in a unique fashion, by exclusive reliance upon iron absorption (1). Though the daily intake of iron can range from 10 to 30 mg, only ~5-10% of it is actually absorbed to balance the ~1 mg/day lost through non-specific mechanisms, including cell desquamation (2). Thus, under normal circumstances, iron absorption is adjusted to the needs of the organism and is dictated by both the amount of storage iron and the rate of erythropoiesis (2).

Dietary iron absorption (mostly in the Fe^{3+} form), firstly involves iron's reduction by a ferrireductase, duodenal cytochrome b (3), followed by its transport across the epithelial cell brush border membrane via natural resistance associated macrophage protein 2 (Nramp2), also known as divalent metal transporter 1 (DMT1) (1). Iron then enters a poorly characterized intracellular labile iron pool (LIP), and, following the ferroxidase activity of the molecule hephaestin (4), is finally transferred across the

1

basolateral membrane by transporter ferroportin 1, also called Ireg1 (5). Iron circulates in the plasma bound to the carrier protein transferrin and is finally delivered to cells via receptor-mediated internalization of the iron-transferrin complex (1). Iron is released from transferrin following endosomal acidification and is exported from the endosome by Nramp2/DMT1 (6, 7). The subsequent steps involved in the cellular trafficking of iron, however, remain somewhat more elusive, as do the specific characteristics of the LIP; these aspects of iron metabolism continue to be the subject of intense study.

In developing erythroid precursors, by far the most avid consumers of the metal, the majority of iron (~80-90%) is targeted to the mitochondria and incorporated into heme for the synthesis of hemoglobin, while the remainder may enter the storage form, ferritin (8). When red blood cells (RBC) become senescent, nearing the end of their 120-day course through the circulation, they are engulfed by macrophages predominantly within the spleen, and their hemoglobin-derived iron may be either stored as ferritin or hemosiderin, or delivered back to the plasma complexed with transferrin, completing the cycle. Iron turnover follows this pattern at a rate of 30 mg/day, with an overwhelming 80% of the metal being delivered to the bone marrow to match the demands of hemoglobin synthesis (1). The rest of iron is found in muscle (mostly as myoglobin), hepatocytes, and other parenchymal cells, as well as in its storage form in macrophages (1).

Cellular iron homeostasis is achieved post-transcriptionally by an elegant system comprised of cytosolic iron regulatory proteins (IRP), and key nucleotide sequences known as iron-responsive elements (IRE) (9). The latter are stem-loop structures found in the messenger RNA (mRNA) of two principal proteins of iron metabolism, ferritin and

transferrin receptor. Iron levels in the LIP are "sensed" and articulated by IRP to IRE. This occurs within a complex scheme involving differential binding of IRP to either the 5' or 3' untranslated regions of mRNA (9). For example, in cells where iron is lacking, an increase in iron acquisition and concomitant decrease in synthesis of the storage form of the metal occurs, reflecting the cells' attempt to restore iron balance. In this case, the low level of iron in the LIP elicits a response in the IRE/IRP system, promoting IRP1 binding at the 5' and 3' untranslated regions of ferritin and transferrin receptor mRNA, respectively, repressing ferritin translation and stabilizing the mRNA of the transferrin receptor. The reverse occurs in iron-replete cells, where ferritin synthesis is augmented and transferrin receptor mRNA, predictably, is destabilized (9).

The number of processes designed to maintain intracellular and body iron levels within narrow limits, and the level of sophistication of these processes, underscore the hazards of iron imbalance and emphasize how relatively easily these scales may be tipped. Such a condition of imbalance occurs in thalassemia, a disease in which the toxic effects of excess unbound iron are clearly manifested. This common disorder served as the focus of our research and will now be discussed in more detail.

1.2. Thalassemia

1.2.1. Background

The thalassemias are a heterogeneous group of blood disorders affecting the synthesis of the critical oxygen-carrying component of red blood cells, hemoglobin. The disease was first described in 1925 by Thomas Cooley and Pearl Lee as a severe form of anemia occurring in children of Italian descent and characterized by massive splenomegaly and bone deformities (10). "Thalassa" stems from the Greek term meaning "the sea", in

reference to the Mediterranean Sea. Although thalassemia is thought to have originated from the Mediterranean region, it is now considered a serious cause of morbidity and mortality worldwide with a high incidence observed in the Middle East, Africa, India, Southeast Asia, and even North America, where over two million carriers are estimated in the United States alone (11). The thalassemias are so widespread, in fact, occurring with a gene frequency of up to 10% in some areas and affecting thousands of infants each year; the World Health Organization regards them as the most prevalent group of inherited blood disorders (12). Developing countries are especially affected as the decline in childhood mortality rates has increased the number of adult patients, a phenomenon requiring longer-term and more effective thalassemia management. The drain on health services is made particularly heavy by the fact that no widely available cure for thalassemia exists. Moreover the treatment that *is* available is cumbersome and costly in nature. Since the fundamental defect lies at the level of hemoglobin production, a short review of hemoglobin and its genetic regulation will follow.

1.2.2. Hemoglobin

Hemoglobin is a 64 000 Dalton (Da) tetrameric protein composed of two α- and two "non-α" globin polypeptide chains, each covalently linked to an iron-containing heme prosthetic group. During development, two α- and two γ-chains combine to form fetal hemoglobin (HbF), the predominant hemoglobin as of 10-12 weeks post-conception (13). The γ-chains, however, are replaced shortly after birth by two β-globin subunits which become the principal non-α-chains throughout adult life. Normal adult hemoglobin consists of a major component, HbA, made of two α- and two β-chains non-covalently bound, and a minor component, HbA_2, comprised of two α- and two δ-chains. Normal

4

proportions of hemoglobin types within adult red cells are 98% HbA, ~2% HbA$_2$, and traces of HbF (14).

The primary function of hemoglobin in vertebrates is to deliver O$_2$ from the lungs to the tissues and to carry CO$_2$ back to the lungs. This critical role in gas exchange defines hemoglobin as a molecule essential for life.

The heme iron is responsible for mediating O$_2$ binding, and must be in the ferrous (Fe^{2+}) oxidation state for this to occur (15). The folded helices of globin, meanwhile, form a pocket surrounding the heme to protect it against oxidation. Both structures, therefore, interact in such a way that ensures reversible and co-operative O$_2$ binding. Because the two originate in distinct cellular compartments (heme in cytosol and mitochondria, globin on ribosomes in cytoplasm), their synthesis must be co-ordinately regulated to properly form the final hemoglobin molecule in the nucleated cells of the bone marrow.

Globin formation itself is a complex process relying on key regulatory gene sequences, transcription factors, and feedback regulation for expression that is appropriate to the physiological need and developmental stage of the organism. Genes at the tip of the short arm of chromosome 16 code for α-chains, while a β-globin gene cluster on chromosome 11 codes for "non-α"-chains (16). Subunit production is tightly regulated to ensure matching of α- and β-chains in an exact ratio of 1 ± 0.05 (17). Any disturbance in this balance precipitates a cascade of pathological events related to both the reduction in cellular hemoglobin levels and the reactivity inherent in the unpaired subunits.

1.2.3. Classification of Thalassemias

The thalassemias originate from a state of polypeptide imbalance due to mutations in one or more of the globin-producing genes. They are classified according to the type of subunit affected and the extent to which synthesis has failed. The two most common forms are α- and β-thalassemia, resulting from decreased α- and β-chain output respectively. These two types of thalassemia differ not only in terms of the targeted subunit, but also in the types of mutations they arise from, the RBC membrane properties impaired, the severity of the phenotypes they produce, and even in their geographical distributions (18). The more widespread and often more severe of the two, β-thalassemia, was selected as the disease for study and will therefore be the focus for the remainder of this investigation.

The description of β-thalassemia as minor, intermedia, or major, refers to progressively decreasing levels of β-globin subunit and, correspondingly, increasing clinical severity (19). Though this classification is practical, it is also somewhat imprecise as the underlying defects and genetic modifiers impart a phenotypic heterogeneity to the disease that makes distinctions between types more ambiguous than absolute. Thus, each category includes a broad spectrum of symptoms requiring variable treatment modalities. Inheriting two mutated genes results in the homozygous condition of β-thalassemia major or Cooley's anemia, the most severe form being when virtually no β-chain is produced. The disease is lethal within the first year of life unless patients are transfused (20). Transfusions are subsequently required throughout the lifetime of affected individuals to maintain normal Hb levels. Thalassemia intermedia patients range from completely asymptomatic to moderately anemic individuals, and though some

6

require transfusions, many survive without any treatment at all. β-thalassemia minor patients are heterozygous carriers of the disease and are asymptomatic or only slightly anemic. Because activity of the normal gene undergoes compensatory upregulation, this condition is extremely mild and does not usually necessitate treatment (20).

1.2.4. Pathophysiology of β-Thalassemia

Over 200 mutations resulting in β-thalassemia have been characterized to date, the most common being point and splicing mutations, although frameshift, and occasionally, deletion mutations also occur (21). All share in common the effect of partially or completely reducing β-globin chain output. Interestingly, though the defining feature of the disease is the decreased or absent synthesis of β-subunits, the pathophysiology is not dictated as much by this deficiency as it is by the relative excess of the unaffected α-chains. While the basic defect in thalassemia is genetic in nature, the pathology ultimately manifests itself at the level of erythroid precursors and mature red cells, whose premature destruction produces clinical consequences throughout the organism. It should be noted that while cell death occurs predominantly at the level of erythroblasts within the marrow, both erythrocytes and their precursors share the fundamental process of α-chain deposition. The emphasis here will be on mature red cells since the oxidant injury leading to their hemolysis is more fully understood and because they constitute a more practical tool in which the disorder, and therapeutic approaches to correct it, can be studied.

The pathophysiology of β-thalassemia is determined by the accumulation and instability of α-chains, the susceptibility of RBC membrane components to oxidation, and the oxidative drive of catalytic iron (17). Each factor will be discussed below.

1.2.4.1. Excess α-Hemoglobin Chains

The globin gene mutation governs the degree of chain imbalance. Several mechanisms exist to partially counteract the discrepancy in α- and β-globin chain production. These compensatory mechanisms include α-chain-degrading proteases (22), persistent production of variable levels of γ-globin (and therefore HbF) into adulthood (23), and the induction of a recently discovered α-hemoglobin stabilizing protein that acts as an α-monomer chaperone (24). The phenotype may also appear less severe if chain imbalance is reduced due to co-inheritance of α-thalassemia (25). The methods used to destroy or neutralize excess α-chains, however, are only partially effective in limiting the imbalance, and α-chain synthesis persists unbridled.

Unable to pair with their β-counterparts, "bachelor" chains with hemes still attached accumulate within the cytoplasm of red cells and ultimately precipitate within the RBC membrane (26). Since they lack the conformational constraint usually conferred by α/β-chain interactions in the tetramer, α-monomers become highly unstable (27). This instability relates to their abnormally high susceptibility to autoxidation concurrent with the loss of α/β "packing" contacts. Free α-chains, in fact, autoxidize and liberate their heme moieties approximately eight times faster than their tetrameric counterparts (28-30).

One possible fate of reactive α-subunits involves their oxidative denaturation to methemoglobin (metHb), a hemoglobin derivative, in which Fe^{2+} iron has been oxidized to Fe^{3+}. Further denaturation to the low-spin ferric derivative, hemichrome, also occurs, aggregates of which may damage cells directly or precipitate over time (31). Alternatively, α-chains may be degraded to their constituents, globin and heme, the latter eventually liberating non-heme iron. Released in close proximity to the membrane, each of these metabolites has the potential to cause sheer mechanical or oxidative damage to cytoskeletal and membrane proteins and lipids. Structural alterations of the RBC membrane will compromise its integrity and lead to premature cell destruction by specific immune or mechanical processes (32).

Immune removal of red cells primarily involves the binding of hemichrome to the cytoplasmic domain of integral membrane protein band 3, a chloride-bicarbonate exchanger (33). This abnormal association results in co-clustering of band 3 molecules and subsequent generation of neo-antigenic sites recognized by autologous immunoglobulin G (IgG) antibodies. Through opsonization and complement binding, erythrocytes are then targeted for removal via macrophages (34).

The mechanical removal of erythrocytes from the circulation is triggered by the degradation products of α-chains. Heme and globin may directly associate with peripheral, cytoskeletal, and integral membrane proteins, causing them to cluster and, in so doing, changing the mechanical properties of the cell (35). They may also intercalate within the lipid bilayer, increasing phospholipid spacing in the outer leaflet, which stimulates phagocytosis (32, 36). Most crucial, though, is the action of catalytic iron liberated from heme, which serves as a nidus for oxidant generation (further described in

1.2.4.3.). By relentlessly transmitting oxidative insult to membrane structures, iron promotes protein cross-linking and lipid peroxidation, compounding the structural damage already effected by heme and globin (37). These abnormalities result in RBC instability and fragmentation, prompting their recognition and mechanical removal by macrophages.

1.2.4.2. The Red Blood Cell Membrane

In thalassemic red cells and precursors, a direct relationship exists between the size of the unpaired α-chain pool and 1) membrane protein defects, 2) the degree of hemolysis and, 3) the clinical severity of the disease (38, 39). This underscores the importance not only of surplus α-chains in the pathogenesis but also, the location of the damage – the red blood cell, specifically its membrane. The thalassemic RBC must handle the hazardous combination of continuous oxygen exposure, reactive heme-containing α-chains, and the potential toxicity of heme-derived iron. Furthermore, the very nature of the membrane - an envelope rich in oxidant-sensitive unsaturated lipids - makes the cell particularly vulnerable to iron-mediated peroxidation.

Thalassemic cells have also lost the protection inherent in hemoglobin structure which, by its very design, conceals iron and limits its reactivity. Compromised hemoglobin integrity thus results in iron decompartmentalization, freeing the metal to initiate oxidative damage. In addition, red blood cells from thalassemic patients produce higher amounts of superoxide, hydrogen peroxide, and hydroxyl radical species, and are deficient in antioxidants, such as glutathione and vitamin E (40-44). Though the mechanisms evolved by RBC to cope with oxidant stress are generally effective, they are also located within the cytoplasm, relatively remote from where the major damage is

occurring. Furthermore, the absence of nuclei and mitochondria limits the RBC's capacity for *de novo* synthesis of molecules involved in membrane repair and cytoprotection.

The thalassemic RBC, therefore, represents a highly pathological environment in which failure of normally fastidious iron compartmentalization, loss of cytoprotective mechanisms, and high oxidant generation act synergistically to promote its premature demise. The final details of these processes and the specific membrane structures involved will be discussed next, in the context of iron release from heme.

1.2.4.3. The Role of Iron

Iron has long been deemed a biological paradox; it is indispensable for life, yet harbours a deadly potential - the ability to promote severe oxidative damage within cells (45). Among its many attributes, iron's interconvertibility between two redox states, ferrous (Fe^{2+}) and ferric (Fe^{3+}), is probably its most important. Moreover, its physiological ubiquity in an array of functions ranging from oxygen transport to DNA synthesis, is a testament to how vital and multifunctional it is. However, just as many of iron's essential functions are fulfilled through its potential to redox-cycle, so too are many of its destructive effects.

Iron's ability to catalyze the formation of toxic free radicals places it at the heart of the pathophysiology of thalassemia. The process of iron's release from heme begins with the generation of methemoglobin and superoxide in the heme pocket during α-chain autoxidation (46). Superoxide is then converted to hydrogen peroxide, which can oxidatively cleave the heme ring and liberate iron in proximity to the membrane. This iron is now bioavailable for valence-cycling (47) and, by catalyzing the classic Fenton

reaction ($H_2O_2 + Fe^{2+} \rightarrow OH^- + \cdot OH + Fe^{3+}$), produces the most deleterious of activated oxygen species, the hydroxyl radical (48). As it attacks virtually any organic molecule in its path, the deadly reactivity of the hydroxyl radical will be focused on those structures iron is most intimately associated with: membrane proteins and lipids.

1.2.4.3.1. Protein Oxidation

At the protein level, the major effects of iron-induced damage include amino acid modification, abnormal protein cross-linking, and oxidation of protein thiol groups (49). Excessive oxidation converges on the three major cytoskeletal proteins - spectrin, actin, and band 4.1 (anchors cytoskeleton to the bilayer), as well as peripheral and integral membrane proteins, ankyrin and band 3, respectively (49-51). As a response, the proteins undergo abnormal aggregation and co-clustering, forming rigid patches within the membrane that resemble "islands" of dysfunctional molecules. This oxidative cross-linking not only causes the cells to lose their deformability, but may also expose lipid regions on their outer surface, marking them for destruction (52, 53). Furthermore, oxidation of the K^+/Cl^- co-transporter causes it to become excessively stimulated, producing leakiness of the membrane, and eventually, cellular dehydration (54).

1.2.4.3.2. Lipid Peroxidation

Membrane phospholipids are also a target of iron-initiated oxidative attack. Remarkably, high-affinity binding of non-heme iron to anionic lipids in both sickle and thalassemic red cells has been demonstrated, imparting a sponge-like attraction of iron to the membrane (55-57). As a result, altered phospholipid asymmetry is commonly seen in thalassemic RBC, with phosphatidylcholine being found in the inner leaflet and both

phosphatidylserine (PS) and phosphatidylethanolamine (PE) translocated to the outer surface (32). One of the consequences of this abnormal distribution is the exposure and partial release of phosphatidylserine from the outer bilayer leaflet, which activates the prothrombinase complex and promotes hypercoagulability (58-60). Furthermore, a selective decrease in the percentage of oxidant-sensitive lipids, PS and PE, as well as polyunsaturated fatty acids (PUFA), notably arachidonic acid, suggests ongoing iron-mediated oxidative stress as the driving force behind lipid damage (61). The downstream effects of excessive lipid peroxidation include decreased lipid fluidity, altered cell permeability, cell stiffness and rigidity, and the permanent "locking" of the cell into an abnormal configuration (32, 62). Finally, iron-driven lipid peroxidation has been shown to generate abnormal lipid adducts as well as elevated levels of the by-product of PUFA breakdown, malondialdehyde (MDA), which itself can trigger erythrophagocytosis and opsonization via a specific immunoglobulin (63).

Each of these processes contributes to the hastened destruction of RBC, and is dangerously amplified by the destabilization of normal hemoglobin as it gives up *its* heme-iron to further promote oxidation (64). Moreover, the chemistry of iron reactivity ensures continuous availability of the metal as it is alternately oxidized and reduced, always free for catalysis and relentlessly feeding into the oxidative cycle.

In summary, therefore, iron triggers a self-amplifying, self-propagating cycle of redox-reactions producing hydroxyl radicals that target the RBC membrane and incite the premature death of thalassemic cells. All of these defects, and the pathways involved in their generation, are represented schematically in Fig. 1 (27). As shown, the ultimate consequence of iron-driven injury is accelerated cell destruction - either intramedullary

(precursors) or peripheral (mature RBC) hemolysis, which in turn, dictates the downstream clinical manifestations of the disease.

1.2.5. Clinical Consequences

1.2.5.1. General

The phenotypes observed in thalassemic patients are, as the genetic origins, extremely heterogeneous. Accelerated destruction of erythroid precursors in the bone marrow occurs both as a result of apoptosis as well as direct iron-mediated cellular modifications (65, 66). Up to 80% of erythroblasts may be unable to complete maturation and thus perish within the marrow (17). Many of the surviving cells eventually succumb to the same oxidative damage while in circulation, and are prematurely destroyed peripherally. Shortened RBC survival due to hemolysis results in clinical anemia, a hallmark of the disease. The decrease in oxygen delivery to tissues stimulates the production of erythropoietin by the kidneys and massive expansion of the marrow to compensate for the cell loss.

There is a fundamental flaw in the physiological response, however, as failure to correct the basic genetic defect permits the oxidative cycle to continue unabated, destined to repeat itself in each new cell formed. Thus, increased erythroid production is futile, and the successive destruction and compensatory production of precursors lead to an important phenomenon in β-thalassemia known as ineffective erythropoiesis (67).

Under this condition of enormous erythropoietin-driven pressure towards erythroid differentiation, erythroid mass has been shown to increase up to 30 times its normal size (27), the consequences of which are manifold, as outlined in Fig.2. Skeletal deformities result from the grossly expanded marrow, and extensive hypertrophy of both

liver and spleen occurs as a result of RBC entrapment (27, 68) and storage of iron (discussed in 1.2.5.2.). Dysregulated iron metabolism is perhaps the most devastating complication of thalassemia, however. The excessive dietary absorption and tissue deposition of iron, which in large part determines patient survival, will now briefly be considered.

1.2.5.2. Iron Overload

Iron overload in target tissues is the major cause of morbidity and mortality in β-thalassemic patients, and has been shown to increase proportionally with the rate of erythropoiesis (69). The insidiously high turnover rate of red cells creates a metabolic drive for continuous iron absorption; however, since no physiological mechanism for iron excretion exists, the amount of iron in the circulation eventually exceeds the capacity of its plasma carrier protein, transferrin, to bind and detoxify it. As iron loading progresses, an unbound fraction, known as non-transferrin-bound iron (NTBI), appears in plasma (70). Intracellularly, meanwhile, iron accumulates in parenchymal cells, notably hepatocytes, from its intracellular storage protein, ferritin. Cells of the reticuloendothelial system also amass iron derived from the hemoglobin of senescent RBC. The iron loading in hepatocytes, macrophages, and other tissues is aggravated by cellular uptake of iron from NTBI. Moreover, iron from NTBI in circulation is weakly bound to physiological ligands (e.g. citrate or albumin), and is available to participate in the production of membrane-damaging free radicals (71-73). Over time, iron's steady accumulation in organs such as the liver, spleen, heart, endocrine and other tissues, leads to their extensive damage and, ultimately, organ failure. Cardiac cells are particularly

vulnerable and their progressive loss of function commonly leads to congestive heart failure or arrhythmias, both of which can be deadly (74).

Spontaneous iron loading is further exacerbated by the very treatment used to manage the disease, transfusion therapy. Before describing this in further detail, it is critical to mention that this systemic iron overload is a phenomenon distinct from, and unrelated to the primary, intraerythrocytic iron accumulation discussed up to now.

1.2.6. Current Treatment

1.2.6.1. Transfusion Therapy

Transfusion therapy is the current mainstay treatment for thalassemia. Though allogenic bone marrow transplantation would be curative, it is limited to a small fraction of individuals for whom histocompatible donors can be found and is, therefore, not an option for most patients. As no definitive cure exists, disease management demands continual care and must be maintained over a patient's lifetime to ensure his or her survival. When thalassemia presents during the first year of life, diagnosis is made by blood test, appearing as a hypochromic, microcytic anemia; thalassemia diagnosis may then be confirmed by hemoglobin electrophoresis. Upon diagnosis, the transfusion regime is prescribed according to clinical parameters, the usual requirement being treatment every 2 to 4 weeks (75). The aim of transfusion is to counteract the anemia, suppress excessive erythropoiesis, and prevent the enhanced dietary absorption of iron and its subsequent tissue deposition. However, the inevitable by-product of repeated transfusions is the further "feeding" of iron from transfused cells into patients, leading to secondary, or transfusional, iron overload. Again, since no physiological system exists to rid the body of the excess metal, a complementary practice must be instated to administer

agents that bind and remove surplus iron before it amounts to dangerous levels; these compounds are known as iron chelators (discussed in 1.4.).

1.2.6.2. Iron Chelation Therapy

The only currently approved chelator in North America is the compound desferrioxamine (DFO), a bacterial siderophore (76). Unfortunately, DFO suffers from a number of serious disadvantages, the most critical, perhaps, being its lack of oral absorption and short plasma half-life necessitating long, subcutaneous or intravenous infusions. The drug is thus given continuously over 8-10 hours, 5-7 times a week (77). Due to the cumbersome and often painful nature of administration, as many as 50% of patients do not comply with the therapy protocol; such a lack of compliance leads to serious cardiac and metabolic abnormalities (78). Other reported side effects of DFO include painful local reactions or infections at the injection site (79), as well as dose-related toxicity in a small number of people (80). Finally, it is an extremely costly drug to synthesize, prohibiting its use by at least 90% of thalassemic patients (81), these being individuals living in developing countries – ironically, the same patients who need treatment the most.

Although an exhaustive selection of chelators now exists, including compounds designed and synthesized since the introduction of DFO therapy in the 1960's, many have been subject to controversy regarding their safety and effectiveness, and none have exhibited a clinical profile favourable enough to replace DFO as the chelator of choice. Thus, despite its cumbersome mode of delivery, DFO continues to be the gold standard in iron chelation therapy and the only agent accepted as viable on a long-term basis. The search continues, then, to find orally available compounds that would maintain the

17

effectiveness of DFO while circumventing the difficulties associated with its administration. A more comprehensive discussion of iron chelation as well as novel compounds that have emerged will follow next, in the context of our hypothesis.

1.3. Rationale and Hypothesis of Study

Despite major advancements in thalassemia research over the past several decades, ultimate management of the disease may require alternative, more curative treatment approaches. The schema of current therapy may be represented as follows:

intraerythrocytic iron ⟶ pathology
↓
transfusion
↓
side effect: secondary iron overload
↓
iron chelation
↓
side effect: chelator-related complications
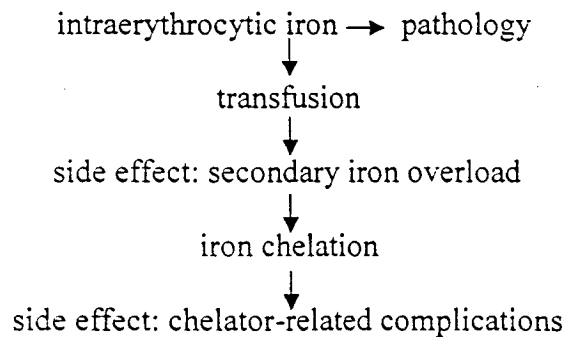
The goal of replacing defective cells with healthy ones is undoubtedly achieved using this strategy, however, the complications of secondary iron overload and non-compliance with chelation regimes make it sub-optimal. Moreover, chelation is aimed at reducing tissue iron and neither accounts for, nor attempts to pursue, the proximate α-chain-derived iron at the source of the damage. Therefore, given the shortcomings of current therapy and the magnitude of the effects triggered by intraerythrocytic iron in the pathophysiology of β-thalassemia, it is conceivable that targeting this iron for removal could be of significant therapeutic benefit. Since this is the most proximal iron compartment in the chain of pathological events, we hypothesize that intercepting it within erythrocytes may diminish metal-catalyzed oxidative damage to membrane

proteins and lipids, and perhaps slow or even prevent accelerated RBC destruction. Clinically, this would be expected to enhance RBC survival and, correspondingly, decrease the transfusion burden in thalassemic patients, ultimately improving their quality of life.

1.3.1. Preliminary Supportive Evidence

We propose, at this juncture, an alternative treatment paradigm for β-thalassemia that would be based on RBC iron chelation *prior to* transfusion therapy as a means of circumventing the cycle of iron-mediated damage and premature cell clearance. This could be accomplished in a practical and therapeutically feasible way by using iron chelators capable of penetrating the red blood cell membrane and accessing abnormal metal deposits therein. Preliminary evidence exists to support this concept: iron chelator deferiprone (L1), has meaningfully improved RBC pathology in β-thalassemic mice (82), and promoted both membrane-bound iron removal (35, 83), and enhanced K^+/Cl^- status in L1-treated human thalassemics (84). However, these have been the only trials to date and have been limited to the study of L1 and DFO. They have also focused exclusively on red blood cells and associated parameters. These preliminary investigations have been significantly broadened in our laboratory, both in terms of the compounds tested and in the scope of cell types examined. Before describing our research objectives and experimental models, a brief overview of iron chelation and selected chelating agents will be presented.

1.4. Iron Chelators

The term "chelator" is derived from translation of the Greek word for claw ("chele"), and aptly refers to the ability of such compounds to bind metal ions like the claws of a lobster. Though a somewhat elementary analogy, it does convey the prime objective of chelators: to bind metals specifically and with high-affinity, and in the case of iron chelators, to keep iron chemically inert and prevent its participation in redox-reactions.

1.4.1. Mechanism of Action

Iron chelators function by binding and inactivating iron either intracellularly, from the labile iron pool, or extracellularly, usually in the form of toxic NTBI in plasma. Iron that is not co-ordinated to high-affinity ligands such as transferrin, or molecules such as hemoglobin, is amenable to chelation; this includes, importantly, intraerythrocytic non-heme iron. Once the chelator binds iron, the complex is transported in the circulation and excreted through feces or urine.

Detoxification by iron chelators requires a biodistribution granting them access to the "toxic" iron pools, and the formation of stable iron-chelate complexes that are rapidly excreted to avoid their redistribution. The stability of these complexes directly depends on how tightly the metal is bound to the chelator. Since iron has six co-ordination sites, all must be liganded to completely prevent it from redox-cycling (85). Hexadentate chelators, binding iron in a 1:1 ratio, thus form the most kinetically stable complexes. Tridentate and bidentate chelators, on the other hand, bind iron in a 2:1 and 3:1 ratio respectively. Therefore, at low concentrations of these chelators, the iron neutralization reaction is incomplete and partial co-ordination complexes containing bioactive iron may be formed - these complexes are free to generate reactive oxygen species (77).

The overall rate of iron removal is dependent, predictably, on both the rate of iron accumulation and the rapidity with which the chelator depletes it (modulated by dose, duration of treatment, etc), while the rate of iron mobilization at the cellular level is dictated by the lipophilicity of both the free chelator and the iron-chelator complex (86). For chelators of the PIH family, the speed of iron mobilization is specifically governed by the rate of efflux of the iron-chelator complexes from the cell (87). Greater ease of chelator diffusion across cell membranes not only expedites translocation of the complex but also minimizes exposure of cell contents to any toxic, "loosely" bound iron.

1.4.2. Criteria for Selection

In designing novel, more optimally performing iron chelators, an extensive range of biochemical and pharmacological properties must be possessed by an agent for it to be considered worthy of pursuit. The criteria for an ideal iron chelator are extremely stringent and no single compound has been identified which could meet them all. A strong candidate would demonstrate the following: high selectivity and affinity for iron, absence of interaction with metabolic iron pools (e.g. iron-dependent enzymes), oral bioavailability, gastrointestinal absorption, and lack of toxicity. Furthermore, the iron-chelator complex should display efficient mobilization, that is, the complex should possess a lipophilicity similar enough to that of the free ligand, allowing effective cell permeation of the chelator without accumulating toxic products once inside the cell. Finally, the ideal chelator should be relatively inexpensive to synthesize and capable of achieving and maintaining negative iron balance (85, 88).

1.4.3. Iron Chelators Under Investigation

Previous studies have supported the idea that intraerythrocytic non-heme iron contributes to the pathogenesis of thalassemia; this was demonstrated by showing the benefits of chelator-mediated iron removal from RBC (50, 82, 83). As will be presented below, our studies have expanded this concept considerably by including an array of iron chelators, some of which are relatively novel. The compounds selected include DFO, the current mainstay in chelation therapy (89) and L1, the only orally available alternative (82-84, 89-93), as well as PIH and its most promising analog, o-108, both highly effective *in vitro* and *in vivo* (87, 94-101). These four chelators span an entire spectrum of properties, varying in their origins, structures and sizes, stoichiometric interactions with iron, lipophilicities, bioavailabilities, and degrees of novelty and clinical use. Table 1 illustrates their basic structures and characteristics.

1.4.3.1. Desferrioxamine (DFO)

DFO occurs naturally as a bacterial siderophore. It is a large (657 Da) hexadentate chelator of the hydroxamic acid family, binding iron with high specificity and affinity, and maintaining it in a metabolically inactive form. DFO is generally non-toxic and effectively depletes tissue iron stores due to its capacity to excrete iron via both urine and feces (80). However, despite its routine clinical use for over thirty years, it is far from meeting the criteria of an ideal drug for the treatment of iron overload. Because of its large size and hydrophilicity, cellular uptake of DFO is slow and its gastrointestinal absorption, negligible (102). Moreover, it is rapidly metabolized (plasma $t_{1/2}$ ~5-10 min), limiting its administration to continuous parenteral infusion (103). The majority of patients do not tolerate DFO treatment well, finding it burdensome and painful. This

chelation protocol frequently results in a lack of patient compliance, inevitably leading to a decrease in life expectancy due to iron overload. It has thus been a major goal of chelator research to identify new formulations of DFO, new methods of its administration, or new treatment options involving DFO's combination with other chelators to improve compliance and decrease the risk of toxicity.

1.4.3.2. Deferiprone (L1)

Deferiprone is a relatively small (139 Da) compound belonging to a class known as α-ketohydroxypyridinones, and has been used in therapeutical trials for over fifteen years (104). It is the only chelator approved for oral application, although exclusively available in Europe and India (92). Excretion of iron using L1 is predominantly urinary. Its small size, neutral charge and bidentate nature predict many of its benefits, including fast gastrointestinal absorption and high cell permeability.

However, the properties of L1 are altered once bound to intracellular iron, resulting in a larger, more hydrophilic and relatively cell impermeable complex that may accumulate dangerously within the cytosol (105). L1 also has the potential to inhibit iron-containing enzymes such as ribonucleotide reductase, necessary for DNA synthesis (106, 107). Another disadvantage of L1 is the instability of its iron complex because of its failure to occupy all six iron co-ordination sites. Thus, at low drug concentrations, biochemically active intermediate products may drive the generation of free radicals (108). Manifestations of this toxicity and other undesirable side effects of L1 in humans include agranulocytosis and neutropenia (109), arthritis (80), musculoskeletal pain (110), and gastric intolerance (93). Independent of these potential risks, L1's widespread implementation and general acceptance by the biomedical community has been hampered

by the sheer controversy surrounding it (110-117). The results of several major long-term trials investigating the effects of L1 on 1) iron burden, 2) hepatic fibrosis, and 3) serum ferritin levels, are conflicting and have yet to be resolved (90, 93, 110-117). Thus, despite clinical scrutiny spanning almost two decades, no consensus regarding the safety and efficacy of L1 has been reached, further warranting the search for alternative, orally administrable iron chelators.

1.4.3.3. Pyridoxal Isonicotinoyl Hydrazone (PIH)

PIH was discovered serendipitously by Ponka *et al.* when its constituents, pyridoxal (vitamin B6) and isonicotinic acid hydrazide (anti-tuberculin drug), unexpectedly mobilized radioiron from mitochondria of reticulocytes previously incubated with an inhibitor of heme synthesis and transferrin-bound radioiron (94). The resultant compound was synthesized, yielding the high affinity iron chelator now known as pyridoxal isonicotinoyl hydrazone, or, PIH. It was later characterized as a 287 Da member of the aroyl hydrazone class and found to bind iron in a 2:1 ratio, qualifying it as tridentate. Its many attributes include its cell permeability, both as a free ligand and as a complex with iron, and its substantial activity when given orally (95, 118). It is uncharged at physiological pH and is extremely selective for iron, which it avidly binds in both ferrous and ferric forms. Most importantly, PIH demonstrates high chelation efficiency both *in vitro* (98, 119-123) and *in vivo* (96, 97, 100, 118), even surpassing DFO in a number of studies (95, 124). It is also highly non-toxic, and cost-effective to synthesize. Iron excreted using this lipophilic chelator is mostly via the fecal route (125).

One of the major drawbacks of PIH is that its complex with iron is more charged than the free ligand, causing slight retardation of PIH-iron efflux from cells. Therefore,

mobilization of iron by PIH has been postulated to rely on an energy-dependent carrier (120, 126). Another disadvantage of PIH is its rapid hydrolysis at acidic pH, such as that found in the stomach. In fact, because of its administration in a non-soluble form during Phase I clinical trials, the efficacy of PIH has likely been underestimated. New studies examining the benefits of PIH administration while fasting or in a coated formulation are thus needed in order for it to be fairly evaluated (99). Results from trials in animals given PIH on an empty stomach yielded a much higher efficiency, and would support this contention (95, 100). The present challenge, then, lies in the attempt to maximally enhance the bioavailability of PIH. Given its relatively few shortcomings and its ability to successfully bind and detoxify iron, PIH merits further consideration as a potentially strong candidate for the treatment of β-thalassemia.

1.4.3.4. Pyridoxal *ortho*-Chlorobenzoyl Hydrazone (*o*-108)

Once PIH was identified as a therapeutically viable iron chelator, a series of analogs were synthesized in the attempt to improve on its chelation efficiency. One such derivative is *o*-108 (320 Da) which, like its PIH parent compound, is a tridentate member of the aroyl hydrazone family. This agent, too, is readily absorbed from the gut, is highly cell permeable and efficiently mobilizes iron both *in vitro* (87, 98, 123, 124, 127-129) and *in vivo* (97, 100, 101), resulting in fecal excretion. However, because of its modified structure, it possesses biochemical and pharmacokinetic properties distinct from PIH. In *o*-108, a weaker electron-withdrawing halogenated benzene ring replaces the pyridine of PIH, rendering it more lipophilic and potentially more adept at accessing intracellular iron pools. This would explain its superior capacity to mobilize iron compared to both PIH and DFO in the aforementioned studies. Finally, *o*-108 is highly non-toxic (128) and

also reasonably inexpensive to synthesize. Though it has not yet reached the clinical trial stage, and remains the most novel chelator of the four, preliminary results obtained with o-108 *in vitro* and in animals are sufficient to corroborate its safety and effectiveness, and highlight its potential as a powerful orally-active iron chelator of the future. We have thus selected it as a representative PIH analog to be the final compound for our study.

1.5. Objectives and Models of β-Thalassemia

1.5.1. Testing the Hypothesis: Objectives

To test the hypothesis that intracellular iron removal via highly selective iron chelating agents could ameliorate the pathophysiology of β-thalassemia, we evaluated the effects of iron chelators DFO, L1, PIH, and o-108 on β-thalassemic erythrocytes, reticulocytes, and tissues. Our goal was to cover a range of possible chelator effects and explore their full potential, rather than simply to compare the compounds relative to each other.

The chelators were tested in two distinct and complementary models of β-thalassemia: *in vitro*, exploiting prepared human erythrocytes loaded with α-globin chains as models of thalassemic cells, referred to simply as model β-thalassemic erythrocytes (51), and *in vivo*, in β-thalassemic mice generated following transplantation of murine thalassemic bone marrow into irradiated recipients. The former would provide insight into the feasibility of this application in *human* cells specifically, while the latter would report on the effects of chelators in a physiological environment, from a whole-body standpoint.

It was anticipated that intraerythrocytic iron chelation would alleviate oxidative damage to membrane structures and thereby, improve overall RBC status in both models. As a result, iron chelators would be expected to correct hematological abnormalities and,

consequently, perhaps prolong RBC survival *in vivo*. Finally, we reasoned that effects of chelation might extend beyond red cells to improve conditions in their precursors and even, possibly, within tissues. It was our hope that by studying these factors concurrently in two different models, a more global appreciation of the therapeutic potential of intraerythrocytic iron chelation would be achieved.

The first goal was to prepare each model and confirm its functionality and accurate representation of human β-thalassemia. Second, it was vital to verify that all chelators were, in fact, able to remove membrane-bound iron, so as to attribute downstream consequences to their iron binding and not other, non-specific properties. The final objective was to assess various indices of pathology within red cells, and additionally, *in vivo*, in erythroid precursors and mouse tissues. As described below, the parameters chosen for evaluation reflected the most salient pathologic features of thalassemic cells, the same ones that would likely be the most amenable to improvement. Before proceeding to the methodology, both models will briefly be discussed.

1.5.2. *In Vitro* - Human Model β-Thalassemic Red Blood Cells

Though ideal *in vitro* testing would use genuinely pathological cells derived from thalassemic patients, such cells are difficult to obtain and are not always appropriate for several reasons. Firstly, thalassemic patients undergo a rigorous regime of transfusion, coupled with chelation therapy, to prevent transfusional iron overload. Their red blood cells would thus not be expected to exhibit the full-blown damage characteristic of untreated patients. Moreover, the most pathological cells are often the first destroyed and therefore, would not be present in peripheral blood, causing underestimation of the level of damage. Finally, the relevant injury to patient cells would have already occurred *in*

vivo, precluding the study of developmental alterations and the involvement of iron therein.

In light of these shortcomings, a model of thalassemic RBC was devised in which disease biogenesis could be tracked, and therapeutic compounds could be tested without compromising the validity of the results. It was found that healthy human erythrocytes, loaded with purified α-hemoglobin subunits via gentle osmotic lysis and resealing, display the abnormalities characteristic of actual β-thalassemia (51, 130, 131). The damage incurred by the modified cells is a direct result of, and proportional to, the concentration of the encapsulated α-chains. These cells represent an experimentally-generated, and thus, readily available population in which the sequence of oxidative events, and the effects of iron chelators at each stage, can be monitored. By minimizing dilution of intracellular constituents and cell membranes during lysis, the resultant erythrocytes are initially, physiologically sound. They display normal morphology, phospholipid composition and membrane permeability, as well as unaltered enzyme concentrations (ATP, glutathione, catalase), and intact membrane transport systems. Conceptually, therefore, they act as a "blank canvas" over which the abnormalities induced by α-chains can be illustrated as they emerge in real-time. As the α-chains adhere to the membrane, they trigger structural and functional modifications that closely parallel the pathophysiological changes underlying human β-thalassemia, specifically, excess membrane-bound iron, exaggerated protein oxidation, and finally, loss of deformability (130, 131). By treating model cells with iron chelators, it should be possible to evaluate their potential protective effects on each of these aspects of cell dysfunction.

In order to generate model β-thalassemic erythrocytes, we first needed to isolate the α-globin to be entrapped within RBC, ascertain its purity, then test for its universal loading; that is, ensure that the majority of cells were indeed being lysed, and that they successfully engulfed exogenous α-chains. Fig. 3 schematically depicts the steps involved in model β-thalassemic RBC preparation.

Human model β-thalassemic cells would be incubated in the presence or absence of iron chelators, and while untreated cells would reproduce the key pathological features of the disease, the chelator-treated ones would demonstrate the potential of each compound to remove membrane iron and curb Hb oxidation. The *in vitro* stage of testing, therefore, constituted a primary checkpoint for chelator efficiency, ensuring the basic ability of each compound to ameliorate cell status. *In vitro* studies also reported on the response of human cells to iron chelation and, thus, addressed the clinical viability of this strategy in thalassemic patients. Provided the efficiency of iron chelators in these initial experiments, we would then evaluate them in a pathophysiologically realistic model *in vivo*, using β-thalassemic mice.

1.5.3. *In Vivo* - Animal Model of β-Thalassemia

1.5.3.1. Murine β-Thalassemia

The first mouse model of β-thalassemia arose through a spontaneous mutation discovered by Johnson and Lewis in 1981 (132). A number of models have since been generated through selective deletions in the β-globin gene locus, which in adult mice normally contains two distinct β-globin genes: β-globin major and β-globin minor ("diffuse" mouse haplotype). Due to polymorphisms, another mouse haplotype contains two genes

forming an identical β-globin subunit, β-single (133). The murine models of thalassemia characterized to date include: 1) mice homozygous for a deletion in β-globin major, 2) mice heterozygous for an insertional disruption of β-globin major (milder phenotype), and recently, 3) mice engrafted with β-globin null fetal liver cells, displaying the equivalent of Cooley's anemia (133-135). The last model is the only one representing true adult thalassemia major and is the most severe, requiring animal euthanasia just 7-9 weeks after the transplant. Yet another model exists which is more severe than 1) and 2), but whose lifespan enables more extended study than model 3), making it ideal for our experiments. This model, generated in 1995 by Townes *et al.* (136), consists of mice hemizygous for the deletion of both β-major and β-minor genes. The mice are termed hemizygous β-globin knockout (though referred to here simply as β-thalassemic), and as a result of their mutation, produce only 70-75% of the normal amount of β-globin protein (136).

Due to the decreased production of β-globin polypeptide chains, mouse models of thalassemia exhibit anemia, abnormal RBC morphology and hematological indices, spontaneous tissue iron deposition, and organ pathology – each with varying degrees of severity. Importantly, the biochemical and functional defects observed in the RBC membranes of these mice also mirror those found in thalassemic humans and critically, include the hallmark intraerythrocytic iron overload, as well as shortened RBC lifespan (49, 82). Combined, these data suggested the suitability of these animals for study (137-139).

Our objectives *in vivo* were, firstly, to generate a high number of thalassemic mice and establish a chelator treatment regimen using the selected compounds. At the cellular

level, our goal was to evaluate the effects of chelators on RBC membrane-associated non-heme iron and hemoglobin oxidation, as was done *in vitro*. Next, we planned to examine hematological parameters and, crucially, track RBC survival for signs of chelator-mediated improvements. Finally, one of the aims of this study was to explore chelator-mediated benefits outside the red cell by evaluating hematological indices in late RBC precursors and iron accumulation and related injury in tissues. Using these animals not only offered the advantage of heightened physiological relevance over isolated cell systems, but it enabled us to evaluate parameters which were inaccessible *in vitro*, such as RBC half-life and organ damage – both important endpoints in determining the overall impact of the chelators.

Again, similar to *in vitro* methodology, β-thalassemic mice were either chelator-treated or untreated; the latter serving as "controls" to confirm the expected disease phenotype – the touchstone against which chelator-treated groups would ultimately be compared. This will be further explained in section 3.2.1.

Finally, an important point regarding our very first objective, the generation of the animal models, should be mentioned at this time. Though our initial intent was to breed colonies of the hemizygous β-thalassemic mice, this prospect proved extremely difficult, due in part to the severity of the disease, the affected animals breeding so inefficiently, it was not feasible to generate sufficiently large, age-matched treatment groups. Faced with this unforeseen challenge, we sought out alternative means of obtaining a meaningful population of thalassemic mice.

1.5.3.2. Hematopoietic Reconstitution Model

Animal studies have often been hindered by the lack of availability of models, and/or by potentially high variability amongst animals due to genetic or age-related heterogeneity. A strategy used by Trudel and colleagues (140) to attain high animal numbers while circumventing both of these difficulties, was to utilize bone marrow transplantations (BMT) to transfer a deficit (sickle cell anemia) into normal mice. Since the marrow contains the blood-forming cells, then blood disorders may be transmitted from relatively rare donors expressing the disease, to readily available recipients whose marrow has been ablated. Using this technique, starting with a single donor mouse, Dr. Trudel's laboratory generated a homogeneous population of age-matched, hemoglobinopathic mice, exhibiting virtually identical degrees of disease severity - essentially "siblings" of a lone pathological "parent" (unpublished). Success was also obtained recently by Rivella and colleagues using a similar procedure, fetal liver cell transplants, to generate large numbers of severely thalassemic mice (135).

We attempted the BMT method, using two hemizygous β-thalassemic donors, in hopes of conferring the disease to nearly thirty control mice. Though BMT may be increasingly commonly used to generate animal models, particularly when the diseases are rare and the animals scarce, it has never been attempted using this specific mouse model before. Therefore, a small-scale pilot study was conducted to ensure the long-term survival of transplanted mice and appropriate manifestation of the disease therein; it was also vital to confirm that the features displayed by recipients were identical to those from donor mice (original colony). Once these questions were resolved, we carried out the transplants, carefully monitoring the status of recipients at each stage of recovery, and

confirming full hematological and phenotypic adoption of the disease. After generating

the mouse models, we proceeded with the investigation of our hypothesis *in vivo*.

2. Materials and Methods

2.1. Materials

2.1.1. Chemicals and Equipment

Michel suture clips were from Aesculap (Tuttlingen, Germany). Thiourea, standard 1 N

NaOH, 1 N HCl, control valve and CGA Teflon sealing washer for CO tank were

obtained from Aldrich (Oakville, Ontario). 2001 Model osmotic pumps and filling tubes

were from Alzet Corporation (La Jolla, CA). Trichloroacetic acid was from American

Chemicals Ltd. (Montreal, Quebec). NaCl, acetic acid, KPO_4, and $MgCl_2$ were from

BDH (Toronto, Ontario). BioRad reagent dye, Chelex, and Wheaton glass tissue

homogenizer were obtained from BioRad (Richmond, CA). Powder HCl, NaOH,

KH_2PO_4, glucose, agar, and reagents for ferrozine assay (with noted exceptions) were

obtained from Bioshop (Burlington, Ontario). Tris was obtained from Boehringer

(Ingelheim, Germany). Biotin-X-NHS was obtained from Calbiochem (San Diego, CA).

Centrifuge tubes, polystyrene tubes for FACS, and 96-well plates were from Falcon

(Franklin Lakes, NJ). Dialysis tubing (SpectraPor3, 3,500 Da MW), sodium

metabisulfite, and all chromatography columns were purchased from Fisher (Fair Lawn,

NJ). HBSS, IMDM, and 10,000 U penicillin/10 mg streptomycin were from Gibco

(Burlington, Ontario). Glucose phosphate isomerase (Gpi) assay was performed using

Helena UK equipment and reagents (Newcastle, UK). FITC-conjugated Egg-White

Avidin was obtained from Jackson Laboratories (West Grove, PA). Centricon Plus-80

centrifugal filters (5,000 Da MW) were from Millipore Corporation (Bedford, MA). CO, parahydroxymercuribenzoate (PMB), β-mercaptoethanol, fluorescein isothiocyanate-dextran (FITC-Dex; 9,500 Da MW), ascorbate, ferrozine, fructose-6-phosphate, 3-(4,5-dimethylthiazol-2-yl)-2,5-diphenyltetrazolium bromide (MTT), glucose-6-phosphate dehydrogenase, nicotinamide adenine dinucleotide phosphate (NADP), phenazine methosulfate (PMS), trizma, glycine, trypan blue, and all other chemicals were obtained from Sigma (St. Louis, MO). The lysis buffer used for dialysis of RBC samples in model thalassemic cell preparation consisted of 5 mM KPO_4 (pH 7.4, ice cold); the resealing buffer was identical, but with the addition of 170 mM NaCl and 5 mM glucose (pH 7.4, heated to 37°C). The buffers used in ghost RBC membrane preparation were as follows: lysis buffer A consisted of 5 mM sodium phosphate + 0.5 mM ethylene diamine tetraacetic acid (EDTA) pH 8.0, lysis buffer B was identical but without EDTA and with the pH adjusted to 7.4; both were ice cold. In the ferrozine assay, reagent A (distinct from lysis buffer A), was prepared as 3 g sodium dodecyl sulfate (SDS) in 5 mL 0.2 M sodium acetate stock buffer (pH 4.5), then brought to 50 mL with iron-free double distilled water (ddH_2O). Reagent B was prepared by adding 30 g ascorbic acid and 1 g sodium metabisulfite to 50 mL 0.2 M acetate stock buffer, then brought to 500 mL with ddH_2O (chelating resin added then removed immediately). The ferrozine reagent consisted of 0.4 g ferrozine and 2.5 g thiourea brought to 100 mL with iron-free ddH_2O. Gey's solution for BMT (Dr. Marie Trudel, unpublished protocol) was prepared as 8.3 g NH_4Cl, 1 g $KHCO_3$, and 1 mL phenol red in 1 L ddH_2O; this was filtered through a 0.22 micron membrane, the pH adjusted to 7.2, and the final solution kept at 4°C. Chelators: DFO was obtained from Novartis (Dorval, Quebec), L1 was a gift from Dr. Robert W.

Grady (Medical College of Cornell University, New York, NY), and PIH and *o*-108 were synthesized in our laboratory as previously described (141). A 100% tribromoethanol (Avertin) stock solution was prepared by combining 10 g tribromoethanol with 10 mL tert-amylalcohol, then diluting to 2.5% in warm PBS just before injecting as either 0.017 mL/mg animal body weight (anaesthetic) or 1 mL/animal (lethal dose).

2.1.2. Instruments

Mass spectrometry was performed by Dr. Andrea Romeo, Concordia Chemistry Department (Montreal, Quebec), using a Finnigan SSQ7000 single quadrupole electrospray ionization (ESI) mass spectrometer (Finnigan, Bremen, Germany). Spectrophotometric assays were conducted using a CARY 13E spectrophotometer (Varian, Australia). Fresh mouse blood samples were shipped to ClinTrials BioResearch Ltd. (CTBR, Senneville, Quebec) for hematological analysis using an Advia 120 automated analyzer. FACS was performed using an EPICS XL-MCL flow cytometry system, Beckman-Coulter Ltd. (Mississauga, Ontario). Fixed mouse tissue sections underwent routine histological processing followed by staining with Perls' Prussian blue for the detection of tissue iron according to standard methods (142). Staining was performed at the IRCM (140), by histologist Annie Vallée.

2.2. Animals

Four- to five-month-old male and female C57BL/6J^{GPI-1a} and C57BL/6J^{GPI-1b} controls, as well as β-globin knockout mice (Hbb^{tm1Tow}/Hbb^s) hemizygous for the deletion of murine β-major and β-minor globin genes, were used in these studies. The congenic C57BL/6J^{GPI-1a} and C57BL/6J^{GPI-1b} mice were obtained from Jackson Laboratories (Bar

Harbor, ME) and mice were used as controls. The hemizygous β-knockout mice (Hbb^{tm1Tow}/Hbb^s), referred to simply as β-thalassemic, were originally obtained from Dr. T. Townes (136) and since backcrossed for > 16 generations to C57BL/6J^{GPI-1b} inbred animals to preclude genetic variability between backgrounds. β-thalassemic mice were identified following PCR amplification and characterized as having intermediate to severe β-thalassemia as previously described (143). All animals were generously provided by Dr. Marie Trudel (140), and were maintained in microisolator cages.

2.3. Methods

In Vitro

2.3.1. Preparation of Model β-Thalassemic Erythrocytes

2.3.1.1. Purification of α-Hemoglobin Chains

Pure α-globin subunits were isolated from whole blood as previously described (144-146), and as summarized briefly below:

Preparation of RBC Hemolysate:

40 mL of blood was collected in heparinized tubes from a healthy volunteer and centrifuged at 1000 g for 5 minutes (min). The plasma was aspirated and red blood cells were washed three times with PBS. The cells were then lysed by adding 1 volume of ddH$_2$O and freeze-thawing three times in acetone/dry ice. The hemolysate was centrifuged at 15,000 g for 30 min then exposed to CO at 4°C for 1 min while mixing.

Dialysis of RBC Hemolysate:

The CO-treated hemoglobin was dialyzed against 2 L ddH$_2$O for 4 hours (h) after which the protein content of the concentrated Hb was measured. KH$_2$PO$_4$ and NaCl were then added to a final concentration of 10 mM and 80 mM, respectively.

PMB Treatment of $\alpha_2\beta_2$-Hb:

The amount of PMB was calculated so as to be in 10 M excess of the heme concentration present in the hemolysate. The PMB was dissolved in 0.5 mL ddH$_2$O by adding 2 drops of 1 M NaOH then 2-3 drops of 1 M acetic acid until the precipitate just redissolved. The PMB was added to the CO-Hb, the pH adjusted to 6.0 with 1 M acetic acid, and the solution left at 4°C overnight.

Separation of α- and β-PMB Chains:

The hemolysate was centrifuged at 1000 g for 5 min, reserving and CO-treating the supernatant as previously described. To isolate the α- from the β-chains, PMB-Hb was passed through a coarse G-25 Sephadex column equilibrated with 10 mM KPO$_4$ buffer (pH 8.15), and the elution volume concentrated to 20 mL. The concentrate was passed through a Whatman DE52 column equilibrated with 10 mM KPO$_4$ buffer (pH 8.15). The α-PMB chains, which eluted first, were collected and exposed to CO.

Regeneration of Purified α-Chain -SH Groups:

The α-PMB chains were adjusted to pH 6.5 with 10 mM KH$_2$PO$_4$ and loaded onto a 4 cm CM23 column equilibrated with 10 mM KPO$_4$ (pH 6.5). The α-PMB chains were mobilized onto the column as a single band and were concentrated through this process. The column was washed for 15 min with 10 mM KPO$_4$ (pH 6.5) first containing, then

devoid of 15 mM β-mercaptoethanol. The α-SH chains were finally eluted with 20 mM Tris-HCl (pH 8.0) then CO-treated, pelleted in liquid nitrogen, and stored at -80°C until use.

2.3.1.2. Protein Concentration of Purified α-Chains

The final protein concentration of the α-hemoglobin was evaluated using the Bradford protein assay (147). Briefly, a dye reagent (BioRad) was diluted 1:4 with ddH$_2$O and the protein solution added in a 1:500 volume ratio. Samples were incubated for 5 min at room temperature and read in triplicate at 595 nm. Absorbance units (AU) were recorded and divided by 0.13 (this number corresponds to the extinction coefficient obtained from the standard curve using BSA, and corrects for dilution), to yield results in μg protein/μL.

2.3.1.3. α-Chain Purity

The α-hemoglobin was analyzed by electrospray ionization-mass spectrometry (ESI-MS) in order to confirm a molecular mass equivalent to previously established values. Fresh α-globin chain samples were diluted 1:150 with ddH$_2$O and analyzed according to standard technique (148).

2.3.1.4. Hemoglobin Oxidation

To ensure the hemoglobin subunits were not oxidatively damaged during the purification process, a well-established spectrophotometric assay (149-151) was used to assess the relative concentrations of intact (oxy), oxidized (met), and denatured (hemichrome) hemoglobin present in the α-hemoglobin-derived lysate. The α-chains were diluted 1:100 with ddH$_2$O, the hemolysate scanned, and absorbance values recorded at 560, 576, 630, and 700 nm. The α-subunits were then incubated overnight at 25°C and the

spectrum re-recorded to examine changes in methemoglobin generation over time. It should be noted that the response of functional hemoglobin subunits to oxidation is firstly, the formation of metHb, followed eventually by that of readily precipitating hemichromes, the latter being a prime determinant of anemia severity (31). The calculations, based on the method of Winterbourn *et al.* (151), are as follows:

Using mM extinction coefficients:

oxyhemoglobin (mM) = $29.8(OD_{576} - OD_{700}) - 9.8(OD_{630} - OD_{700}) - 22.2(OD_{560} - OD_{700})$

methemoglobin (mM) = $7(OD_{576} - OD_{700}) + 76.8(OD_{630} - OD_{700}) - 13.8(OD_{560} - OD_{700})$

hemichrome (mM)* = $33.2(OD_{576} - OD_{700}) - 36(OD_{630} - OD_{700}) - 58.2(OD_{560} - OD_{700})$

* When no hemichrome was present, the concentrations of oxyHb and metHb were added and their sum considered as total hemoglobin (100%). Each was divided by total Hb concentration and multiplied by 100 to determine their relative proportions, expressed as a percentage. The change in metHb generation over time (Δ % metHb), when required, was determined by the percent $metHb(t_{final})$ – percent $metHb(t_{initial})$.

2.3.1.5. Osmotic Lysis and Resealing

Loading erythrocytes with the purified α-chains was performed according to the method of Scott *et al.* (152, 153). Briefly, blood was collected from healthy human volunteers in heparinized tubes. The samples were centrifuged and the plasma and buffy coat aspirated. Packed erythrocytes were washed three times in PBS (pH 7.4) and the following RBC populations were prepared: 1) control normal, 2) control-resealed, and 3) α-chain loaded. A 250 μL aliquot of washed pRBC was reserved as the first control. A mixture of 500 μL pRBC and 275 μL PBS (no α-chains) constituted the second control,

undergoing osmotic lysis and resealing in the absence of α-chains to exclude any adverse effects due to the procedure itself. Finally, 500 μL pRBC were admixed with 250 μL α-chains (33.75 mg) and 25 μL 10X PBS to eventually comprise the model β-thalassemic cell population. After thorough mixing of cells and added solutions, samples 2) and 3) were dialyzed against 1 L of ice cold 5 mM KPO_4 lysis buffer (pH 7.4) for 45 min at 4°C with constant stirring. The membranes were then transferred to 1 L of warm 5 mM KPO_4 resealing buffer (pH 7.4) and dialyzed for another 45 min at 37°C with stirring. All samples, including reserved controls, were then transferred to centrifuge tubes and washed 7 times with PBS. Washed control, resealed, and α-chain loaded pRBC were resuspended to 5% hematocrit in HBSS supplemented with 5 mM glucose and containing 100 U penicillin/mL and 100 μg streptomycin/mL. Samples were then incubated at 37°C with gentle shaking and aliquots removed at 0, 1, 3, 5 and 20 h to determine levels of hemoglobin oxidation. Samples recovered after 20 h were used to determine erythrocyte membrane-bound non-heme iron.

2.3.1.6. Determination of Universal Loading

Previous studies have calculated the efficiency of encapsulation, proportional to the mean intraerythrocytic α-chain concentration, using α-chains radiolabeled with [^{3}H]-NEM. This value has repeatedly been shown to correspond to 3-5% of the total RBC hemoglobin when resealing 10 mg α-chains/mL packed cells (51, 130, 154). An alternative test examines whether loading is universal or not, that is, whether a high enough proportion of cells incorporates exogenous material. The "universality" of loading can be determined by co-entrapment of a fluorescent dextran (FITC-Dex) of

similar molecular weight (MW) to α-chains. Since incorporation of the fluorescent marker parallels that of exogenous chains, cells exhibiting fluorescence should likewise contain the subunits. Using this technique, other laboratories found more than 95% of resealed cells to effectively incorporate α-chains (51, 130). To confirm this value in our studies, we loaded RBC with α-chains as above (2.3.1.5.) in the presence or absence of 5 mg FITC-Dex/mL pRBC. The percentage of cells exhibiting fluorescence, and thus containing FITC-Dex along with α-chains, was then determined using FACS.

2.3.2. Characterization of Model β-Thalassemic Erythrocytes and *In Vitro* Evaluation of Iron Chelators

Once the α-chains had been purified and their encapsulation into RBC verified, we characterized the model β-thalassemic cells and assessed potential chelator-mediated benefits therein. We therefore repeated the cell preparation procedure as above, this time treating samples of α-chain loaded cells with the selected iron chelators. After the 20 h incubation, control, control-resealed, and model β-thalassemic RBC (untreated or chelator-treated) were characterized in terms of: 1) membrane-associated non-heme iron, and 2) hemoglobin oxidation (metHb generation). These parameters reflect the importance of intraerythrocytic iron in disease pathophysiology, and represent two of the most prominent features of β-thalassemic cells.

2.3.2.1. Iron Chelator Solutions

Stock solutions of 5 mM chelator were prepared in ddH$_2$O (DFO and L1) or 1 M NaOH (PIH and *o*-108, subsequently neutralized through the addition of 1 M HCl), and

dissolved in HBSS to a final concentration of 50 μM. This is within the lower range of concentrations routinely used to test iron chelators *in vitro* (50-1000 μM) (119-121), and has been reported as the minimum concentration required to achieve maximal iron release using radioiron-labeled reticulocytes (155).

2.3.2.2. Incubation Conditions

The process of osmotic lysis and resealing was repeated as above (2.3.1.5.), preparing a larger volume of α-chain loaded cells to be distributed among four iron chelator treatment groups. Thus, 2.5 mL pRBC were admixed with 1.25 mL α-chains (168.75 mg) dissolved in 125 μL 10X PBS. Samples were dialyzed against lysis and resealing buffers, and washed with PBS. An aliquot of α-chain loaded cells was reserved (untreated) and the remainder divided into four chelator treatment groups. Washed erythrocytes were suspended at 5% hematocrit in HBSS or HBSS/chelator solution and incubated for 20 h at 37°C with gentle shaking.

2.3.2.3. Membrane-Associated Non-Heme Iron

Measuring non-heme iron adherent to the RBC membrane was an important objective in the evaluation of selected iron chelators, as any subsequent chelator action should be related to their ability to strip this pathological iron from the membrane milieu. Non-heme iron present in RBC membranes was quantified by: 1) preparing ghost RBC membranes, then 2) using an iron-binding reagent to determine the exact concentration of iron in ghost samples. All buffers and solutions used were rendered iron-free by pre-treatment with chelating resin, Chelex (2.1.1.).

2.3.2.3.1. Ghost RBC Preparation

In order to quantify strictly the iron that was membrane-associated, RBC were lysed, their cytosolic contents expelled, and the resultant "ghost" membranes washed exhaustively until no further hemoglobin could be removed; this was done according to the method of Dodge *et al.* (156, 157). Briefly, after 20 h of incubation, RBC samples were washed 3 times in PBS. Aliquots (0.5 mL) of pRBC were each lysed in 45 mL ice cold lysis buffer A and centrifuged at 13,000 rpm for 15 min at 4°C. Supernatants were aspirated and pellets resuspended by drawing and expelling them five times through a 1 mL syringe fit with a 22-gauge needle, ensuring thorough break-up of ghosts and freeing any hemoglobin embedded within membranes. Exhaustive washing continued until control ghosts were milky-white (a total of 5 washes). Membranes were then washed twice in lysis buffer B, and finally stored at 50% hematocrit in buffer B at -80 °C until use.

2.3.2.3.2. Ferrozine assay

Free, non-heme iron associated with ghost membranes was quantified by convention of its reaction with the compound, ferrozine, within two minutes of its addition; a standard method known as the ferrozine assay (157). When the ferrozine chromophore binds ferrous iron, a rich magenta complex is formed whose depth of colouration is proportional to the concentration of iron in the sample. Ghost membranes, prepared as above, were resuspended in 5 mM sodium phosphate buffer (pH 7.2) to 1 mg/mL. Three cuvettes were prepared for each sample: buffer blank (100 µL buffer), ghost blank (100 µL iron-free control ghosts), and sample of interest (100 µL ghost sample). The first accounts for the colour produced by the buffer itself, the second reports the absorbance of ghosts in absence of ferrozine, and the last is the colour produced by the

ghosts of interest from the reaction with ferrozine. The first two served as controls and were eventually subtracted from the sample of interest. SDS (275 µL of 10%), reagent A (100 µL), and just before reading, reagent B (725 µL), were added to each sample. Finally, 100 µL ferrozine reagent was quickly added (except to ghost blank) and the sample was read over 2 min at 562 nm. For the ghost blank, 100 µL phosphate buffer was added instead of ferrozine in this final step. Calculations used to determine levels of membrane non-heme iron were based on a protocol by Dr. Mark Scott (146).

Calculations:

[OD ghost sample of interest - (OD buffer blank + OD ghost blank)] X 465.9/ 1mg/mL
= nmoles non-heme iron/mg

In this equation:

- OD (optical density) denotes absorbance values ranging from 0 to 1.0

- OD of buffer blank and ghost blank are subtracted from OD of ghost sample of interest, yielding the absorbance due exclusively to membrane-bound iron

- value 465.9 represents the molar extinction coefficient of the iron-ferrozine complex after correcting for dilution; standard value = 28,000 liters mol^{-1} cm^{-1} (158)

- 1 mg/mL is the protein concentration in each sample

- final results are expressed as nanomoles of non-heme iron per milligram of membrane protein

2.3.2.4. Hemoglobin Oxidation Assay

Levels of methemoglobin were measured as an index of total cellular oxidative stress, expected to be elevated in model β-thalassemic RBC due to iron-catalyzed oxidation of membrane components, and potentially decreased in chelator-treated cells due to removal of that iron. During cell incubation, aliquots were removed at 0, 1, 3, 5, and 20 h,

centrifuged, and packed erythrocytes diluted 1:500 with ddH₂O. Using the described method (2.3.1.4.), RBC lysates were analyzed for their respective concentrations of oxyhemoglobin and its oxidized form, methemoglobin.

In Vivo

2.3.3. Generation of Mouse Models of β-Thalassemia

2.3.3.1. Bone Marrow Transplantation

Several mouse models of β-thalassemia exist (132-138, 159, 160), arising either through spontaneous mutations or more commonly, targeted deletions of the β-globin gene locus. The mice used in this study are hemizygous for the deletion of murine β-major and β-minor globin genes, and are characterized as having intermediate to severe β-thalassemia. However, due to their phenotype and poor breeding efficiency, only a limited number are available at any one time. Thus, in order to have a population large enough to form meaningful treatment groups, murine thalassemic bone marrow was transplanted into a substantial number of control mice. Two β-thalassemic adult donor mice were thus sacrificed, and both hind and forelimbs were dissected and thoroughly cleaned. Using a 3 mL syringe and 26$^{1/2}$-gauge needle, BM cells were harvested by perforating and flushing bones with IMDM containing 5% serum. Cells were centrifuged at 1200 rpm for 5 min at 4°C, the supernatant aspirated, and Gey's solution (2.1.1.) added to lyse the RBC. Lysis was stopped after 3 min with 3 mL IMDM containing 5% serum. The cells were centrifuged again, the supernatant aspirated, and the pellet resuspended in 2 mL serum-free IMDM. Cells were counted using the trypan blue exclusion method and resuspended in serum-free IMDM in preparation for transfer.

Twenty-eight C57BL/6J$^{\text{GPI-1a}}$ mice were lethally irradiated at 152 rads/minute for a total of 875 rads (cGy), and following a 4 h recovery period, injected intravenously (tail vein) with 1.8 million BM cells in 350 µL volume. The chimeric mice were monitored for hematopoietic engraftment at 4, 7, and 10 wk post-transplant before commencing the iron chelator regimen on wk 12.

2.3.3.2. Monitoring Engraftment: Glucose Phosphate Isomerase Assay

The two murine electrophoretic isoforms of the enzyme, glucose phosphate isomerase-1, can be separated by their different migration rates on cellulose acetate membranes using standard Gpi-phenotyping methods (161, 162). Recipient and donor mice expressing alternate forms of the enzyme, Gpi-1a and Gpi-1b, respectively, were thus used in this study. Peripheral blood of transplanted mice was analyzed at the protein level to determine the proportion of endogenous RBC remaining, and the proportion contributed by the donor (Gpi-1b) at different stages following BMT. As per standard protocol from Dr. Marie Trudel (unpublished), cellulose acetate membranes were soaked 60 min in Gpi running buffer (3.0 g trizma, 14.4 g glycine in 1 L ddH$_2$O, pH 8.7). Approximately 50 µL tail vein blood was collected into heparinized hematocrit tubes and centrifuged for 3 min at 13,000 rpm. The pRBC contained within 0.5 cm of tube were lysed in 125 µL ddH$_2$O and 8 µL of this, transferred onto the membranes. Samples migrated from cathode to anode for 60 min at 200 Volts. Gpi-1 bands were then revealed using an enzymatic colorimetric reaction based on the Gpi-1-mediated conversion of fructose-6-phosphate to glucose-6-phosphate, which, in the presence of NADP and glucose-6-phosphate dehydrogenase, drives the reaction toward the formation of product, NADPH.

When NADPH reacts with MTT in the presence of PMS, the latter is reduced, yielding the intensely purple-coloured product, formazon. Briefly, therefore, a 2% agar preparation was heated to 55°C and maintained at that temperature until use. A first reagent was made, consisting of 2 mL of 0.2 M Tris-HCl (pH 8.0), 120 μL of 0.2 M MgCl$_2$, 150 μL of 100 mg/mL fructose-6-phosphate, and 120 μL of 10 mg/mL MTT. Just before the end of migration, a second reagent was made (120 μL of 10 mg/mL NADP, 120 μL of 2.4 mg/mL PMS, and 4 μL of glucose-6-phosphate dehydrogenase), and added to the first. The migration was stopped and the membrane blotted dry. Finally, 2 mL of the hot agar was added to the above admixed solutions (total volume ~4.5 mL) and, using a 3 mL syringe, distributed evenly over the membrane, brightly staining Gpi-1 bands. Once control bands appeared sharp, membranes were fixed in 5% acetic acid to stop the staining. The intensity of the signal was then quantified by Image Quant software.

2.3.4. Preparation of Chelator Solutions for *In Vivo* Testing

The osmotic pumps used for drug delivery in this study were designed to dispense 1 μL solution/hour, and contained a reservoir which could be filled to a maximum of 168 μL ± a built-in margin of error of a few μL (163). The total volume of 168 μL reflects the constant delivery of 1 μL solution/hour X 24 hours/day X 7 days total. In order to achieve administration of 50 mg/kg/day, chelator stock solutions of DFO, L1, PIH, and o-108 were prepared by dissolving 92 mg of each into 2 mL of 25-30% NaOH/PBS (1M NaOH diluted to 0.25-0.3 M with PBS), depending on their solubilities. This concentration would be considered conservative and highly non-toxic, as

47

pharmacological doses routinely administered to humans range between 30-100

mg/kg/day (89, 99, 111) and those to animals, between 100-500 mg/kg/day (96, 97).

Doses were adjusted to weight by varying the chelator concentration inside the pump, and

solutions sterilize-filtered before filling the pumps to capacity. Pumps containing a

vehicle solution of 25% NaOH in PBS were also prepared as controls.

2.3.5. Osmotic Pump Implantation

After filling osmotic pumps, animals were anaesthetized with avertin and the pumps

implanted into their backs subcutaneously as per manufacturer's directions (163).

Briefly, a small incision was made in the skin between the scapulae. A hemostat was

used to spread apart the connective tissue, creating a small pocket. The pump was

inserted into the pocket with flow moderator end (end from which solution is dispensed),

pointing towards the animal's posterior, and sterile suture clips then used to seal the

wound. New pumps containing fresh chelator solutions were implanted to replace the old

ones every 7 days for a total of 4 procedures.

2.3.6. Characterization of Murine β-Thalassemic Erythrocytes and *In Vivo* Evaluation of Iron Chelators: Erythrocyte and Precursor Pathology

In addition to the tests described below, mice were monitored daily throughout the course

of treatment for signs of chelator toxicity and/or morbidity, including: lack of grooming,

changes in appearance of coat, inability to eat or drink, 20% weight loss/gain, and

behavioural abnormalities.

2.3.6.1. Membrane-Associated Non-Heme Iron

Following 4 weeks of iron chelator treatment, mice were sacrificed and total blood volumes collected. RBC ghost membranes were prepared exactly as above (2.3.2.3.1.), and the non-heme, non-ferritin iron reacting within 2 min in the presence of ferrozine was assessed as described (2.3.2.3.2.). This test served to determine, *in vivo*, the effectiveness of iron chelators in mobilizing RBC membrane-bound iron from actual murine thalassemic cells.

2.3.6.2. Hemoglobin Oxidation Assay

Spectrophotometric evaluation of oxidized and reduced components of mouse hemoglobin was conducted as above (2.3.2.4.) prior to, and following the chelation regime. Methemoglobin generation was initially examined at 10 wk post-transplant by withdrawing a small amount of blood (~150 μL) via tail snip. Final levels were taken within 24 h of sacrificing the animals. As before, this assay would indicate the potential of iron chelators to, as a function of their iron-binding capacity, attenuate oxidative stress in thalassemic erythrocytes *in vivo*.

2.3.6.3. Hematological Parameters

Fresh blood samples, collected immediately into EDTA-coated microtubes following each animal's sacrifice, were shipped to CTBR for complete hematological analysis (2.1.2.). Erythrocyte and reticulocyte parameters were established using flow cytometry-based measurements obtained on an Advia 120 automated blood cell analyzer. The mouse archetype of multi-species software version 2.2.06 was used in analysis (Bayer Diagnostics, Tarrytown, NY). Hematocrits (Hct) were measured manually, and mean

cellular volume (MCV) and red cell Hb concentration were determined using two (low- and high-angle) light scatter measurements. From the measured Hct and Hb concentration, the mean cell hemoglobin concentration (MCHC) was derived (164). Reticulocyte counts were determined using the RNA-staining dye, oxazine 750, and expressed as a percentage of total red cells. Sub-populations of reticulocytes were quantified based on their levels of maturation, designated as follows: 1) L RETIC (low staining-intensity, most mature), 2) M RETIC (medium staining-intensity, intermediate maturation), and 3) H RETIC (high staining-intensity, most immature). The relative proportions of these groups provided information regarding the effectiveness of erythropoiesis, and correspondingly, the severity of the disease, since thalassemia is characterized by fewer mature reticulocytes and abnormally high numbers of immature ones. Reticulocyte mean cell volume (MCVr), an indicator of hydration status specific to reticulocytes, was also measured using the reticulocyte channel of the analyzer.

2.3.6.4. Erythrocyte Survival

Labeling RBC *in vivo* using the compound biotin, is a safe and useful alternative to radiolabeling for the determination of erythrocyte survival. Biotin-labeled cells are discriminated from newly-produced, unlabeled ones, using the fluorescent conjugate FITC-Avidin. FITC-Avidin specifically binds biotin, causing labeled cells to fluoresce, allowing them to be quantified by FACS analysis. This technique was used to track RBC lifespan in the various mouse populations (165), and is briefly summarized here.

2.3.6.4.1. *In Vivo* Biotinylation of Erythrocytes

A biotin solution of 1.2 mg biotin dissolved in 45.6 µL N, N,-Dimethylformamide, then added to 300 µL PBS, was prepared for each mouse. All mice (except for reserved non-biotinylated controls) received tail vein injections of 280 µL biotin/mouse/day for three consecutive days. Twenty-four hours following the final injection was regarded as the 100% labeling point, and the first day of FACS analysis.

2.3.6.4.2. FITC-Avidin Incubation

Tail vein blood (2-3 µL) was collected on days 1, 3, 4, 5, 6, then on alternate days for a total of 21 days. 2 µL blood was measured out from each heparinized capillary tube and admixed with 4 mL PBS. 1 mL of this was reserved as FITC-negative control while another 1 mL was transferred into an Eppendorf tube and incubated with 10 µL FITC-Avidin for 30 min at 4°C. All samples were centrifuged at 2500 rpm for 10 min at 4°C, after which the supernatant was aspirated and the small RBC pellet resuspended in fresh PBS and washed twice. The final pellet was resuspended in 1000 µL PBS, and all samples then analyzed by flow cytometry. Controls included non-biotinylated RBC as well as FITC-negative and FITC-positive biotin-labeled ones. All steps involving FITC-Avidin were performed in the dark to prevent fluorescence quenching by direct exposure to light.

2.3.6.4.3. Flow Cytometry

Flow cytometry was used to distinguish the fluorescently labeled cell population from the unlabeled one. The fate of labeled cells was monitored by the progressive decay of fluorescence over the course of their destruction. Gates were first set to exclude the

analysis of aggregated cells or non-cellular debris. Then, background fluorescence of untreated (non-biotinylated) FITC-incubated syngeneic erythrocytes was counted and new gates set to exclude inherent cellular fluorescence of control cells. Control histograms were generated through this process and subsequent histograms gated to account for the background. Erythrocytes were counted (10,000 cells/sample) and biotinylated cells expressed as a percentage of the total using FACScan software. To determine erythrocyte half-life, the percentage of biotinylated cells was first plotted against time. The day at which 50% of labeled cells remained in circulation was calculated from the linear equation derived from each plot using Sigma Plot scientific graphing software (Version 3.0), and established as the RBC $t_{1/2}$ for that animal.

2.3.7. Characterization of Murine β-Thalassemic Tissues and *In Vivo* Evaluation of Iron Chelators: Organ Pathology

2.3.7.1. Spleen/Body Weight Ratio

Animals were sacrificed by avertin injection and total body, liver, and spleen weights were determined. The spleen to body weight ratio (spleen/body weight), calculated as wet weight of the organ divided by total body weight, is a well-known indicator of disease severity (137). A high ratio reflects hyperactivity of the spleen during accelerated hemolysis, as the spleen constitutes the primary organ for destruction of damaged or senescent RBC in mice.

2.3.7.2. Liver Iron Content

To quantify the accumulation of non-heme iron in mouse liver, a major organ for iron storage in addition to spleen, a protocol was adapted from Pountney et al. (166). Livers were dissected and fresh sections were weighed and frozen at -80°C until the time of assay. Tissues were homogenized with 700 μL iron-free ddH$_2$O in a 1 mL glass homogenizer, then boiled in 20 μL 12 N HCl for 10 min after which 200 μL 50% trichloroacetic acid was added, and the samples cooled on ice for 15 min. Samples were finally centrifuged at 14,000 rpm for 15 min, and 40 μL 10 M NaOH added to supernatants (yielding a final pH of 4.5 in the medium). A ferrozine reagent was prepared (0.88 g ascorbate, 4.3 g sodium-acetate, and 98 mg ferrozine in 50 mL ddH$_2$O), and 500 μL added to each sample before reading the absorbance over 2 min at 562 nm. All solutions were rendered iron-free as above (2.3.2.3.). Final liver iron concentrations were expressed as nmoles/mg wet tissue.

2.3.7.3. Perls' Iron Staining in Liver and Spleen

A standard method used to demonstrate iron accumulation in tissues is the Perls' Prussian blue stain (142). The iron demonstrable by this assay must be in the ferric form, as most human and mouse tissue iron is. Whole spleens and liver lobes were fixed in formalin (10% formaldehyde in PBS) overnight with gentle shaking. The organs were then transferred to cassettes and kept in PBS at 4°C until the time of histological sample preparation (no more than one day). The organs were embedded in paraffin, sectioned, dehydrated in graded alcohol and stained with Prussian blue using a hematoxylin and eosin counterstain (137). Tissues were scored for blue-positive iron deposits at 20 X

magnification using a Zeiss Axiophot image analysis microscope. Five non-overlapping fields were systematically examined for each organ. Areas staining positive for iron were quantified by conversion to pixels, which were then expressed as a percentage of total surface area examined using Northern Eclipse software Version 6.0. The percentage values from all five fields assessed were averaged and considered as the total stainable iron in that particular organ.

Statistical Analysis

The probability of a statistically significant difference between the mean values of 2 data sets was determined using the unpaired Student t test or Mann-Whitney test (murine RBC membrane-associated iron).

3. Results

3.1. *In Vitro Studies*

Model β-thalassemic erythrocytes were an innovative design by Scott *et al.* that helped elucidate the sequence of events occurring during the development of the thalassemic phenotype in RBC (51, 153). In essence, model thalassemic erythrocytes are normal human red cells manipulated into a diseased state through the insertion of excess, heme-containing α-chains, and therefore, represent a readily available and unique tool in which the effects of therapeutic agents can be evaluated. Despite extensive characterization of these cells, however, the benefits of intraerythrocytic iron chelation therein have been minimally explored, with very few compounds having been tested to this end. These include DFO and its high molecular weight derivative, plasma tripeptide H-Gly-His-Lys-OH, and N,N-bis(2-hydroxybenzyl)ethylenediamine-N,N-diacetic acid, also known as HBED (146). Because some of the more potent iron chelators, including novel compounds that have since been designed, have never been investigated in this model, the full potential of intraerythrocytic iron chelation in thalassemic RBC is not truly known. Therefore, the prime objective *in vitro* was to examine iron chelator-mediated improvements in human thalassemic type cells using four diverse agents, two of which constitute the mainstay in treatment, and two comparatively new and promising oral candidates. The experiments involved, firstly, purifying and characterizing α-Hb subunits, then encapsulating them into normal erythrocytes. The model thalassemic cells were then confirmed as appropriate correlates of human disease and the iron chelators tested therein for their respective abilities to: 1) remove abnormal membrane-bound iron, and 2) curtail the oxidative destruction of hemoglobin; thereby probing two key features

of the disease. Importantly, because model β-thalassemic RBC were elaborated from human erythrocytes, they provided insight into the applicability of this strategy to *human* cells specifically. Furthermore, findings from the *in vitro* studies helped to validate and develop the ensuing animal studies.

3.1.1. Purification of α-Hemoglobin Chains

Once isolated, the α-chains were determined to have a protein concentration of 0.135 g/mL. This value was similar to those obtained in other laboratories using the same method (51, 154). In order to confirm the identity of the subunits, ESI-MS, a highly accurate technique for measuring protein molecular weights, was used. This type of mass spectrometry enables analysis of the different globin chain varieties and heme moieties of hemoglobin as separate entities, as well as any modified forms of either. As a reference, Fig. 5 A depicts the standard ESI mass spectra of normal human blood diluted 500-fold (148), while panel B shows the spectra obtained from α-chains purified in our laboratory (diluted 1:150). Both spectra consist of a characteristic peak at 15,126 Da, due to the contribution of α-globin protein (no heme), and a peak at 15,741 Da that represents the entire α-hemoglobin peptide (globin with attached heme). Both peaks obtained from isolated α-chains were consistent with the reference peaks and accepted mass values, authenticating the prepared subunits as pure α-hemoglobin monomers.

Furthermore, analysis of the subunits' initial oxidation state and time-dependent oxidative response helped establish their functional properties. An assay which proved indispensable in this regard, and which was used throughout the course of both *in vitro* and *in vivo* testing, was the spectrophotometric measurement of hemoglobin oxidation (2.3.1.4.). Fig. 6 depicts sequential scans of RBC hemolysate over a 20 h period at 37°C,

illustrating the range of Hb oxidation states from intact, 100% oxyHb (pronounced peaks, solid line) to oxidized 100% metHb (flattened peaks, broken line). When the α-globin isolated in our laboratory was scanned in the same way, the expected spectrum of oxyHb was observed at t = 0, confirming the chains had not been oxidized during purification (Fig. 7, solid line). Also, the spectrophotometric changes recorded in α-hemoglobin over time were consistent with a functional oxidative denaturation response, as the subunits yielded solely methemoglobin after a 20 h incubation at room temperature (Fig. 7, dotted line). Evidence of α-chain integrity was obtained by analyzing the subunits via the ferrozine assay (2.3.2.3.2.). This test confirmed the absence of non-heme iron in α-chain samples, suggesting that iron was appropriately sequestered within heme and, thus, supporting the intact condition of subunits following purification (data not shown). The characterization of isolated α-chains through a combination of ESI-MS and spectrophotometry, therefore, established not only the identity of the subunits, but also their purity and integrity. We consequently pursued their encapsulation into healthy human erythrocytes in order to generate model β-thalassemic cells.

3.1.2. Universal Loading of α-Chains

The preparation of reliable model β-thalassemic cells depends on the efficient loading of excess, heme-containing α-globin chains into normal human erythrocytes. To ensure incorporation of the purified subunits, RBC underwent regurgitation-resealing using α-chains in parallel with a comparably heavy fluorescent Dextran (FITC-Dex, 9,500 Da). After re-annealing and washing, the cells were analyzed for uptake of the fluorescent molecule using flow cytometry (2.3.1.6.). Fig. 8 first illustrates the background

fluorescence intensities of control (A) and control-resealed (B) cells in absence of FITC-Dex; an identical background pattern was observed for α-chain loaded cells (not shown). These control histograms were used to set "gates" excluding non-specific fluorescence from subsequent samples. Cells exhibiting relative fluorescence intensities greater than 1 (within region "D"), were considered to have incorporated FITC-Dex while values below 1 reflected typical low-level inherent cellular fluorescence. The fluorescence intensities of cells lysed and resealed in the presence of either 5 mg FITC-Dex/mL pRBC alone or FITC-Dex in suspension with α-subunits (13.5 mg α-chains/mL pRBC) are seen in panels C and D, respectively. When fluorescent RBC were expressed as a percentage of the total counted (5000 cells), more than 98.5% of red cells were found to have incorporated the extracellular material. Samples were prepared in triplicate and representative histograms for each condition are shown. The data obtained helped to establish the generation of truly α-globin-containing RBC in which the effects of iron chelators could then be investigated.

3.1.3. Characterization of Model β-Thalassemic Erythrocytes and *In Vitro* Evaluation of Iron Chelators

Since reversible osmotic lysis and resealing alone do not have any substantial effects on normal red cell behaviour (50, 51, 153, 154), changes observed in RBC loaded with purified α-hemoglobin must be due exclusively to the effects of the iron-containing hemoglobin subunits. The indices monitored during evaluation of iron chelators *in vitro* included erythrocyte membrane-associated iron, as well as extent of oxidative attack on cellular Hb, reflecting the central oxidative mechanisms involved in the development of thalassemia. Both parameters were examined in control and control-resealed

erythrocytes, as well as in α-chain loaded cells that were either untreated or chelator-treated.

3.1.3.1. Quantification of Membrane-Associated Non-Heme Iron

Model β-thalassemic erythrocytes were untreated or incubated with 50 μM of one of four iron chelators for 20 h at 37°C with gentle shaking. In order to measure the amount of non-heme iron embedded specifically within cell membranes, Hb-free ghost erythrocytes were prepared. This step was effected as above (2.3.2.3.1.), and the iron-binding chromophore, ferrozine, was used to spectrophotometrically quantify the concentration of non-heme ferrous iron in each sample.

In control and control-resealed cells, levels of non-heme iron were 0.37 and 0.47 nmoles/mg membrane protein, respectively, while α-chain loaded cells carried a burden equivalent to nearly 4.0 nmoles/mg membrane protein – approximately 10 times that of controls. Treatment of cells with iron chelators, however, significantly depleted cell membranes of this abnormal iron fraction: final values ranged from 0.85 to 1.05 nmoles/mg membrane protein, using DFO and *o*-108 respectively, representing ~4-5 times less iron than in untreated α-chain loaded cells. As Fig. 9 A illustrates, all iron chelators were effective in dislodging a significant amount of non-heme iron from the membranes of model β-thalassemic RBC ($p < 0.002$). The concentration of iron indicated for each sample represents the average of three independent experiments.

3.1.3.2. Hemoglobin Oxidation Assay

In β-thalassemia, unstable α-subunits are not only prone to *auto*xidation but act additionally, via the toxic iron they liberate, to destabilize normal hemoglobin and trigger *its* oxidation to metHb, further promoting iron release (64). Agents that even partially remove injurious iron at the root of this reaction would be expected to short-circuit the oxidative cascade and, consequently, limit the production of metHb. Because the level of methemoglobin mirrors the total oxidative injury incurred by cells, its concentration within RBC was monitored for chelator-mediated improvements throughout the 20 h incubation, as described (2.3.2.4.). The overall change in the concentration of metHb from 0 to 20 h is depicted in Fig. 9 B. Control and control-resealed cells exhibited increases of 1.9% and 4.4% metHb, respectively, while the increase in model β-thalassemic cells exceeded 30%, signalling considerable oxidative damage. When model cells were treated with iron chelators, metHb levels were reduced from untreated values by at least 50% ($p < 0.01$), and remarkably, approximated normal values in L1- and PIH-treated samples, suggesting maximal protection against Hb oxidation by those compounds. Without exception, though, iron chelators demonstrated a high level of efficiency in mitigating oxidative damage to model β-thalassemic erythrocytes, conceivably due to their iron removal properties.

The *in vitro* studies yielded encouraging results: the human model β-thalassemic erythrocytes that were prepared appropriately displayed the excessive membrane-associated iron and abnormally high metHb levels characteristic of the disease. All four of the iron chelators tested significantly improved these erythrocyte parameters, reducing membrane iron burden and providing relief from oxidative stress. Though they

accomplished this with relatively similar degrees of efficiency, DFO and PIH displayed a slight advantage in iron removal, while L1 and PIH did so in attenuating oxidation. Because model β-thalassemic erythrocytes mimicked the early stages of human thalassemia (likened to the first months of a patient's life), and because iron chelation achieved beneficial results in the absence of transfusion, this therapeutic strategy, applied clinically, would be expected to slow disease development and, perhaps, bypass transfusion altogether. Thus, insofar as human β-thalassemic erythrocytes are concerned, intraerythrocytic iron chelation appears to be a valid strategy to prevent damage caused by excess α-chains, if initiated at an early enough clinical stage.

Next, to determine the far-reaching effects of iron chelators in a physiological milieu, we evaluated the same compounds *in vivo*, using β-thalassemic mice with a disease severity comparable to β-thalassemia intermedia-to-major, in humans.

3.2. *In Vivo Studies*

In light of the benefits mediated by iron chelators *in vitro*, we hypothesized that through the same mechanism of binding intraerythrocytic iron and preventing consequent membrane damage, these compounds could extend the lifespan of model β-thalassemic RBC *in vivo*. We planned to transfuse labeled murine model thalassemic cells (murine RBC loaded with human α-chains) into control mice, then follow the survival of labeled thalassemic RBC in untreated and chelator-treated animals. To this end, murine blood was collected and red cells loaded with purified human α-chains as described above (2.3.1.5.), then biotin-labeled for tracking (2.3.6.4.1.), and injected into normal mouse recipients. Using flow cytometry to quantify the labeled population, it was found,

unexpectedly, that only a slight proportion of modified cells remained in circulation after injection. To clarify their precise fate, we labeled murine model β-thalassemic RBC with radioactive ^{59}Fe and counted the fractions of radioactivity in circulation, spleen, and liver following their injection (data not shown). The majority of α-chain loaded RBC, and even control-resealed cells, were cleared abnormally rapidly by the spleen of injected mice. This observation suggested that in the process of generating murine model β-thalassemic cells, perhaps some incompatibility due to the combination of lysis-resealing and biotin-labeling, or through immunogenic-related modifications (168), they became altered in such a way as to no longer be suitable for *in vivo* tracking. Thus, although human model β-thalassemic cells faithfully resembled their clinical counterparts in the nature and severity of α-globin-induced damage, more subtle alterations may have developed during the preparation and labeling of murine model β-thalassemic cells, limiting them for our purposes, to *in vitro* systems. We promptly shifted our methodology to a more physiologically meaningful model, namely, the β-thalassemic mouse.

3.2.1. Mouse Model of β-Thalassemia

Since the first description of a mouse model for β-thalassemia in the early 1980's, several different models have been generated and they are now widely accepted as suitable paradigms of human β-thalassemia (132-139). A shared feature of the biogenesis of disease in both species is the fundamental role played by excess α-chains and the related membrane defects (138). Unfortunately, however, the high level of heterogeneity amongst sick animals and their relative shortage due to poor breeding make the prospect

of studying β-thalassemic mice especially challenging. For the *in vivo* studies, therefore, we used a novel approach to overcome the limiting number of pathologic mice at our disposal. By performing a series of bone marrow transplantations, we attempted to transfer the hematological deficit from a small number of β-thalassemic mice to a sufficiently large number of healthy ones.

3.2.1.1. Donor Animals

Hemizygous β-globin knockout mice, the mouse model used in these studies, were identified following PCR amplification and were characterized via hematological analysis as having severe β-thalassemia (143). These mice exhibited dramatically decreased RBC counts, hemoglobin content, hematocrit, cell volume and cell hemoglobin concentration. They also displayed marked reticulocytosis and elevated red cell distribution widths, indicating abnormally high erythropoiesis and anisocytosis (cell heterogeneity), respectively. Two of these mice were selected from the original colony to act as BM cell donors. Because donor animals had already been thoroughly characterized (136, 143), and because the animals of interest were the transplanted recipients, developing features identical to those of the original colony (section 3.2.2.), all data presented will be from the transplanted mice.

3.2.1.2. Recipient Hematopoietic Reconstitution

Following BM transplants, the chimeric mice were monitored for hematopoietic engraftment at 4, 7, and 10 wk post-transplant by the cell marker, glucose phosphate isomerase-1. An assay combining electrophoretic and enzymatic techniques was used to reveal the relative proportions of blood cells derived from recipients and donors at

various stages of engraftment. To avoid redundancy, data from ten representative recipients are shown for each assay (Fig. 10). In all three membranes, the first two lanes indicate the positions of Gpi-1 isotypes "a" and "b" derived from C57BL/6J^{GPI-1a} (recipient) and C57BL/6J^{GPI-1b} (donor) mice, respectively. Lanes 1-10 reveal the Gpi-1 isotypes of ten transplanted animals. The first assay demonstrated the majority of recipient RBC to be of endogenous origin, as Gpi-1a was the principal form of the enzyme detected (Fig. 10, first membrane). After 7 wk however, over 50% of recipient RBC expressed Gpi-1b; these cells must have, therefore, been contributed by the donor (Fig. 10, second membrane). By 10 wk, 100% of recipient RBC expressed the donor-derived marker (Fig. 10, third membrane), confirming the switch to β-thalassemic RBC production, exclusively. These data, therefore, corroborated successful transfer of functional BM from the original β-thalassemic donors to recipients by demonstrating the production of donor-type pathological erythrocytes by these recipients.

While the Gpi test explicitly reported on the engraftment status, other indices monitored throughout the 10 wk period established engraftment indirectly by detailing the development of disease; these included hematocrit and metHb levels, which changed appropriately in the transplanted mice (data not shown). All subsequent data (see section 3.2.2.) clearly characterized these mice as having adopted a β-thalassemic phenotype, providing further evidence of hematopoietic reconstitution. Therefore, from this point, all transplanted animals were considered hemizygous β-thalassemic, just as the BM donors from the original colony.

3.2.1.3. Treatment Groups

Three control and three thalassemic mice received no treatment at all, while three more of each were implanted with 25% NaOH vehicle-containing pumps; this was done to ensure that neither pump implantation nor vehicle solution had any adverse effects. Each of the chelator treatment groups consisted of five β-thalassemic animals. Animals from each group were matched for weight, sex, and age. Below is a summary of the treatment groups:

Treatment Groups:

Control (C57BL/6J^{GPI-1b})		$n = 6$	β-Thalassemic (Hbb^{tm1Tow}/Hbb^{s})		$n = 26$
no treatment*	} untreated	$n = 3$	no treatment*	} untreated	$n = 3$
vehicle		$n = 3$	vehicle		$n = 3$
			DFO-treated		$n = 5$
			L1-treated		$n = 5$
			PIH-treated		$n = 5$
			o-108-treated		$n = 5$

* Because data from mice receiving no treatment and those receiving vehicle showed no statistical difference, they were combined to form a single group of $n = 6$, designated "untreated".

3.2.2. *In Vivo* Administration of Iron Chelators to β-Thalassemic Mice

The iron chelator regime began 12 wk post-transplant. Compounds were administered subcutaneously by osmotic pump (2.3.5.), a method that minimized animal handling. It also allowed for constant, stable delivery of a low drug concentration, thereby limiting potential toxicity and preserving the natural pharmacokinetics of the iron chelators.

Continuous delivery was especially useful in determining the effects of chelators with shorter half-lives, such as DFO (plasma $t_{1/2}$ = 5-10 min), which are not effective when given by bolus administration (103).

To ensure chelator composition did not change appreciably throughout the 7 days, spectrophotometric tests were conducted on days 1 and 7 of each implantation. Since variations in chelator solutions can be detected spectrophotometrically, we reserved aliquots of the same solutions administered *in vivo* and monitored them *ex vivo* immediately after implantation and again after 7 days incubation at 37°C (mimicking the state *in vivo*). As anticipated, the chelators showed no significant changes in their structure over this time period (data not shown). Also, to confirm that the iron chelators were being dispensed accurately, all residual solutions were aspirated and quantified upon pump removal. Again, the built-in margin of excess designed for the pumps was respected, and no major discrepancies between actual drug volume delivered and the theoretical quantity defined by the manufacturer, were observed. Finally, mice were carefully monitored on a daily basis and exhibited no changes in weight or behaviour that may signal chelator toxicity or related morbidity.

3.2.2.1. Quantification of Membrane-Associated Non-Heme Iron

To ensure the reported effects of chelators were in fact due to their iron chelating properties, it was critical to evaluate chelator-induced changes in RBC membrane iron. Animals were sacrificed upon termination of the RBC survival assay (after 4 wk chelator-treatment) to provide total blood volumes required for these tests. The results described below are summarized in Table 2.

Erythrocyte ghost membranes derived from β-thalassemic mice harboured extensive iron deposits compared to non-detectable levels in controls ($p < 0.001$), marking a fundamental feature of the disease and supporting the validity of the transplantation method. After 4 wk, L1 and PIH diminished membrane-bound iron by 45% and 38%, respectively, relative to untreated ($p < 0.05$). Although iron mobilization did not reach a similar degree of significance with the other compounds, all of them reduced RBC iron by at least 30%, as demonstrated by the ferrozine assay (2.3.2.3.2.). Because all chelators successfully mobilized iron from β-thalassemic RBC membranes, we could rationalize any further effects as being, very likely, due to this defining property.

3.2.2.2. Hemoglobin Oxidation Assay

Just as the iron chelators were tested for their ability to attenuate hemoglobin oxidation in model β-thalassemic RBC *in vitro*, the same was investigated in thalassemic mice *in vivo*. Initial methemoglobin levels determined prior to treatment with iron chelators were compared with values obtained following the 4-wk treatment regime. As depicted in Fig. 11, RBC from control mice generated extremely low levels of metHb at the study's onset; these levels increased only slightly (3%) by the end of the study. Murine β-thalassemic RBC, in contrast, displayed endogenously high levels of metHb initially, ~25-fold in excess of controls, and experienced a greater increase in the percentage of metHb over the 4 weeks. Finally, though untreated and chelator-treated thalassemic cohorts displayed similarly high metHb values *initially*, the chelator-treated animals were found to generate significantly less metHb than untreated cohorts by the study's end (Fig. 11). The most dramatic positive effect was exerted by PIH, which decreased metHb by 4%, followed by

DFO, L1, and *o*-108. All observed differences were statistically significant (p < 0.03). This data suggested that by removing adventitious membrane iron, iron chelators not only limited the extent of hemoglobin oxidation, but also, likely conferred the same protection to other proteins, thereby diminishing total oxidative impact to cells.

3.2.2.3. Hematological Parameters

After 4 weeks of receiving iron chelators, total mouse blood volumes were collected and samples immediately sent for hematological analysis. Hematocrit, mean cell volume, mean cell Hb concentration, and reticulocyte counts were averaged for each treatment group and compared; these results are summarized in Table 3. Untreated β-thalassemic mice displayed hematological abnormalities consistent with the disease: reduced hematocrit (50%) and mean cell volume (~20%) were indicative of profound anemia and cell dehydration, respectively, while an abnormally high reticulocyte count (10-fold) was reflective of stimulated erythropoiesis. All values in β-thalassemic mice differed significantly from controls (p < 0.001).

Iron chelators improved hematological parameters in β-thalassemic mice with varying degrees of significance. Chelator-treated mice had modestly corrected hematocrits and saw even more meaningful changes in MCV and MCHC. Cell volume was increased by all iron chelators, most significantly by DFO (p < 0.05), while MCHC, an index of cell volume, was significantly improved by all compounds (p < 0.05). Partially normalized values of MCV and MCHC were indicative of chelator-mediated protection against the hallmark cellular dehydration of β-thalassemia. This effect was likely achieved by attenuating oxidative damage to the membrane transport proteins involved in regulating cell volume, demonstrating substantial benefits of iron removal on

both membrane structure *and* function. Iron chelators also significantly reduced the abnormally high number of reticulocytes present in peripheral blood of untreated mice; DFO and PIH had the highest impact, decreasing levels by ~20% and 45% respectively ($p < 0.05$).

Reticulocyte parameters, distinct from those obtained in mature red cells, have the unique potential to convey information pertaining to the earlier stages of erythroid development. In addition to erythrocytes, therefore, reticulocytes were also examined for signs of chelator-mediated improvements. Reticulocytes were first classified into sub-populations based on their level of maturation. As a convention, categories designated L, M, and H reflect low, intermediate, and high RNA staining-intensity, respectively; denoting decreasing levels of maturity. In normal mice, the vast majority of reticulocytes were from the mature sub-population, displaying the least RNA staining (Table 3). Proportions were skewed towards immature cells in untreated β-thalassemics however, with over 50% of cells demonstrating high RNA staining. A significant shift back towards normal proportions occurred in chelator-treated animals, where the majority of reticulocytes were in mature and intermediate populations ($p < 0.05$, DFO and PIH). Finally, although not statistically significant, a trend toward enhanced mean cell volume in reticulocytes from chelator-treated mice was also observed (Table 3). Collectively, the reticulocyte data supported beneficial effects of iron chelators not only in mature cells but even earlier, within their precursors, explaining, in part, their high therapeutic activity *in vivo* thus far.

3.2.2.4. Erythrocyte Survival

One week was allowed for the effects of the chelators to develop before commencing RBC survival studies at 13 wk post-transplant. Murine erythrocytes were then biotin-labeled *in vivo* and their survival monitored by FACS analysis. The turnover rate of labeled cells provided values of RBC half-life for each animal. Figure 12 reports the final average $t_{1/2}$'s for each treatment group. RBC half-life in control mice was 21.6 days, similar to values determined in other laboratories, establishing the validity of the assay and healthy status of control mice (165, 167). The cells of untreated β-thalassemic mice, by contrast, exhibited an appreciably shortened half-life of 12.6 days, nearly 50% lower than controls (p < 0.001). Remarkably, RBC of all chelator-treated thalassemic mice exhibited $t_{1/2}$'s intermediate between those of controls and those of untreated thalassemics. Animals receiving DFO had the longest-surviving RBC with $t_{1/2}$ of 15.8 days, followed by those treated with L1 ($t_{1/2}$ = 15.0), PIH ($t_{1/2}$ = 14.0), and finally, *o*-108 ($t_{1/2}$ = 13.9). Though approaching but not achieving statistical significance, likely due to variability within groups, these results suggested that even conservative doses of iron chelators improved membrane parameters substantially enough to slow RBC destruction. This observation is best illustrated by the representative RBC survival curves depicted in Fig. 12. Iron chelators attenuated red cell hemolysis in thalassemic animals, resulting in RBC survival curves closer to those of control animals. As will be discussed in section 4.4., this finding was perhaps the most pivotal in terms of the clinical potential and applicability of iron chelators. Evidence that these agents extended RBC lifespan in untransfused thalassemic mice by virtue of binding iron, firstly, highlighted iron's pathophysiological importance. Furthermore, it supported the hypothesis that removal of

this proximal iron compartment could put a brake on abnormal red cell clearance and consequently, disease progress. This is a promising finding for many thalassemic patients in whom (insofar as the results from mice can be extrapolated to humans) chelator administration at an early enough stage should prevent the need for transfusion altogether. Instead, a minimal and more convenient iron chelation regimen would form the basis of disease management, thereby avoiding secondary iron overload and improving patients' quality of life.

Examining the effects of intraerythrocytic iron chelation on RBC survival was a primary investigative objective. Because of the striking improvements observed in thalassemic erythrocytes and precursors *in vivo*, we postulated that iron chelators might likewise, have a beneficial effect in tissues. This question was addressed by measuring iron content and iron-mediated damage in liver and spleen tissues from untreated and chelator-treated β-thalassemic mice.

3.2.2.5. Assessment of Organ Pathology and Tissue Iron

All experiments conducted thus far have examined the effects of iron chelators within a framework of erythroid pathology. However, a defining feature of β-thalassemia is the accumulation of iron not only in erythrocytes, but also within such organs as the liver, spleen, heart, kidneys, and endocrine tissues. In order to assess which organ parameters were most dysfunctional in thalassemic mice, we performed an initial characterization study, comparing a small number of β-thalassemic animals ($n = 6$, original colony) to controls ($n = 3$). The livers, spleens, hearts, kidneys, and femurs of all nine animals were dissected and evaluated by gross and microscopic examination in terms of general appearance, weight and size. Organs were then prepared for histological analysis and the

distribution of iron was determined by the Perls' Prussian blue staining method (2.3.7.3.). The β-thalassemic mice exhibited massive splenomegaly relative to healthy littermates, while the size of other organs appeared normal. This is in contrast to human β-thalassemic patients, who not only display hypertrophy of the spleen but also typically, liver, kidney, bone marrow, and heart tissue. Humans can also store iron extensively in each of these organs, while β-thalassemic mice presented visible iron deposits only in liver and spleen. Similar findings were reported by other laboratories using different β-thalassemic mouse models (135, 137, 160), and helped confirm which organ parameters would best inform our studies.

Given the data from this small-scale characterization pilot, we planned, for the full-scale experiment, to examine the benefits of iron chelators in thalassemic tissues by specifically assessing: 1) spleen/body weight ratio, 2) non-heme iron content of liver, and 3) extent of Prussian blue iron staining in liver and spleen.

3.2.2.5.1. Spleen/Body Weight Ratio

Examining the weight of the spleen in the context of total body weight provides insight into the extent of splenomegaly, a product of the accelerated RBC clearance, extramedullary hematopoiesis, and iron storage central to murine β-thalassemia (143). Mouse spleens were dissected and weighed, then expressed as a percentage of total body weight. In this case, the improvements mediated by iron chelation were conservative. Still, a tendency towards reduced spleen/body weight ratio in the chelator-treated groups was observed. As presented in Table 4, the normal range for spleen/body weight ratio was between 0.2 and 0.3. In untreated β-thalassemic mice, this value increased nearly

6-fold, then fell slightly to ~5 to 5.5 times control values in chelator-treated mice. Though the decrease was subtle, the fact that a trend could be observed at all revealed how rapid and far-reaching the effects of the iron chelators could be. While reduction in spleen/body weight was encouraging to observe as an overall phenomenon, it did not provide mechanistic details regarding specific sites of chelator action or the aspects of splenic dysfunction being improved. Iron chelators may act directly at the level of the spleen, or may improve splenic function indirectly by normalizing RBC parameters and curtailing RBC clearance. It is conceivable, either way, that longer term or higher dose chelator treatment could be of substantial benefit to target tissues, and could even promote regression of pathology by depleting iron stores through a number of possible mechanisms.

3.2.2.5.2. Liver Iron Content

The liver is a primary site for iron loading in murine β-thalassemia as well as the spleen (137). We thus conjectured that it would be one of the organs most affected by iron chelation and therefore, a likely location to observe potential improvements mediated by the chelators. Using the same spectrophotometric principle of iron detection as in erythrocyte membranes, non-heme iron was quantified per milligram of liver wet weight. Results described below are summarized in Table 4. Hepatic iron content in control and thalassemic mice was 0.78 and 1.65 nmoles iron/mg wet weight, respectively ($p < 0.001$). Remarkably, all chelators depleted liver iron stores, most significantly to 1.19 nmoles/mg using o-108 ($p < 0.05$). Direct hepatic iron measurements, therefore, supported the ability of iron chelators to mobilize injurious iron not only from within red cells but perhaps, also from principal organ storage sites. This again, occurred within a relatively short

period of time and at a remarkably moderate dose. To further evaluate iron chelator effects in tissues, the classic iron detection technique of Perls' staining was used in mouse liver and spleen. Though the assay is qualitative, the intensity of staining is considered an accurate indicator of iron content (169), making visual or graphical "scoring" of stained tissues a highly acceptable method of quantitating iron (2.3.7.3.). Also, because the method permits visual examination of tissue make-up and iron deposition, the cells expressly affected can be identified, offering insight into the direct targets of iron chelator action.

3.2.2.5.3. Perls' Iron Staining in Liver and Spleen

Perls' Prussian blue staining is a sensitive and reliable method for detecting ferric iron in tissue samples. Sections are first treated with acid to release ferric ions, then as the cation of potassium ferrocyanide is replaced by the ferric ion, insoluble ferric ferrocyanide is formed and readily precipitates, staining bright blue (169). Both liver and spleen sections were examined using a hematoxylin and eosin counterstain, and stainable iron expressed as a percentage of the total surface area examined.

As reported in Table 4, liver sections from control mice revealed no stainable iron while 0.23% staining was seen in untreated β-thalassemics. Iron chelators reduced the extent of iron accumulation by at least 50%, with the greatest effect being achieved by o-108, which reduced stainable iron by 90% relative to untreated animals ($p < 0.05$).

Perls' Prussian blue-stained liver sections are shown in Fig. 13. Each section represents the average percent stainable iron for that treatment group. Sections from control liver (first panel), revealed normal histology and no detectable iron. Tissues from untreated β-thalassemic mice, however, contained noticeable iron deposits in the

cytoplasm of Kupffer cells, identified by their characteristic "half-moon" shape and location, directly surrounding the hepatocytes. Some darker, more granular-appearing deposits may represent stainable iron from phagocytosed RBC, seen most prominently in untreated β-thalassemic tissue. Liver tissues from chelator-treated animals showed no treatment-related abnormalities. In DFO-treated animals, moderate iron staining was observed within Kupffer cells, again, proximate to hepatocytes. Deposits, however, appeared less extensive and less heavily-embedded than in untreated β-thalassemics. Staining in tissues from mice treated with L1, PIH, and o-108, was even more faint and more restricted than in untreated or DFO-treated cohort tissues. Sections from o-108-treated mice, especially, revealed remarkably scant iron staining (p < 0.05), and an overall appearance that was very close to normal.

Perls' staining was next used to assess iron deposition in the spleen, the primary organ for clearance of damaged and senescent RBC in mice, which was far more extensive than in the liver, for all animals. As reported in Table 4, 1.39% stainable iron was measured in control spleens, while a 4-fold excess was found in those from untreated β-thalassemics. Impressively, all chelators, with the exception of DFO, promoted a statistically significant decrease in the extent of staining; final values were intermediate between untreated thalassemics and normal controls (p < 0.05). Still, a more dramatic effect was seen in o-108-treated samples, where stainable iron was ~60% less than in untreated mice (p < 0.001).

Representative spleen tissues from each group are depicted in Fig. 14. Control spleens displayed intact architecture and overall normal histology: red and white pulp appeared in approximately equal proportion and only slight iron staining was visible. By

contrast, the splenic architecture in untreated β-thalassemic mice was virtually destroyed and the boundaries separating red and white pulp, unclear. Furthermore, iron staining was rife throughout the parenchyma, revealing splenic macrophages gorged with ferric iron. In the DFO-treated group, iron still pervaded the tissues, though less prominently than in the untreated group. In tissues from animals treated with L1, PIH, and o-108, splenic architecture was greatly improved, as evidenced by a clearer distinction and more normalized ratio between red and white pulp. As well, in all three of these groups, iron staining was considerably less intense and less diffuse than in untreated and DFO-treated mice ($p < 0.05$). Notably, tissues from o-108-treated animals showed improvements beyond those seen with other chelators: white pulp could actually be discerned, iron staining was minimal, and a close resemblance to normal tissues was evident. Interestingly, these results corresponded with those obtained in liver, the data from both organs highlighting o-108 as a superior iron chelator in tissues, surpassing the effectiveness of its peer candidates by an appreciable margin.

The observed benefits of iron chelators in thalassemic tissues were reflective of a number of possible mechanisms resulting from iron chelation in tissues, red cells, erythroid precursors, or a combination thereof. Factors contributing to the alleviation of tissue pathology may include attenuated RBC removal, diminished extramedullary erythropoiesis, and reduced iron loading.

Examined collectively, the results characterizing the erythrocytes and tissues of untreated and chelator-treated β-thalassemic mice confirmed success of the BMT technique in generating severely β-thalassemic mice. Moreover, the data established active iron chelation by each of the compounds tested and identified this iron-

mobilization activity as central to restoration of cell function and tissue reconstitution. Consideration of iron chelator effects in the various compartments tested, as well as a summary and discussion of both *in vitro* and *in vivo* results, will be the focus of the final section.

4. Discussion

4.1. Thalassemia: Pathophysiology and Current Treatment

The thalassemias encompass an extremely prevalent and debilitating group of diseases that target the essential oxygen carrier, hemoglobin. Though recognized as a major cause of morbidity and mortality worldwide, there is still no widely available cure for it, and the remedial measures that *are* available, are largely unsatisfactory. Because thalassemic infants born in developing countries, where the disease is most endemic, are surviving increasingly later into adulthood, there is an urgent need for a more practical treatment; one that is both therapeutically effective and economically viable. Furthermore, as the demography of the illness has changed, so has its geography, with high rates of immigration no longer relegating thalassemia to a "disease of the Mediterranean" but rather, expanding its borders, making it a serious global threat.

The disease arises from mutations in the α- or β-globin genes, causing a decrease in α- or β-globin polypeptide synthesis, respectively. Such genetic defects result in a fatal imbalance: the deficiency or total absence of one of the globin chains, and the insidious production of the other unaltered "bachelor" chain. Due to the loss of conformational stability inherent in α/β contacts, the monomeric subunit, whose synthesis is in relative excess, becomes highly unstable and readily precipitates within erythrocyte precursors and later in mature RBC. In β-thalassemic erythrocytes,

spontaneously high levels of free radicals and the newfound susceptibility of α-chains to autoxidation result in the release of heme moieties from their globin polypeptide chains. Though the globin and liberated heme can, themselves, cause mechanical damage by binding to membrane structures, it is the heme-derived iron that becomes the major culprit in the pathophysiology of the disease. As the heme ring is cleaved by hydroperoxides present in excess in patient cells, the iron that is normally so diligently sequestered becomes liberated in the vicinity of the membrane. Free to valence cycle between the ferric and ferrous forms, it functions as a catalyst in the Fenton redox-reaction, generating the deadly hydroxyl radical. It is this role in oxidant generation that endows iron with an inherent and devastating toxicity.

Critical to the development of thalassemia is not simply the excess of injurious oxygen species, but also their location. Cell structures critical for maintenance of deformability and integrity (spectrin, ankyrin, band 3, protein 4.1, membrane phospholipids, etc), act collectively as a sink for iron, drawing it onto binding sites on the cytoplasmic leaflet. Because of this intimate yet highly inappropriate association, iron's toxic potential becomes focused on the cell membrane, specifically, cytoskeletal proteins and membrane phospholipids. Iron also induces more of its own release by destabilizing and oxidatively denaturing normal hemoglobin and other α-chains, amplifying the vicious cycle of oxidant production and membrane destruction.

Also aggravating the pathology at the cellular level are some of the unique characteristics of the RBC itself, namely its excessive exposure to high oxygen concentrations, its limited *de novo* protein synthesis, its imbalance in pro-oxidant and antioxidant factors, and the restricted access of its membrane to intracellular oxidant

scavengers. The erythrocyte is also particularly vulnerable as the most ferruginous somatic cell, having to maintain 20 mM of iron fully liganded and meticulously compartmentalized (64).

The endpoint of the oxidative cascade is modification of the membrane that is so severe as to cause premature RBC removal from the circulation. The major anomalies precipitating erythrophagocytosis stem from cytoskeletal impairments and include cation leakiness, cellular dehydration and rigidity, reduced lipid fluidity, and the loss of phospholipid asymmetry. Phagocytosis of damaged red blood cells occurs via either MDA generation from peroxidized lipids or the binding of autologous antibodies recognizing band 3 protein on the cell surface (53).

Accelerated RBC breakdown accounts for the trademark anemia and stimulates splenic activity, resulting in massive splenic enlargement (also a product of iron loading and red blood cell production). Meanwhile, compensatory erythropoiesis leads to gross expansion of the bone marrow and characteristic bone deformation, as well as a spectrum of metabolic and endocrine abnormalities, including excessive gastrointestinal iron absorption (69). Clinically, therefore, the thalassemic phenotype develops to a large extent from the premature RBC destruction initiated by the presence of intraerythrocytic non-heme iron.

Despite considerable knowledge of its pathophysiology and its high frequency in the population, the only existing treatment for thalassemia, as mentioned, is non-curative and consists of chronic blood transfusions. This therapy exacerbates pre-existing iron overload by relentlessly supplying patients with surplus iron from breakdown of transfused RBC. Because its physiological excretion is limited, iron accumulates to toxic proportions in the liver, spleen, and heart, proving fatal if not removed – a task which is

accomplished by iron chelators designed specifically to bind the metal and promote its elimination. However, the only approved compound to this end is DFO, a drug which despite its clinical use since the 1960's suffers from significant drawbacks, most notably, its cumbersome parenteral method of administration. The majority of patients find the long-term use of DFO-dispensing portable pumps highly inconvenient and extremely taxing, both physically and financially, the latter prohibiting DFO's widespread use in socioeconomically disadvantaged countries. The high rate of non-compliance owing to the above complications results in failure to chelate surfeit iron in major organs, and eventually leads to organ shutdown and early patient mortality.

4.2. Summary of Hypothesis and Experimental Models

Thalassemic patients endure a triple threat from potentially toxic iron: it accumulates proximally at the red blood cell membrane, secondarily within major organs as a result of dysregulated metabolism and, finally, paradoxically, throughout tissues due to the very blood transfusions intended to treat it. Most research has been aimed at prenatal diagnosis, improving transfusion regimes, and reducing secondary tissue iron by ways of modulating DFO's mode of administration or developing orally available iron chelators. However, these strategies neither account for, nor attempt to pursue the *proximate* intraerythrocytic iron at the *source* of the damage. Given our limited therapeutic armamentarium in the treatment of thalassemia and the paramount importance of iron in its pathophysiology, it is conceivable that targeting the primary pathological iron "core" could provide the basis for an alternative treatment paradigm. Since iron's interception within the membrane would be expected to slow or reverse oxidative damage, then exploiting iron chelation before even attempting transfusion could improve cell

parameters sufficiently to prolong their circulation. The ultimate goal of this strategy is to allow patients to survive indefinitely without the need for transfusion - an exciting prospect that would undoubtedly increase their quality of life.

A practical and therapeutically feasible way to target intraerythrocytic iron is by using chelators capable of penetrating cell membranes and inactivating the iron contained therein. To test our hypothesis, two established and two comparatively novel iron chelators, spanning a range of properties, were used. DFO represents the current mainstay in therapy, while L1 is the only orally available alternative. However, a controversial history related to the effectiveness and potential toxicity of L1 has precluded its clinical approval in North America. The search for safer, more effective, and orally bioavailable chelators has yielded two promising candidates: PIH, and its most effective analog as per *in vitro* and *in vivo* screenings, *o*-108; neither of which has, until now, been tested in the context of thalassemia. These two cell permeable, tridentate iron chelators, by their very design, retain the effectiveness of DFO and oral bioavailability of L1, while circumventing the cumbersome method of delivery of the former, and the safety risks of the latter (127-129).

The iron chelators were evaluated in two complementary models of disease: *in vitro*, using human model β-thalassemic erythrocytes and *in vivo*, in a murine model of β-thalassemia. The former assessed effects within human cells, while the latter did so in a functionally integrated, physiological system. Finally, the remedial consequences of membrane iron chelation were demonstrated not only in mature cells but also in their precursors and further, in target organs, where the activity of compound *o*-108 was found to be particularly high. This was the first study, to our knowledge, addressing iron

chelation via standard and novel compounds in human and murine prototypes simultaneously. The research was also not limited to red blood cell analysis and examined, for the first time, the impact of iron chelators in immature erythroid cells and affected tissues. A discussion of our findings *in vitro* and *in vivo*, as well as a short synthesis of the two is presented below.

4.3. *In Vitro* Studies

The main objective of the *in vitro* experiments was to test the ability of selected iron chelators to ameliorate the pathophysiology of human thalassemic cells. Theoretically, studies should have been conducted using erythrocytes obtained directly from patients. However, because the cells exhibiting the most damage are the first to be cleared *in vivo*, and because the severity of the disease may be "diluted" by the presence of healthy transfused cells, information from thalassemic patients (inevitably undergoing treatment) is difficult to obtain and does not always accurately portray the pathology. Mouse models, while approximating the pathophysiology and phenotype of the disease (to be discussed below in 4.4.), are still not the perfect substitute for human cells, as their RBC are more fragile *ex vivo* and their α-chains possess distinct biochemical properties, allowing us only to extrapolate data to humans (146). Examining therapeutic interventions directed at human β-thalassemic erythrocytes was therefore, until just over a decade ago, seriously compromised. It was the development of model β-thalassemic erythrocytes in the early 1990's that finally deepened our knowledge of the mechanisms of α-chain-induced injury in human thalassemic cells. Such model cells consist of normal human erythrocytes loaded with purified human α-chains; they have been extremely well- characterized as exhibiting the same structural, functional, and metabolic

abnormalities as β-thalassemic patient cells (130, 131). The favourable exception to model cells is that they are readily available and more highly amenable to testing of new pharmacological agents and strategies for disease management.

We exploited this model of thalassemia to investigate the therapeutic potential of the selected iron chelators. As proposed, model β-thalassemic cells were prepared (depicted schematically in Fig. 3), first by isolating and characterizing α-hemoglobin subunits from normal human RBC. Purity of the α-chains was confirmed by mass spectrometry and their functionality was assessed through spectrophotometric analysis. As indicated by the characteristic oxyhemoglobin spectrum in Fig. 7, chains were not oxidized during preparation and no presence of Hb degradation by-products was detectable. However, over a 20 h incubation at 37°C, the α-chains oxidized completely to metHb, enabling them to exert their pathophysiological effects. We established the value of the aberrant, modified cells *in vitro* by assessing their non-heme iron and oxidative stress levels as compared to control and control-resealed RBC. Cells loaded with an excess of α-chains contained excessive membrane-bound iron as well as elevated metHb levels, simulating the pathology of true β-thalassemic cells (Fig. 9). Furthermore, α-chains incorporated into normal RBC in graded concentrations were shown through spectral analysis to cause dose-dependent oxidative damage to RBC (data not shown). Therefore, the model cells displayed the fundamental oxidative damage evocative of their clinical human counterparts and were considered a suitable model in which iron chelators could be tested.

As depicted in Fig. 9, model β-thalassemic cells incubated for 20 h in the presence of 50 μM iron chelator, contained 4- to 5-fold less membrane iron than

untreated cells. A similarly significant effect was observed in comparing metHb levels following incubation, which were reduced by at least 50% in all chelator-treated samples. Importantly, iron mobilization results correlated directly with those from Hb oxidation studies, implying that the protection against oxidative damage conferred by iron chelators was due to their iron binding properties. Interestingly, all compounds promoted cellular improvements with relatively equal levels of efficacy; no single compound distinguished itself as much more or less effective than any other. This could be true to the nature of these chelators under these conditions or could, alternatively, be a product of the sensitivities of the assays, perhaps not revealing the full potency or range of chelator effects at these moderate concentrations. Therefore, from the *in vitro* results, we determined that iron chelators acting in human thalassemic-like cells were successful in stripping iron from cell membranes, and in the process, significantly relieving oxidative injury. Moreover, the damage effected by the α-chains was extremely rapid, as was the action of the iron chelators themselves. The fast kinetics of iron mobilization, with chelators permeating cells and effluxing a substantial iron load within only 20 h, lends credibility to the "chelation before transfusion" principle. One could rationalize that the more rapid the iron removal, the more preventative the nature of the treatment - and hence, the less likely a patient will be to require transfusion.

The sudden onset of the damage is suggestive of a primordial role for α-chain-derived iron, inducing lethal alterations early on in erythroid development. This broadens the concept of intraerythrocytic iron chelation by raising the possibility of targeting therapeutic agents not only to red cells, but also, perhaps more importantly, to their precursors (to be discussed in section 4.4.).

Another exciting finding pertaining to the rapidity of chelator action came from a secondary experiment which, although not directly included in our objectives, still supported our hypothesis. In it, o-108 was supplemented to the incubation medium of model β-thalassemic cells at either t = 0 or t = 4 h. This test revealed that its addition, even several hours after the α-chains had adversely precipitated, still produced remarkably beneficial effects by decreasing metHb levels back to their initial, t = 0 values, essentially reversing the oxidative injury already induced. This observation implied that early incubation with chelators could not only avert α-chain-induced toxicity, but moreover, could rescue already damaged cells. On a clinical level, this would suggest iron chelation to be a countermeasure against transfusion when instituted early on in the disease, while chelation in later stages could still, likely, repair injury already incurred by cells.

One final point worthy of note relates to the unexpected efficiency of DFO in these studies, as well as in vivo. Recalling its relative cell impermeability and high MW, DFO was not predicted to chelate intracellular iron as well as it did. Knowing that the ability of agents to cross biological membranes depends largely on their size and lipophilicity, it was natural to question why and how DFO accomplished its iron chelation at a level comparable to other, smaller cell permeable molecules. Though it is not possible to answer this definitively from our data, one possibility includes its partial entry into cells via pinocytosis or other means besides passive diffusion, shown to be the case when using cell impermeable drugs (170). Alternatively, because lysis-resealing results in some cells which experience a slight leak, or in which resealing is partial, DFO may be taken up, to some degree, through the remainder of transient pores opened during

α-chain encapsulation. Another viewpoint is that since α-chains are loaded *in vitro* as a relatively large mass at once, they achieve higher intraerythrocytic concentrations compared to those found *in vivo* in human β-thalassemic RBC, which experience α-chain deposition continuously and at a constant rate. Hence, the "one-shot" loading method of unstable globin chains into RBC to create the model cells may enable even minor chelator penetration to achieve a seemingly dramatic effect. Since chelation efficiency does in fact depend on the concentration of iron present (86), it would follow that a spike from α-chain encapsulation may cause slight overestimation of chelation efficiency, making DFO appear equally beneficial as the other compounds. Therefore, while not entirely expected, iron chelation by DFO in this *in vitro* model system may occur through a number of mechanisms, attesting to its high iron binding and removal capacity in spite of its unfavourable charge and size.

We can conclude from the *in vitro* studies, therefore, that iron chelators possess a high potential to mobilize iron and, as a direct result, improve cellular oxidative parameters in model human β-thalassemic cells. All chelators in this setting behaved with comparable efficiency, thus, no compounds were singled out for more extensive testing and none were excluded from the study – each warranted further examination *in vivo*. These experiments informed us of the mechanisms and impact of iron chelation as they pertain to cells specifically of *human* origin, and supported our hypothesis insofar as thalassemic patient cells in isolation are concerned. Regarding this data as strong evidence for chelator effectiveness in protecting human β-thalassemic cells, we pursued testing of our hypothesis in a more physiological setting, *in vivo*.

4.4. *In Vivo* Studies

The objectives *in vivo* were to study the potential benefits of iron chelation on the pathophysiology of β-thalassemia from the perspective of the whole organism; a mouse model of β-thalassemia was therefore used. Mice hemizygous for deletion of the two tandemly-organized adult β-globin genes, β-globin major and β-globin minor, produce only 70-75% of β-globin protein compared to wild-type mice (136). As a result, they exhibit characteristics analogous to human thalassemia, including a hypocellular, hypochromic, microcytic anemia, abnormal RBC morphology, and a host of hematologic alterations. At the tissue level, they manifest grossly enlarged spleens and spontaneous iron overload. Given the severity of their disease, β-thalassemic mice do not breed efficiently, and furthermore, studies with them may be hampered by high variability amongst animals. To circumvent these obstacles, we used serial bone marrow transplantations to artificially generate a homogeneous population of age-, sex-, and weight-matched β-thalassemic mice, all with a similar degree of pathology. After monitoring for hematopoietic reconstitution, we confirmed the replacement of normal RBC production by donor-type thalassemic cell production in all transplanted mice. Features identical to the original colony and consistent with the disorder were established in transplanted recipients throughout the study, validating their use as models of β-thalassemia and supporting the transplantation method used to obtain them. The newly-generated β-thalassemic mice were treated with iron chelators over 4 weeks, and the same indices used to characterize human model β-thalassemic cells *in vitro* were examined in murine RBC and precursors. We also investigated fundamental indicators of disease that were inaccessible *in vitro*, including hematological data, RBC survival rates,

and tissue iron levels. In each case, values were compared between untreated and chelator-treated β-thalassemic mice.

The first assay, quantification of non-heme membrane iron, served as the primary and most direct measure of chelator effectiveness, ensuring each compound's ability to remove iron deposits from β-thalassemic cells before pursuing any other tests. Effective iron mobilization would suggest the outcome of subsequent assays to be a direct result of iron binding, as opposed to other ligand properties. RBC from untreated β-thalassemic animals showed explicit evidence of α-chain-induced damage, documented by excessive membrane-associated iron (Table 2) and metHb levels that were spontaneously ~30% higher than normal controls (Fig. 11). RBC from these animals suffered an oxidative disturbance corresponding in nature to that found in both human model and actual β-thalassemic cells. By contrast, after receiving iron chelators subcutaneously for 4 weeks, all treated animals showed a substantial reduction in erythrocyte membrane iron. Significantly, compounds L1 and PIH mobilized nearly 50% of membrane iron relative to untreated values (Table 2). Moreover, both normal control and untreated β-thalassemic mice showed a moderate increase in metHb from initial values after the 4 weeks, an effect that was more pronounced in the thalassemic population. This increase would not be considered unusual even in normal mice, however, since slight changes in metHb may also reflect native responses to stress, fluctuations with age and possibly other conditions (171, 172). Remarkably, this minor increase in metHb generation was absent in chelator-treated groups; in fact, chelators *decreased* metHb levels significantly from their original $t = 0$ values (Fig. 11). This was a powerful observation implying, as *in vitro*, a cause-effect relationship between iron chelation and the manifest decline in oxidant generation.

It also revealed chelator-related effects beyond normalization, that is, Hb oxidation was not only prevented from attaining as high a level as in untreated thalassemics but was actually reduced, a response not even seen in control mice. This would suggest a protective or preventative effect of chelators even in absence of disease, inhibiting the natural, progressive rise in metHb (produced spontaneously at ~0.5-3% per day), conceivably of bearing to normal, biological cell senescence (171, 172). Though outside the scope of this study, the application of iron chelators in systems of cell aging is one worthy of further consideration.

Next, hematological screening provided detailed information about chelator-mediated improvements in a more meaningful context, reporting on cell function and metabolism in both mature and immature erythroid cells. Briefly, we examined the most salient hematological features relating to thalassemia – those expected to be the greatest beneficiaries of chelator-mediated iron removal: hematocrit, MCV, MCHC, and reticulocyte count.

The hematocrit reports the ratio of pRBC volume to whole blood volume, and is invariably reduced in thalassemia due to the high rate of hemolysis. This index is proportional to the degree of anemia and also forms the grounds for the decision to transfuse or not, making it a critical value to examine. In these studies, the measured hematocrits were appropriate to each treatment group: reduced by 50% in untreated β-thalassemic mice, confirming severe anemia, and mildly improved in chelator-treated cohorts (Table 3), indicating reduced hemolysis as a function of iron chelation, thereby corroborating our hypothesis.

Another hematological parameter examined was the mean cell volume, often considered the most clinically useful as it serves to diagnostically flag diseases involving structurally abnormal hemoglobin and/or cellular ionic imbalance. This value, too, was abnormally low in β-thalassemic mice due to iron-driven oxidation of transport proteins, making the cells more susceptible to leaks and, ultimately, causing their dehydration. Chelator-treated animals, in contrast, had cell volumes almost exactly midway between untreated β-thalassemics and normal controls (Table 3), revealing significant amelioration in cell function, notably, cell volume regulation.

Two more important parameters pertaining to cell hydration status are mean cellular Hb and mean cellular Hb concentration, which respectively convey the amount of hemoglobin per cell, or in a given volume of packed cells. Decreased MCHC (expressed in g/dL) commonly reflects hypochromic cells resulting from decreased production of hemoglobin, leading to a lower cell Hb content. However, in a condition where the cell Hb content (reported in picogram) does not appreciably change, variations in the MCHC will entirely reflect changes in cell volume. This proved to be the case in our study, where chelator-treated mice had unchanged MCH, but significantly reduced MCHC relative to untreated cohorts, signalling that the overall change observed must have been due to an increase in cell volume. This improvement in cell hydration further supported conclusions drawn from MCV values, establishing enhanced cell function as a result of chelator-mediated iron removal.

The final hematological marker examined was the reticulocyte count. Expressed as a percentage of the total number of erythrocytes, it reflects the rate of RBC production and is also of critical diagnostic value. Reticulocytes are young, RNA-containing,

anucleate erythrocytes found almost exclusively in the marrow; they can be distinguished from mature cells by staining with an RNA-specific dye. Normally, very few reticulocytes are found in peripheral circulation (1-3%). However, if the demand for RBC production increases, as in certain pathological conditions, an abnormally high number of reticulocytes may be delivered to the blood before fully maturing. In our study, reticulocyte counts in untreated β-thalassemic mice were elevated 10-fold from control, suggesting highly stimulated erythropoiesis (Table 3). This finding is consistent with a compensatory response to accelerated erythroid cell destruction from iron-triggered mechanisms. In chelator-treated mice, however, reticulocyte counts were favourably decreased by 20-45% compared to untreated animals (Table 3), a plausible explanation being enhanced "effective" erythropoiesis and consequent normalization of metabolic demands. It is conceivable that iron chelation initiated a corrective cycle to counteract the pathological one, making toxic iron mobilization a primary step to ameliorating cell function and possibly prolonging RBC survival. If cell circulation time was improved, stress on the erythropoietic system would be relieved, and the need for extra RBC to sustain homeostasis, presumably decreased, resulting in substantially fewer reticulocytes being released prematurely. Meaningful inferences were drawn from these results: for the first time, iron chelators were shown not only to restore cellular features in isolation, but moreover, to produce functional improvements within the organism as a whole. This was the first opportunity to put formerly observed cellular changes into greater perspective, demonstrating that correction at the earliest stage of the pathophysiological program (iron removal, in this case) had downstream, physiological repercussions on the animals.

The ultimate endpoint in this study was to redress the condition of β-thalassemic erythrocytes via intraerythrocytic iron chelation sufficiently to prolong their survival in circulation. Though our previous observations suggested enhanced RBC $t_{1/2}$, they did not explicitly demonstrate it. Therefore, to confirm improved lifespan, red cells were labeled *in vivo* and monitored over the treatment period; final RBC $t_{1/2}$ values were then determined. In all cases, erythrocyte kinetics were remarkably improved by iron chelation, the RBC $t_{1/2}$ extended to values intermediate between untreated β-thalassemic and normal mice (Fig. 12). Though results clearly indicated a reduced hemolytic rate in chelated animals, the observed differences were not statistically significant. Several factors may account for this, including the rather high background rate of cellular destruction found in mice, making it difficult for alterations in kinetics patterns to emerge (165). Thus, seemingly moderate improvements in RBC lifespan, in the face of such adverse conditions, speak to a much more profound effect than is revealed through these methods. The most direct explanation for the lack of statistical significance may, in fact, stem from technical aspects of the study itself. For instance, the number of animals per treatment group (though adequate to derive meaning from these studies, ideally *"n"* would have been much larger) created unusually high variability in this assay. Moreover, the conservative chelation regime, in terms of both dosage and treatment period, likely masked the full potential of the iron chelators. Supportive of this assumption was that intraerythrocytic iron removal was only partial in each case. It is thus probable that additional iron chelation via higher drug concentrations and/or prolonging the treatment period, would have increased β-thalassemic RBC $t_{1/2}$ further. Finally, the increase in RBC $t_{1/2}$ must be considered in the larger context of the total lifespan of the cell. While

an increase of 3.2 days was reported in DFO-treated mice, for example, the increase in total lifespan would be twice that, i.e. 6.4 days. In the scheme of normal murine RBC circulation time, generally 45-50 d, this would represent a ~15% extension in lifespan, but because β-thalassemic RBC survive roughly half as long, this would be closer to a ~25-30% increase in RBC lifespan. Since a considerable number of transfused β-thalassemic patients are considered "borderline", that is, on the threshold of transfusion, this calibre of RBC lifespan improvement could, for them, mean the difference between a lifelong burden and living transfusion-free.

The specific reasons for the improvement in RBC $t_{1/2}$ could lie in any of the aforementioned cellular benefits of iron chelation. Though the increase in cell circulation time is probably an outcome contributed to by a number of functional changes working in concert, two of the most important are likely to be i) enhanced cell hydration and ii) reduced band 3 co-clustering. Critically, at the root of each of these positive modifications lies the primary removal of iron.

The red blood cell survival assay, therefore, yielded extremely encouraging results and supported the proposed hypothesis. The assay demonstrated, unequivocally, that RBC membrane-bound iron chelation could serve as a springboard for a series of restorative mechanisms, leading ultimately to the extension of red cell lifespan. It also underlined intraerythrocytic iron chelation via specific metal-binding ligands as a valid and potentially widely applicable therapeutic solution to managing β-thalassemia. This strategy would clearly need to be tested in humans before drawing conclusions about its clinical efficacy. Nonetheless, our study offers convincing preliminary evidence to support such testing, ideally, prior to instituting transfusion in young thalassemic patients.

The pathophysiological role of iron in thalassemic precursors is considerably less well-understood than in mature red cells. As indicated in a previous section (3.2.2.3.), the fast rate of α-chain accumulation and iron deposition would almost require iron chelators to act at earlier stages in erythroid development (normoblast and/or reticulocyte), to arrest disease progression with greatest efficiency. To investigate whether iron chelators could access abnormal iron compartments at the onset of disease in cells upstream from mature erythrocytes, we assessed reticulocyte parameters. Even though α-chains begin to accumulate earlier, at the polychromatophilic normoblast stage (143), reticulocyte indices were the most practical to evaluate (164). We thus hoped to determine, at least indirectly, whether primitive red cells could equally benefit from membrane iron chelation and, thus, whether chelators targeted specifically at precursors would be worth considering. Because reticulocytes lose RNA as they develop, decreased cell staining with RNA-specific dye, oxazine 750, is observed progressively throughout maturation, with no staining detectable by the erythrocyte stage. If iron chelation were to promote precursor maturation, it would be reflected in decreased staining with oxazine 750. The reticulocyte population was thus divided into categories based on staining intensity, and each sub-population was quantified and compared between untreated and chelator-treated β-thalassemic mice. Chelator-treated precursor populations contained a preponderance of mature cells relative to untreated. Furthermore, the mean reticulocyte volumes, independent of mature RBC volumes, were invariably increased from untreated (Table 3), suggesting reduced oxidation of membrane structures and improved cell function. These observations, together, strengthened the premise that chelators may be acting directly at the level of reticulocytes (or earlier precursors) within the bone marrow,

restoring cell integrity sufficiently to promote their maturation and longevity. Diminished intramedullary hemolysis would concretely benefit thalassemic patients as it would be expected to repress or even, possibly, completely block the hallmark ineffective erythropoiesis responsible for many of the clinical consequences. More extensive studies would be needed to confirm this through examination of bone marrow cellularity and exact quantification of erythroid precursors. If iron removal from reticulocytes did indeed prolong their survival, then theoretically, chelators targeted specifically at early erythroid lines would possess an even greater potential to alleviate disease.

By examining murine β-thalassemic parameters at the cellular level (mature cells and erythroid precursors), therefore, we confirmed the devastating injury induced by free intraerythroid iron and the benefits of its chelation on the pathophysiology of the disease. In addition to the hallmark cellular features, however, β-thalassemia is also characterized by extensive abnormalities at the tissue level. The liver and spleen are obvious targets due to their role as reticuloendothelial organs. Both organs accumulate iron in part by its translocation from the Hb of red cells into macrophages, and eventually, into parenchymal cells, the latter having the most deleterious consequences. To determine the effects of iron chelators in mouse tissues, therefore, we examined spleen weight, liver iron content, and iron staining in both organs.

Massive splenomegaly was observed in untreated β-thalassemic animals, consistent with other mouse models of the disease, likely resulting from a combination of accelerated hemolysis, extramedullary hematopoiesis and hemochromatosis (173). There was a noticeable trend toward reduced spleen/body weight in chelator-treated animals (Table 4), and while this constituted evidence for reduced spleen pathology, it did not

explicitly confirm improvement in splenic function (though this is also highly likely). The precise reasons for the decrease in splenomegaly can only be speculated. Iron chelators may be purging iron directly from reticuloendothelial or parenchymal cells, or the tissue improvement could occur indirectly as a downstream consequence of intraerythrocytic iron chelation (attenuated hemolysis and ineffective erythropoiesis), or a combination of both. Because tissue iron probably began accumulating shortly after BM transplantation, and had thus reached significant proportions by the time its removal was initiated via chelation, the proposed treatment could be of importance to humans in whom hypersplenism has already developed considerably. Even administered at a more advanced stage of iron overload, iron chelators would still be expected to benefit the patient, at least in part by reducing RBC membrane iron.

Tissue iron distribution was quantitated per mg wet weight of tissue (liver) and was also examined by Perls' staining of liver and spleen. Abnormally high hepatic iron concentrations and stainable iron in untreated β-thalassemic mice were both significantly reduced by o-108, and modestly by all other compounds (Table 4, Fig. 13). In the spleen, all chelators promoted a statistically significant decrease in iron staining; however, o-108 again demonstrated a capacity for iron removal that was far superior (Fig. 14). Another exciting finding concerned the kinetics of iron chelation, as both iron accumulation and subsequent chelation were unexpectedly rapid: within 3-4 months of transplantation, iron loading was substantial in multiple organs. Then, within only 4 wk of iron chelator treatment, tissue pathology had regressed in its development, with o-108 demonstrating particularly high efficacy, virtually "rescuing" affected tissues. Though alleviation of damage must have largely been mediated by o-108's ability to reduce iron burden,

several factors working synergistically may also have contributed to the overall restorative effect. These observations raised important questions regarding the differential effects of iron chelators *in vitro* and *in vivo*, and in various cells and tissue types, both of which will now briefly be considered.

4.5. Comparison of *In Vitro* and *In Vivo* Results

Because *in vivo* results matched those obtained *in vitro* in terms of support for the proposed treatment strategy, we inferred that the oxidative mechanisms dominating human thalassemia were, overall, the same ones responsible for the disease in mice, which was consistent with data from other laboratories (49, 82, 138). Perhaps most vital to our hypothesis, though, was how iron's selective removal from human and murine β-thalassemic cells by all tested chelators put a biochemical "brake" on metHb generation and the ensuing oxidative cascade, enabling cells to remain in circulation considerably longer *in vivo*. Encouragingly, the pathophysiology of the disease was ameliorated in both models.

However, while compounds performed relatively equally well *in vitro* (PIH ~ DFO ~ L1 showing marginal advantage), *in vivo*, their relative efficiencies differed more substantially. This finding could be explained by the nature and limitations of the models themselves. The controlled environment (no positive selection, equally damaged cells) and narrow time frame of observation *in vitro* likely hampered our ability to observe potential differences in chelator performance. While comparatively, iron chelator effects developed more faithfully *in vivo*, given chronic drug administration over a longer period of time. This distinction between the models seemed intuitive, since so many additional variables navigate the biological performance of chelators *in vivo*, thereby creating more

opportunities to observe variance in their effects. Moreover, different rates of α-chain precipitation, proteolysis, and iron release, as well as differential compensatory mechanisms in model human and pathological murine cells may also account for the discrepancy in chelator behaviour (equivalent versus graded efficiencies) in the two models. Despite minor incongruities, human model β-thalassemic RBC and animal models of thalassemia were both valuable in helping further our understanding of the iron-triggered oxidative damage underlying β-thalassemia and its prevention via proximate iron chelation. Together, they helped construct a broad and comprehensive picture of this prospective strategy by examining a composite of isolated human cell and widespread physiological responses to iron chelators.

4.6. Comparison of Iron Chelators in Erythroid and Tissue Compartments

Notable distinctions emerged over the course of *in vivo* experiments when comparing a single chelator's effectiveness across different iron compartments (erythroid cells versus organ storage sites). Interestingly, while relatively uniform efficiency was found at the cellular level (slight advantage of DFO and PIH), a unique and remarkable impact was apparent in the tissues using *o*-108. This observation supported direct activity of the compounds within tissues (macrophages, parenchymal cells, or both), distinct from, and additional to their effects within erythroid cells, designating both sites as potential targets for iron chelators. The exceptional activity of *o*-108 in tissues was not entirely surprising: of the series of halogenated PIH analogs, *o*-108 was one of the most effective in mobilizing iron from a number of cell types *in vitro*, and in promoting iron excretion in rats (100, 128). The overall efficacy of *o*-108 in these studies was superior to that of both DFO and PIH; it bound significantly more iron than either and mobilized it more rapidly

due to efficient efflux of its iron complex (127). The enhanced capacity of o-108 to chelate body iron reported here can also be attributed to the higher lipophilicity of both free ligand and its complex with iron. The explanation for the distinct behaviour of o-108 within different cell types, however, is not as clear, and the reasons why it appeared so much more promising, relatively speaking, within organs than in RBC are subject to much speculation. Perhaps additional iron pools are amenable to chelation in parenchymal and reticuloendothelial cells, or, alternatively, o-108 may possess certain properties which are of greater benefit to, or more exploitable in tissues. The fact that hepatocytes possess alternative means of iron elimination (bile), that are not limited by the translocation of the complex across the plasma membrane, also offers a plausible explanation for o-108's greater chelation in tissues. Conversely, an additional kinetic barrier may be present in red cells during handling of the o-108-iron complex, impeding o-108 from functioning at its full capacity compared to other cell types. It may also be that the iron intercalated within RBC membranes is not as attainable as chelatable iron in other cells, or still, that features of the red cell membrane may modulate o-108's access to internal iron compartments differently than other membrane types. Regardless of the mechanism, it is certainly not unusual for iron chelators to express different levels of effectiveness depending on the cell type examined, as a number of other studies have found (101, 122, 123). More detailed analyses are warranted to explore these differences, as well as the potential overlap between chelation sites (erythroid versus tissues) – perhaps eventually determining the contribution of each to the overall improvement in the thalassemic phenotype. In conclusion, we have established both β-thalassemic erythroid cell membranes and tissues to be laden with free iron, and have found these pools to be

differentially amenable to chelation. Though iron chelators were successful in inhibiting the progress of disease, the exact sequence of events, beginning from initial intraerythrocytic iron chelation to the final functional improvements, still remains to be elucidated.

4.7. Overall Assessment of Iron Chelator Efficiency

Though it was not the direct aim of this study to compare different classes of chelators, an apparent advantage of the two non-standard compounds, PIH and o-108, did emerge. At the cellular level, no obviously superior compound could be distinguished, as mentioned previously. However, a trend *was* observed with PIH (almost equivalent to DFO), slightly surpassing the other compounds in improving cell-related parameters, frequently achieving statistical significance in this regard where others did not. At the tissue level, it was o-108 which stood out among its peer candidates, removing one of the most substantial quantities of liver iron and exerting the most pronounced therapeutic effect in both liver and spleen, as discussed in 3.2.2.5.3. and as seen in Figs. 13 and 14. The superiority of PIH and o-108 may be ascribed to their high lipophilicity and iron-binding capacity, amongst other properties, including antioxidant activity via both iron chelation and hydroxyl scavenging (174). Meanwhile, DFO's efficiency *in vivo* was not as intuitive a projection, and may be reasoned along several possible lines. One explanation relates to its mode of administration, since continuous delivery would be expected to enhance development of its effects, allowing otherwise weak activity to be amplified. Previous studies have supported this notion by showing that sustained chelator presence in blood does, in fact, cause greater iron chelation than would be observed with larger but less frequent doses (175, 176). Thus, for a compound such as DFO, which does not

readily permeate cells, chronic infusion via osmotic pump granted it a privilege denied by most delivery methods - continual access to cells. Even if not taken up rapidly, its stable presence would have ensured at least partial entry into cells, accounting for its efficiency. Another possibility stems from the conservative drug dosage, which may have concealed the actual potency of certain other compounds, artificially "equalizing" or levelling out their apparent effects. Conceivably, administering higher chelator concentrations would have produced more dramatic differences between compounds than were palpable here. Another point of consideration is that iron chelation *in vivo* depends not only on drug dose and its mode and frequency of delivery, but also on the initial iron load of the subject, with the general rule being that higher starting loads result in greater iron excretion (86). Unfortunately, due to experimental design, there was no way of knowing the initial iron burden in individual mice, and so the average levels for each treatment group could only be compared relative to each other, post-treatment. A slight discrepancy in initial iron mass amongst mice may, therefore, be accountable for some of the observed differences in chelator activity, though probably only as a minor contributor. Finally, after interpreting the differences in iron chelation via two established, versus two comparatively novel iron chelators, the latter more capable of accessing abnormal erythroid iron compartments, we found PIH and *o*-108, on a whole, to demonstrate superior effectiveness in improving the pathology of β-thalassemia. This finding underscores the need for future studies with these compounds in a clinical setting and highlights them both as potentially important agents for the treatment of disease via the proposed proximate iron chelation strategy.

A concluding remark should be made concerning the comparative assessment of iron chelator behaviour. Despite implementing a chelation regime that was as tightly controlled and physiologically realistic as possible, results have still been interpreted with caution, as not all the variables that may have meaningfully influenced our findings could be accounted for. Such factors include chelator pharmacokinetics, metabolism, and stoichiometric contributions. Because we were dealing with very low concentrations of iron and chelators, typical of biological systems, the iron-ligand complexes formed were likely incomplete, yielding mixed ligand complexes. This element made it virtually impossible to know the active concentrations of ligand in different tissues at different times, making it even more difficult to draw absolute conclusions about the data. Finally, in the face of so many modifying factors, identification of specific molecular structures and substituents responsible for high chelator activity would be of great advantage in designing more powerful intracellular iron chelators. Compounds capable of selectively accessing iron pools in multiple target sites, including early erythroid membranes, could potentially serve not only in the treatment of thalassemia, but also, in other diseases involving iron toxicity or free radical damage, such as Parkinson's disease, ischemic heart disease, and even cancer (177-179).

4.8. Future Directions

A major goal of iron chelation therapy in the future is to modulate treatment to meet the specific needs of patients, in essence, tailoring the chelation regime to the individual. A breakthrough concept to this end has been combination therapy, which was first used in 1998 using DFO and L1 (180). Several clinical studies have since been reported, with iron excretion at least equal to that achieved with either drug alone. In most cases,

however, the two chelators have produced additive or synergistic effects (181, 182). The basis for combination therapy is the "iron shuttle system", as it has come to be known; drawing on a small, cell permeable chelator to access intracellular iron, diffuse out of the cell, and unload its iron to a larger, cell impermeable compound with higher iron-binding affinity. The relay creates a virtual tag team of chelation, with the first molecule shuttling into cells and scavenging the iron, and the second, acting as a docking molecule, or, a sink for chelated iron. A number of advantages are offered by this strategy, over and above enhanced iron excretion. Because combination therapy does not require as high a dose of either compound, ligands are less likely to access intracellular iron compartments indiscriminately, thereby limiting potential toxicity and preventing iron's redistribution. Furthermore, since the therapy uses orally active lipophilic molecules in the initial chelation phase, it is likely to resolve the problem of non-compliance in many patients.

Another exciting therapeutic advance similarly involves the use of two agents; rather than combine them, however, it advocates their use on an alternating basis to circumvent their potential side effects. For instance, the sequential use of DFO and L1 has been shown to cause significant iron excretion while greatly improving compliance (183). It appears, therefore, that iron chelation in the future is likely to involve not only new chelator designs and drug combinations, but also alternative methods of chelator administration and novel treatment strategies, such as the one we have proposed in this study. Even if not curative, these measures, at the very least, offer a greater number of options to patients – promoting a more individualized approach to treatment that is certain to improve both compliance and therapeutic outcome.

103

In conclusion, almost 80 years after its initial description, β-thalassemia still remains a serious health problem worldwide, and a continued challenge to both researchers and clinicians. Because of the substantial complications of current disease management, a novel treatment strategy has been proposed which could meaningfully enhance the quality of life of patients by preventing the need for transfusion. This approach involves iron chelators as primary pharmacological agents, targeted to abnormal erythroid membrane iron compartments. Compounds capable of safely and effectively permeating red cells and/or their precursors, and rigorously depleting them of toxic iron have been shown, in this report, to rapidly alleviate many of the symptoms of β-thalassemia. Striking effects were observed using two non-standard chelators, PIH and o-108, both meriting serious consideration as potential therapeutic agents for this disease. Through extensive characterization of red cells, their precursors, and thalassemic tissues, our studies substantiate iron's causal role in the biogenesis of β-thalassemia and strongly support a treatment modality whereby its removal via iron chelators would be the first line of defense, eventually relegating transfusion to a therapy of the past.

5. Reference List

1) Ponka P. Recent advances in cellular iron metabolism. The Journal of Trace Elements in Experimental Medicine. 16:201-17, 2003.

2) Wintrobe MM. In: Greer JP *et al.*, ed. Wintrobe's Clinical Hematology. Philadelphia, PA: Lippincott Williams and Wilkins Inc.; 113-22, 1995.

3) McKie AT, Barrow D, Latunde-Dada GO, Rolfs A, Sager G, Mudaly E, Mudaly M, Richardson C, Barlow D, Bomford A, *et al.* An iron-regulated ferric reductase associated with the absorption of dietary iron. Science. 291:1755-9, 2001.

4) Anderson GJ, Frazer DM, McKie AT, and Vulpe CD. The ceruloplasmin homolog hephaestin and the control of intestinal iron absorption. Blood Cells, Molecules and Diseases. 29:367-75, 2002.

5) McKie AT, Marciani P, Rolfs A, Brennan K, Wehr K, Barrow D, Miret S, Bomford A, Peters TJ, Farzaneh F, *et al.* A novel duodenal iron-regulated transporter, IREG1, implicated in the basolateral transfer of iron to the circulation. Molecular Cell. 4:299-309, 2000.

6) Fleming MD, Trenor CC III, Su MA, Foernzler D, Beier DR, Dietrich WF, and Andrews NC. Microcytic anaemia mice have a mutation in Nramp2, a candidate iron transporter gene. Nature Genetics. 16:383-6, 1997.

7) Gunshin H, Mackenzie B, Berger UV, Gunshin Y, Romero MF, Boron WF, Nussberger S, Gollan JL, and Hediger MA. Cloning and characterization of a mammalian proton-coupled metal-ion transporter. Nature. 388:482-8, 1997.

8) Ponka P. Tissue-specific regulation of iron metabolism and heme synthesis: distinct control mechanisms in erythroid cells. Blood. 89:1-25, 1997.

9) Kuhn LC. Molecular regulation of iron proteins. Baillière's Clinical Haematology. 4:763-85, 1994.

10) Cooley TB, and Lee P. A series of cases of splenomegaly in children with anemia and peculiar bone changes. Transactions of the American Pediatric Society. 37:29-30, 1925.

11) *The Tyler Medical Clinic,*
http://www.tylermedicalclinic.com/beta%20thalassemia.htm

12) *World Health Organization,*
http://www.who.int/genomics/public/geneticdiseases/en/index2.html

13) Wood WG, and Weatherall DJ. Developmental genetics of the human haemoglobins. Biochemical Journal. 215:1-10, 1983.

14) Rochette J, Craig JE, and Thein SL. Fetal hemoglobin levels in adults. Blood Reviews. 8:213-24, 1994.

15) Marden MC, Griffon N, and Poyart C. Oxygen delivery and autoxidation of hemoglobin. Transfusion Clinique et Biologique. 2:473-80, 1995.

16) Sanders-Haigh L, Anderson WF, and Francke U. The beta-globin gene is on the short arm of human chromosome 11. Nature. 283:683-6, 1980.

17) Schrier, SL. Thalassemia: Pathophysiology of red cell changes. Annual Reviews in Medicine. 45:211-8, 1994.

18) Advani R, Sorenson S, Shinar E, Lande W, Rachmilewitz E, and Schrier SL. Characterization and comparison of the red blood cell membrane damage in severe human alpha- and beta-thalassemia. Blood. 79:1058-63, 1992.

19) Weatherall DJ, Clegg JB, Wood WG, Old JM, Higgs DR, Pressley L, and Darbre PD. The clinical and molecular heterogeneity of the thalassemia syndromes. Annals of the New York Academy of Sciences. 344:83-100, 1980.

20) Wonke, B. Clinical management of β-thalassemia major. Seminars in Hematology. 38:350-9, 2001.

21) Rund D, and Rachmilewitz EA. Pathophysiology of α- and β-thalassemia: Therapeutic implications. Seminars in Hematology. 38:343-9, 2001.

22) Testa U, Hinard N, Beuzard Y, Tsapis A, Galacteros F, Thomopoulos P, and Rosa J. Excess α chains are lost from β-thalassemic reticulocytes by proteolysis. Journal of Laboratory and Clinical Medicine. 98:352-63, 1981.

23) Olivieri NF, and Weatherall DJ. The therapeutic reactivation of fetal haemoglobin. Human Molecular Genetics. 10:1655-8, 1998.

24) Kihm AJ, Kong Y, Hong W, Rusell JF, Rouda S, Adachi K, Simon MC, Blobel GA, and Weiss MJ. An abundant erythroid protein that stabilizes free alpha-haemoglobin. Nature. 417:758-63, 2002.

25) Wainscoat JS, Kanavakis E, Wood WG, Letsky EA, Huehns ER, Marsh GW, Higgs DR, Clegg JB, and Weatherall DJ. Thalassaemia intermedia in Cyprus: the interaction of alpha and beta thalassaemia. British Journal of Haematology. 53:411-6, 1983.

26) Shinar E, Shalev O, Rachmilewitz RA, and Schrier SL. Erythrocyte membrane skeletal abnormalities in severe β-thalassemia. Blood. 70:158-64, 1987.

27) Weatherall DJ. Pathophysiology of thalassemia. Baillière's Clinical Haematology. 11:127-46, 1998.

28) Bunn HF, and Jandl JH. Exchange of heme among hemoglobins and between hemoglobin and albumin. Journal of Biological Chemistry. 243:465-475, 1967.

29) Brunori M, Falcioni G, Fioretti E, Giardina B, and Rotilio G. Formation of superoxide in the autoxidation of the isolated α and β chains of human hemoglobin and its involvement in hemichrome precipitation. European Journal of Biochemistry. 53:99-104, 1975.

30) Joshi W, Leb L, Piotrowski J, Fortier N, and Snyder LM. Increased sensitivity of isolated alpha subunits of normal human hemoglobin to oxidative damage and crosslinkage with spectrin. Journal of Laboratory and Clinical Medicine. 102:46-52, 1983.

31) Rachmilewitz EA. Denaturation of the normal and abnormal hemoglobin molecule. Seminars in Hematology. 11:441-62, 1974.

32) Shinar E, and EA Rachmilewitz. Oxidative denaturation of red blood cells in thalassemia. Seminars in Hematology. 27:70-82, 1990.

33) Yuan J, Kannan R, Shinar E, Rachmilewitz EA, and Low PS. Isolation, characterization, and immuno-precipitation studies of immune complexes from membranes of β-thalassemic erythrocytes. Blood. 79:3007-13, 1992.

34) Kay MM. Localization of senescent cell antigen on band 3. Proceedings of the National Academy of Sciences, USA. 81:5753-7, 1984.

35) Schrier SL, Rachmilewitz EA, and Mohandas N. Cellular and membrane properties of alpha and beta thalassemic erythrocytes are different: Implication for differences in clinical manifestations. Blood. 74:2194-202, 1989.

36) Pradhan D, Weiser M, Lumley SK, Frazier D, Kemper S, Williamson P, and Schlegel RA. Peroxidation-induced perturbations of erythrocyte lipid organization. Biochimica et Biophysica Acta. 1023:398-404, 1990.

37) Vincent SH. Oxidative effects of heme and porphyrins on proteins and lipids. Seminars in Hematology. 26:105-13, 1989.

38) Rouyer-Fessard P, Scott MD, Leroy-Viard K, Garel MC, Bachir D, Galacteros F, and Beuzard Y. Fate of alpha-hemoglobin chains and erythrocyte defects in beta-thalassemia. Annals of the New York Academy of Sciences. 612:106-17, 1990.

39) Vigi V, Volpato S, Gaburro D, Conconi F, Bargellesi A, and Pontremoli S. The correlation between red cell survival and excess alpha-globin synthesis in beta-thalassemia. British Journal of Haematology. 16:25-30, 1969.

40) Grinberg LN, Rachmilewitz EA, Kitrossky N, and Chevion M. Hydroxyl radical generation in β-thalassemic red blood cells. Free Radical Biology and Medicine. 18:611-5, 1995.

41) Livrea MA, Tesoriere L, Pintaudi AM, Calabrese A, Maggio A, Freisleben HJ, D'Arpa D, D'Anna R, and Bongiorno A. Oxidative stress and antioxidant status in β-thalassemia major: iron overload and depletion of lipid soluble antioxidants. Blood. 88:3608-14, 1996.

42) Rachmilewitz EA, Lubin BH, and Sohet SB. Lipid membrane peroxidation in β-thalassemia major. Blood. 47:495-505, 1976.

43) Chakraborty D, and Bhattacharyya M. Antioxidant defense status of red blood cells of patients with β-thalassemia and Eβ-thalassemia. Clinica Chimica Acta. 305:123-9, 2001.

44) Rachmilewitz EA, Shifter A, and Kahane I. Vitamin E deficiency in beta-thalassemia major: changes in hematological and biochemical parameters after a therapeutic trial with alpha-tocopherol. American Journal of Clinical Nutrition. 32:1850-8, 1979.

45) Halliwell B and Gutteridge JM. Biologically relevant metal ion-dependent hydroxyl radical generation. An update. FEBS Letters. 307:108-12, 1992.

46) Nagababu E, and Rifkind JM. Heme degradation during autoxidation of oxyhemoglobin. Biochemical and Biophysical Research Communications. 273:839-45, 2000.

47) Shalev O, and Hebbel RP. Catalysis of soluble hemoglobin oxidation by free iron on sickle red cell membranes. Blood. 87:3948-52, 1996.

48) Ryan TP, and Aust SD. The role of iron in oxygen-mediated toxicities. Critical Reviews in Toxicology. 22:119-41, 1992.

49) Advani R, Rubin E, Mohandas N, and Schrier SL. Oxidative red blood cell membrane injury in the pathophysiology of severe mouse beta-thalassemia. Blood. 79:1064-7, 1992.

50) Scott MD, van den Berg JJM, Repka T, Rouyer-Fessard P, Hebbel RP, Beuzard Y, and Lubin BH. Effect of excess α-hemoglobin chains on cellular and membrane oxidation in model β thalassemic erythrocytes. Journal of Clinical Investigation. 91:1706-12, 1993.

51) Scott MD, Rouyer-Fessard P, Lubin BH, and Beuzard Y. Entrapment of purified alpha-hemoglobin chains in normal erythrocytes: A model for β-thalassemia. Journal of Biological Chemistry. 265:17953-9, 1990.

52) Browne P, Shalev O, and Hebbel RP. The molecular pathobiology of cell membrane iron: the sickle red cell as a model. Free Radical Biology and Medicine. 24:1040-8, 1998.

53) Mannu F, Arese P, Cappellini MD, Fiorelli G, Cappadoro M, Giribaldi G, and Turrini F. Role of hemichrome binding to erythrocyte membrane in the generation of Band-3 alterations in β-thalassemia intermedia erythrocytes. Blood. 86:2014-20, 1995.

54) Olivieri O, De Franceschi L, Capellini MD, Girelli D, Corrocher R, and Brugnara C. Oxidative damage and erythrocyte membrane transport abnormalities in thalassemias. Blood. 84:315-20, 1994.

55) Kuross SA, and Hebbel RP. Nonheme iron in sickle erythrocyte membranes: Association with phospholipids and potential role in lipid peroxidation. Blood. 72:1278-85, 1988.

56) Shalev O, and Hebbel RP. Extremely high avidity association of Fe (III) with the sickle red cell membrane. Blood. 88:349-52, 1996.

57) Repka T, Shalev O, Reddy R, Yuan J, Abrahamov A, Rachmilewitz EA, Low PS, and Hebbel RP. Nonrandom association of free iron with membranes of sickle and beta-thalassemic erythrocytes. Blood. 82:3204-10, 1993.

58) Helley D, Eldor A, Girot R, Ducrocq R, Guillin MC, and Bezeaud A. Increased procoagulant activity of red blood cells from patients with homozygous sickle cell disease and beta-thalassemia. Thrombosis and Haemostasis. 76:322-7, 1996.

59) Atichartakarn V, Angchaisuksiri P, Aryurachai K, Onpun S, Chuncharunee S, Thakkinstian A, and Atamasirikul K. Relationship between hypercoagulable state and erythrocyte phosphatidylserine exposure in splenectomized haemoglobin E/beta-thalassaemic patients. British Journal of Haematology. 118:893-8, 2002.

60) Eldor A, and Rachmilewitz EA. The hypercoagulable state in thalassemia. Blood. 99:36-43, 2002.

61) Jacob HS, and Lux SE. Degradation of membrane phospholipids and thiols in peroxide hemolysis: Studies on vitamin E deficiency. Blood. 32:549-68, 1968.

62) Rachmilewitz EA, Shinar E, Shalev O, Galili U, and Schrier SL. Erythrocyte membrane alterations in beta-thalassaemia. Clinical Haematology. 14:163-82, 1985.

63) Hebbel RP, and Miller WJ. Unique promotion of erythrophagocytosis by malondialdehyde. American Journal of Hematology. 29:222-5, 1988.

64) Scott MD, and Eaton JW. Thalassemic erythrocytes: cellular suicide arising from iron and glutathione-dependent oxidation reactions. British Journal of Haematology. 91:811-9, 1995.

65) Yuan J, Angelucci E, Lucarelli G, Aljurf M, Snyder LM, Kiefer CR, Ma L, and Schrier SL. Accelerated programmed cell death (apoptosis) in erythroid precursors of patients with severe beta-thalassemia. Blood. 82:374-7, 1993.

66) Schrier SL. Pathophysiology of thalassemia. Current Opinion in Hematology. 9:123-6, 2002.

67) Robinson S, Vanier T, Desforges JF, and Schmid R. Jaundice in thalassemia minor: a consequence of "ineffective erythropoiesis". New England Journal of Medicine. 267:523-9, 1962.

68) Blendis LM, Modell CB, Bowdler AJ, and Williams R. Some effects of splenectomy in thalassaemia major. British Journal of Haematology. 28:77-87, 1974.

69) Pootrakul P, Kitcharoen K, Yansukon P, Wasi P, Fucharoen S, Charoenlarp P, Brittenham G, Pippard MJ, and Finch CA. The effect of erythroid hyperplasia on iron balance. Blood. 71:1124-9, 1988.

70) Ahmed NK, Hanna M, and Wang W. Nontransferrin-bound serum iron in thalassemia and sickle cell patients. International Journal of Biochemistry. 18:953-6, 1986.

71) Jacobs A. Low molecular weight intracellular iron transport compounds. Blood. 50:433-9, 1977.

72) Hershko C, Graham G, Bates GW, and Rachmilewitz EA. Non-specific serum iron in thalassaemia: an abnormal serum iron fraction of potential toxicity. British Journal of Haematology. 40:255-63, 1978.

73) Al-Refaie FN, Wickens DG, Wonke B, Kontoghiorghes GJ, and Hoffbrand AV. Serum non-transferrin-bound iron in beta-thalassaemia major patients treated with desferrioxamine and L1. British Journal of Haematology. 82:431-6, 1992.

74) Vecchio C, and Derchi G. Management of cardiac complications in patients with thalassemia major. Seminars in Hematology. 32:288-96, 1995.

75) Wonke, B. Clinical management of β-thalassemia major. Seminars in Hematology. 38:350-9, 2001.

76) Propper RD, Shurin SB, and Nathan DG. Reassessment of the use of desferrioxamine B in iron overload. New England Journal of Medicine. 294:1421-3, 1976.

77) Gutteridge JM, and Halliwell B. Iron toxicity and oxygen radicals. Baillière's Clinical Haematology. 2:195-256, 1989.

78) Modell B, Khan M, and Darlison M. Survival in beta-thalassaemia major in the UK: data from the UK Thalassaemia Register. Lancet. 355:2051-2, 2000.

79) Richardson, DR. Therapeutic potential of iron chelators. Expert Opinion on Investigational Drugs. 8:2141-58, 1999.

80) Olivieri NF, and Brittenham GM. Iron-chelating therapy and the treatment of thalassemia. Blood. 89:739-61, 1997.

81) Kushner JP, Porter JP, and Olivieri NF. Secondary iron overload. The American Society of Hematology Education Program Book. January, 2001:47-61.

82) Browne PV, Shalev O, Kuypers FA, Brugnara C, Solovey A, Mohandas N, Schrier SL, and Hebbel RP. Removal of erythrocyte membrane iron in vivo ameliorates the pathobiology of murine thalassemia. Journal of Clinical Investigation. 100:1459-64, 1997.

83) Shalev O, Repka T, Goldfarb A, Grinberg L, Abrahamov A, Olivieri NF, Rachmilewitz EA, and Hebbel RP. Deferiprone (L1) chelates pathologic iron deposits from membranes of intact thalassemic and sickle red blood cells both in vitro and in vivo. Blood. 86:2008-13, 1995.

84) De Franceschi L, Shalev O, Piga A, Collell M, Olivieri O, Corrocher R, Hebbel RP, and Brugnara C. Deferiprone therapy in homozygous human β-thalassemia removes erythrocyte membrane free iron and reduces KCl cotransport activity. Journal of Laboratory and Clinical Medicine. 133:64-9, 1999.

85) Liu DY, Liu ZD, and Hider RC. Oral iron chelators - development and application. Best Practice and Research. Clinical Haematology. 15:369-84, 2002.

86) Zanninelli G, Glickstein H, Breuer W, Milgram P, Brissot P, Hider RC, Konijn AM, Libman J, Shanzer A, and Cabantchik ZI. Chelation and mobilization of cellular iron by different classes of chelators. Molecular Pharmacology. 51:842-52, 1997.

87) Buss JL, Arduini E, and Ponka P. Mobilization of intracellular iron by analogs of pyridoxal isonicotinoyl hydrazone (PIH) is determined by the membrane permeability of the iron-chelator complexes. Biochemical Pharmacology. 61:1689-701, 2002.

88) Richardson DR, and Ponka P. Development of iron chelators to treat iron overload disease and their use as experimental tools to probe intracellular iron metabolism. American Journal of Hematology. 58:299-305, 1998.

89) Beutler EA, Hoffbrand V, and Cook JD. Iron deficiency and overload. The American Society of Hematology Education Program Book. January, 2001:40-47.

90) Olivieri NF, Brittenham GM, McLaren CE, Templeton DM, Cameron RG, McClelland RA, Burt AD, and Fleming KA. Long-term safety and effectiveness of iron-chelation therapy with deferiprone for thalassemia major. New England Journal of Medicine. 339:417-22, 1998.

91) Rombos Y, Tzanetea R, Konstantopoulos K, Simitzis S, Zervas C, Kyriaki P, Kavouklis M, Aessopos A, Sakellaropoulos N, Karagiorga M, et al. Chelation therapy in patients with thalassemia using the orally active iron chelator deferiprone (L1). Haematologica. 85:115-7, 2000.

92) Richardson DR. The controversial role of deferiprone in the treatment of thalassemia. Journal of Laboratory and Clinical Medicine. 137:324-9, 2001.

93) Cohen AR, Galanello R, Piga A, De Sanctis V, and Tricta F. Safety and effectiveness of long-term therapy with the oral iron chelator deferiprone. Blood. 102:1583-7, 2003.

94) Ponka P, Borova J, Neuwirt J, and Fuchs O. Mobilization of iron from reticulocytes: Identification of pyridoxal isonicotinoyl hydrazone as a new iron chelating agent. FEBS Letters. 97:317-21, 1979.

95) Cikrt M, Ponka P, Necas E, and Neuwirt J. Biliary iron excretion in rats following pyridoxal isonicotinoyl hydrazone. British Journal of Haematology. 45:275-83, 1980.

96) Hershko C, Avramovici-Grisaru S, Link G, Gelfland L, and Sarel S. Mechanism of in vivo iron chelation by pyridoxal isonicotinoyl hydrazone and other imino derivatives of pyridoxal. Journal of Laboratory and Clinical Medicine. 98:99-108, 1981.

97) Johnson DK, Pippard MJ, Murphy TB, and Rose NJ. An in vivo evaluation of iron chelating drugs derived from pyridoxal and its analogs. Journal of Pharmacology and Experimental Therapeutics. 221:399-403, 1982.

98) Ponka P, Richardson D, Baker E, Schulman HM, and Edward JT. Effect of pyridoxal isonicotinoyl hydrazone and other hydrazones on iron release from macrophages, reticulocytes and hepatocytes. Biochimica et Biophysica Acta. 967:122-9, 1988.

99) Brittenham GM. Pyridoxal isonicotinoyl hydrazone: an effective iron-chelator after oral administration. Seminars in Hematology. 27:112-6, 1990.

100) Blaha K, Cikrt M, Nerudova J, Fornuskova H, and Ponka P. Biliary iron excretion in rats following treatment with analogs of pyridoxal isonicotinoyl hydrazone. Blood. 91:4368-72, 1998.

101) Link G, Ponka P, Konijn AM, Breuer W, Cabantchik I, and Hershko C. Effects of combined chelation treatment with pyridoxal isonicotinoyl hydrazone analogs and deferoxamine in hypertransfused rats and in iron-loaded rat heart cells. Blood. 101:4172-9, 2003.

102) Bottomley SS, Wolfe LC, and Bridges KR. Iron metabolism in K562 erythroleukemic cells. Journal of Biological Chemistry. 260:6811-5, 1985.

103) Hallaway PE, Eaton JW, Panter SS, and Hedlund BE. Modulation of deferoxamine toxicity and clearance by covalent attachment to biocompatible polymers. Proceedings of the National Academy of Sciences, USA. 86:10108–12, 1989.

104) Savulescu J. Thalassemia major: the murky story of deferiprone. British Medical Journal. 328:358-9, 2004.

105) Shalev O, Hileti D, Nortey P, Hebbel RP, and Hoffbrand VA. Transport of ^{14}C-deferiprone in normal, thalassemic and sickle red blood cells. British Journal of Haematology. 105:1081-3, 1999.

106) Kayyali R, Porter JB, Liu ZD, Davies NA, Nugent JH, Cooper CE, and Hider RC. Structure-function investigation of the interaction of 1- and 2-substituted 3-hydroxypyridin-4-ones with 5-lipoxygenase and ribonucleotide reductase. Journal of Biological Chemistry. 276:48814-22, 2001.

107) Porter JB. Evaluation of new iron chelators for clinical use. Acta Haematologica. 95:13-5, 1996.

108) Dobbin PS, Hider RC, Hall AD, Taylor PD, Sarpong P, Porter JB, Xiao G, and van der Helm D. Synthesis, physicochemical properties and biological evaluation of N-substituted-2-alkyl-3-hydroxy-4(1H)-pyridinones. Journal of Medicinal Chemistry. 36:2448-58, 1993.

109) Hershko C, Konijn AM, and Link G. Iron chelators for thalassaemia. British Journal of Haematology. 101:399-406, 1998.

110) Cohen A, Galanello R, Piga A, Vullo C, and Tricta F. A multi-center safety trial of the oral iron chelator deferiprone. Annals of the New York Academy of Sciences. 850:223-6, 1998.

111) Tricta F, and Spino M. Iron chelation with oral deferiprone in patients with thalassemia. New England Journal of Medicine. 339:1710, 1998.

112) Hoffbrand AV, Al-Refaie F, Davis B, Siritanakatkul N, Jackson BF, Cochrane J, Prescott E, and Wonke B. Long-term trial of deferiprone in 51 transfusion-dependent iron overloaded patients. Blood. 91:295-300, 1998.

113) Tondury P, Zimmermann A, Nielsen P, and Hirt A. Liver iron and fibrosis during long-term treatment with deferiprone in Swiss thalassaemic patients. British Journal of Haematology. 101:413-5, 1998.

114) Lucas GN, Perera BJ, Fonseka EA, De Silva DD, and Fernandopulle M. A trial of deferiprone in transfusion-dependent iron overloaded children. Ceylon Medical Journal. 45:71-4, 2000.

115) Wanless IR, Sweeney G, Dhillon AP, Guido M, Piga A, Galanello R, Gamberini MR, Schwartz E, and Cohen AR. Lack of progressive hepatic fibrosis during long-term therapy with deferiprone in subjects with transfusion-dependent beta-thalassemia. Blood. 100:1566-9, 2002.

116) Hoffbrand VA, and Wonke B. Long term deferiprone chelation therapy. Advances in Experimental Medicine and Biology. 509:127-39, 2002.

117) Pootrakul P, Sirankapracha P, Sankote J, Kachintorn U, Maungsub W, Sriphen K, Thakernpol K, Atisuk K, Fucharoen S, Chantraluksri U, et al. Clinical trial of deferiprone iron chelation therapy in beta-thalassaemia/haemoglobin E patients in Thailand. British Journal of Haematology. 122:305-10, 2003.

118) Hoy T, Humphrys J, Jacobs A, Williams A, and Ponka P. Effective iron chelation following oral administration of an isoniazid-pyridoxal hydrazone. British Journal of Haematology. 43:443-9, 1979.

119) Ponka P, Borova J, Neuwirt J, Fuchs O, and Necas E. A study of intracellular iron metabolism using pyridoxal isonicotinoyl hydrazone and other synthetic chelating agents. Biochimica et Biophysica Acta. 586:278-97, 1979.

120) Huang AR, and Ponka P. A study of the mechanism of action of pyridoxal isonicotinoyl hydrazone at the cellular level using reticulocytes loaded with non-heme ^{59}Fe. Biochimica et Biophysica Acta. 757:306-15, 1983.

121) Morgan EH. Chelator-mediated iron efflux from reticulocytes. Biochimica et Biophysica Acta. 733:39-50, 1983.

122) Ponka P, Grady RW, Wilczynska A, and Schulman HM. The effect of various chelating agents on the mobilization of iron from reticulocytes in the presence and absence of pyridoxal isonicotinoyl hydrazone. Biochimica et Biophysica Acta. 802:477-89, 1984.

123) Baker E, Vitolo ML, and Webb J. Iron chelation by pyridoxal isonicotinoyl hydrazone and analogues in hepatocytes in culture. Biochemical Pharmacology. 34:3011-7, 1985.

124) Richardson DR, Tran EH, and Ponka P. The potential of iron chelators of the pyridoxal isonicotinoyl hydrazone class as effective antiproliferative agents. Blood. 86:4295-306, 1995.

125) Pappenhemier JR, Karnovsky ML, and Maggio JE. Absorption and excretion of undegradable peptides: role of lipid solubility and net charge. Journal of Pharmacology and Experimental Therapeutics. 280:292-300, 1997.

126) Richardson DR. Mobilization of iron from neoplastic cells by some iron chelators is an energy-dependent process. Biochimica et Biophysica Acta. 1320:45-57, 1997.

127) Buss JL, Arduini E, Shephard KC, and Ponka P. Lipophilicity of analogs of pyridoxal isonicotinoyl hydrazone (PIH) determines the efflux of iron complexes and toxicity in K562 cells. Biochemical Pharmacology. 65:349-60, 2003.

128) Buss JL, Hermes-Lima M, and Ponka P. Pyridoxal isonicotinoyl hydrazone and its analogues. Advances in Experimental Medicine and Biology. 509:205-29, 2002.

129) Baker E, Richardson D, Gross S, and Ponka P. Evaluation of the iron chelation potential of hydrazones of pyridoxal, salicylaldehyde and 2-hydroxy-1-naphthylaldehyde using the hepatocyte in culture. Hepatology. 15:492-501, 1992.

130) Scott MD, Rouyer-Fessard P, Ba MS, Lubin BH, and Beuzard Y. Alpha- and beta-haemoglobin chain induced changes in normal erythrocyte deformability: comparison to beta thalassaemia intermedia and Hb H disease. British Journal of Haematology. 80:519-26, 1992.

131) Kuypers FA, Schott MA, and Scott M.D. Phospholipid composition and organization in model β-thalassemic erythrocytes. American Journal of Hematology. 51:45-54, 1996.

132) Johnson FM, and Lewis SE. Electrophoretically detected germinal mutations induced in the mouse by ethylnitrosourea. Proceedings of the National Academy of Sciences, USA. 78:3138-41, 1981.

133) Skow LC, Burkhart BA, Johnson FM, Popp RA, Popp DM, Goldberg SZ, Anderson WF, Barnett LB, and Lewis SE. A mouse model for β-thalassemia. Cell. 34:1043-52, 1983.

134) Shehee WR, Oliver P, and Smithies O. Lethal thalassemia after insertional disruption of the mouse major adult beta-globin gene. Proceedings of the National Academy of Sciences, USA. 90:3177-81, 1993.

135) May C, Rivella S, Chadburn A, and Sadelain M. Successful treatment of murine β-thalassemia intermedia by transfer of the human β-globin gene. Blood. 99:1902-8, 2002.

136) Ciavatta DJ, Ryan TM, Farmer SC, and Townes TM. Mouse model of human β^o thalassemia: targeted deletion of the mouse β^{maj}- and β^{min}-globin genes in embryonic stem cells. Proceedings of the National Academy of Sciences. 92:9259-63, 1995.

137) Garrick LM, Strano-Paul LA, Hoke JE, Kirdani-Ryan LA, Alberico RA, Everett MM, Bannerman RM, and Garrick MD. Tissue iron deposition in untransfused beta-thalassemic mice. Experimental Hematology. 17:2423-8, 1989.

138) Rouyer-Fessard P, Leroy-Viard K, Domenget C, Mrad A, and Beuzard Y. Mouse β Thalassemia, a model for the membrane defects of erythrocytes in the human disease. Journal of Biological Chemistry. 265: 20247-51, 1990.

139) Kean LS, Brown LE, Nichols JW, Mohandas N, Archer DR, and Hsu LL. Comparison of mechanisms of anemia in mice with sickle cell disease and β-thalassemia: Peripheral destruction, ineffective erythropoiesis, and phospholipid scramblase-mediated phosphatidylserine exposure. Experimental Hematology. 30:394-402, 2002.

140) Dr. Marie Trudel, Molecular Genetics and Development Laboratory, Institut de Recherches Cliniques de Montreal, 110 Avenue des Pins Ouest, Montreal, Quebec, Canada, H2W 1R7.

141) Edward JT, Gauthier M, Chubb FL, and Ponka P. Synthesis of new acylhydrazones as iron-chelating compounds. Journal of Chemical and Engineering Data. 33:538-40, 1988.

142) Ferreira C, Santambrogio P, Martin M-E, Andrieu V, Feldmann G, Hénin D, and Beaumont C. H ferritin knockout mice: a model of hyperferritinemia in the absence of iron overload. Blood. 98:525-32, 2001.

143) Beauchemin H, Blouin MJ, and Trudel M. Differential regulatory and compensatory responses in hematopoiesis/erythropoiesis in α- and β-globin hemizygous mice. Journal of Biological Chemistry. 279:19471-80, 2004.

144) Bucci E, and Fronticelli C. A new method for the preparation of α and β subunits of human hemoglobin. Journal of Biological Chemistry. 240:551-2, 1965.

145) Turci SM, and McDonald MJ. Isolation of normal and variant hemoglobin chains. Journal of Chromatography. 343:168-74, 1985.

146) Scott MD, personal communication.

147) Bradford MM. A rapid and sensitive method for the quantitation of microgram quantities of protein utilizing the principle of protein-dye binding. Analytical Biochemistry. 72:248, 1976.

148) Wild BJ, Green BN, Cooper EK, Lalloz MRA, Erten S, Stephens AD, and Layton DM. Rapid identification of hemoglobin variants by electrospray ionization mass spectrometry. Blood Cells, Molecules and Diseases. 27:691-704, 2001.

149) Szebeni J, Winterbourn CC, and Carrell RW. Oxidative interactions between haemoglobin and membrane lipid: A liposome model. Biochemical Journal. 220:685-92, 1984.

150) Winterbourn CC. Reactions of superoxide with hemoglobin. In: Greenwald RA, ed. CRC Handbook of Methods for Oxygen Radical Research. Boca Raton, FL: CRC Press; 137-41, 1986.

151) Winterbourn CC. Oxidative reactions of hemoglobin. Methods in Enzymology. 186:256-72, 1990.

152) Scott MD, Eaton JW, Kuypers FA, Chiu DT-Y, and Lubin BH. Enhancement of erythrocyte superoxide dismutase activity: Effects on cellular oxidant defense. Blood. 74:2542-9, 1989.

153) Scott MD, Kuypers FA, Butikofer P, Bookchin RM, Ortiz O, and Lubin BH. Effect of osmotic lysis-resealing on red cell structure and function. Journal of Laboratory and Clinical Medicine. 115:470-80, 1990.

154) Scott MD. Entrapment of purified alpha-hemoglobin chains in normal erythrocytes as a model for human beta-thalassemia. In: Magnani M, and DeLoach JR, eds. The Use of Resealed Erythrocytes as Carriers and Bioreactors. New York, NY: Plenum Press; 133-8, 1992.

155) Mouralian, C. Evaluation of novel iron chelators for therapeutic use in secondary iron overload disorders. M. Sc. Thesis, McGill University, Montreal, Quebec (2000).

156) Dodge JT, Mitchell C, and Hanahan DJ. The preparation and characteristics of hemoglobin-free ghosts of human erythrocytes. Archives of Biochemistry and Biophysics. 100:119-30, 1963.

157) Kuross SA, Rank BH, and Hebbel RP. Excess heme in sickle erythrocyte inside-out membranes: Possible role in thiol oxidation. Blood. 71:876-82, 1988.

158) Artiss JD, Vinogradov S, and Zak B. Spectrophotometric study of several sensitive reagents for serum iron. Clinical Biochemistry. 14:311-5, 1981.

159) Popp RA, Popp DM, Johnson FM, Skow LC, and Lewis SC. Hematology of a murine β-thalassemia: a longitudinal study. Annals of the New York Academy of Sciences. 445:432-44, 1985.

160) Yang B, Kirby S, Lewis J, Detloff PJ, Maeda N, and Smithies O. A mouse model for β°-thalassemia. Proceedings of the National Academy of Sciences. 92:11608-12, 1995.

161) Ansell J, and Micklem H. Genetic markers for following cell populations. In: Weir DM, Herzenberg LA, and Blackwell CC, eds. Handbook of Experimental Immunology. Edinburgh, Scotland: Blackwell Publishers, 4th Edition; 4:56.1-56.18, 1986.

162) Ploemacher RE, van Os RP, Van Beurden CA, and Down, JD. Murine hematopoietic stem cells with long-term engraftment and marrow repopulating ability are less radiosensitive to gamma-radiation than are spleen colony forming cells. International Journal of Radiation Biology. 61:489-99, 1992.

163) Alzet Mini-Osmotic Pump Model 2001 Instruction and Specification Sheet, Alzet Technical Information Services. DURECT Corporation, Cupertino, CA.

164) Diep H, Boyer G, McCartney J, and Deschamps Y. ClinTrials BioResearch Ltd. Hematology ADVIA 120 Technical Manual. Senneville, Quebec, Canada.

165) Hoffmann-Fezer G, Maschke H, Zeitler HJ, Gais P, Heger W, Ellwart J, and Thierfelder S. Direct in vivo biotinylation of erythrocytes as an assay for red cell survival studies. Annals of Hematololgy. 63:214-7, 1991.

166) Pountney DJ, Konijn AM, McKie AT, Peters TJ, and Raja KB. Iron proteins of duodenal enterocytes isolated from mice with genetically and experimentally altered iron metabolism. British Journal of Haematology. 105:1066-73, 1999.

167) de Jong K, Emerson RK, Butler J, Bastacky J, Mohandas N, and Kuypers FA. Short survival of phosphatidylserine-exposing red blood cells in murine sickle cell anemia. Blood. 98:1577-84, 2001.

168) Muzykantov VR, Murciano JC, Taylor RP, Atochina EN, and Herraez A. Regulation of the complement-mediated elimination of red blood cells modified with biotin and streptavidin. Analytical Biochemistry. 241:109-19, 1996.

169) *Stainsfile: Perls' Prussian Blue,*
http://members.pgonline.com/~bryand/StainsFile/stain/pigment/perls.htm

170) Richardson DR, and Ponka P. Pyridoxal isonicotinoyl hydrazone and its analogs: potential orally effective iron-chelating agents for the treatment of iron overload disease. Journal of Laboratory and Clinical Medicine. 131:306-15, 1998.

171) Signorini C, Ferrali M, Ciccoli L, Sugherini L, Magnani A, and Comporti M. Iron release, membrane protein oxidation and erythrocyte ageing. FEBS Letters. 362:165-70, 1995.

172) Giardina B, Scatena R, Clementi ME, Ramacci MT, Maccari F, Cerroni L, and Condo SG. Selective binding of met-hemoglobin to erythrocytic membrane: a possible involvement in red blood cell aging. Advances in Experimental Medicine and Biology. 307:75-84, 1991.

173) Persons DA, Allay ER, Sabatino DE, Kelly P, Bodine DM, and Nienhuis AW. Functional requirements for phenotypic correction of murine β-thalassemia: implications for human gene therapy. Blood. 97:3275-82, 2001.

174) Mauricio AQ, Lopes GKB, Gomes CS, Oliveira RG, Alonso A, and Hermes-Lima M. Pyridoxal isonicotinoyl hydrazone inhibits iron-induced ascorbate oxidation and ascorbyl radical formation. Biochimica et Biophysica Acta. 162:15-24, 2003.

175) Fassos FF, Klein J, Fernandes D, Matsui D, Olivieri NF, and Koren G. Urinary iron excretion depends on the mode of administration of the oral iron chelator 1,2-dimethyl-3-hydroxypyrid-4-one in patients with homozygous beta-thalassemia. Clinical Pharmacology and Therapeutics. 55:70-5, 1994.

176) Sharma BK, Tavill AS, Louis LN, Wiesen E, and Varnes AW. Enteral pyridoxal isonicotinoyl hydrazone (PIH) is an effective chelator in experimental iron overload by promotion of biliary iron excretion. Hepatology. 10:573, 1989.

177) Halliwell B, and Gutteridge J. Role of free radicals and catalytic metal ions in human disease. Methods in Enzymology. 186:1-85, 1990.

178) Toyokuni S. Iron-induced carcinogenesis: the role of redox regulation. Free Radical Biology and Medicine. 20:553-66, 1996.

179) Meneghini R. Iron homeostasis, oxidative stress, and DNA damage. Free Radical Biology and Medicine. 23:783-92, 1997.

180) Wonke B, Wright C, and Hoffbrand AV. Combined therapy with deferiprone and desferrioxamine. British Journal of Haematology. 103:361-4, 1998.

181) Link G, Konijn AM, Breuer W, Cabantchik ZI, and Hershko C. Exploring the "iron shuttle" hypothesis in chelation therapy: effects of combined deferoxamine and deferiprone treatment in hypertransfused rats with labeled iron stores and in iron-loaded rat heart cells in culture. Journal of Laboratory and Clinical Medicine. 138:130-8, 2001.

182) Giardina PJ, and Grady RW. Chelation therapy in beta-thalassemia: an optimistic update. Seminars in Hematology. 38:360-6, 2001.

183) Aydinok Y, Nisli G, Kavakli K, Coker C, Kantar M, and Cetingul N. Sequential use of deferiprone and desferrioxamine in primary school children with thalassaemia major in Turkey. Acta Haematologica. 102:17-21, 1999.

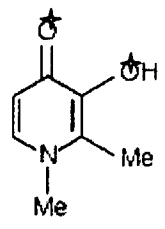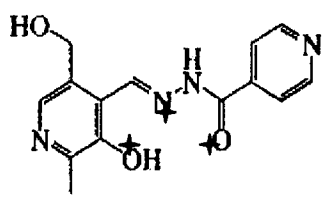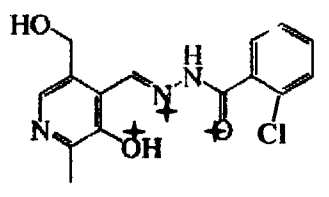## *Table 1.* Characteristics of Iron Chelators Selected for Study

	current standard	only approved substitute	promising oral candidate	novel PIH analog, ↑ efficiency
Chelator	**DFO**	**L1**	**PIH**	*ortho*-**108**
Structure				
	hexadentate	bidentate	tridentate	tridentate

✦ iron binding sites

MW	657	139	287	320
Cell Permeability	negligible	high	high	high
Administration	parenteral	oral	oral	oral
Clinical Experience (yrs)	>30	17	15	na

Table 2. Effects of Iron Chelators on Murine β–Thalassemic RBC Membrane-Associated Iron

	Control (n = 6)	β-Thalassemic				
		Untreated (n = 6)	DFO (n = 5)	L1 (n = 5)	PIH (n = 5)	o-108 (n = 5)
Non-Heme Iron nmoles/mg protein	nd	$23.2^A \pm 8.3$	16.4 ± 4.3	$12.9^B \pm 2.6$	$14.4^B \pm 3.6$	15.8 ± 4.9

Data shown as mean $\pm$ SD for each group. [A] Comparison with control group ($p < 0.001$). [B] Comparison with untreated β-thalassemic group ($p < 0.05$). nd: non-detectable iron content as per the Ferrozine assay (as described in the Methods, section 2.3.2.3.2.).

Table 3. Effects of Iron Chelators on RBC and Reticulocyte Parameters in β–Thalassemic Mice

Mice	RBC Parameters				Reticulocyte Parameters			
	Hct %	Retic %	MCV fL	MCHC g/dL	L % mature	M % interm.	H % immature	MCVr g/dL
Control	49.5 ± 4.7	2.38 ± 0.96	56.8 ± 3.3	24.1 ± 2.8	58.8 ± 13.8	35.3 ± 10.2	5.9 ± 5.2	59.5 ± 4.5
β-Thal.								
Untreated	21.2 ± 1.3	22.0 ± 3.1	46.8 ± 2.45	23.3 ± 0.78	22.6 ± 8.0	23.1 ± 5.1	54.4 ± 12.5	57.8 ± 3.3
+ DFO	22.8 ± 1.8	17.2[A] ± 4.2	50.3[A] ± 1.92	21.2[A] ± 0.87	35.4[A] ± 9.3	33.4[A] ± 5.8	31.2[A] ± 14.7	59.8 ± 2.0
+ L1	22.1 ± 2.3	17.6 ± 4.2	49.2 ± 2.32	21.6[A] ± 1.36	28.6 ± 8.9	28.0 ± 8.5	43.5 ± 17.3	61.6 ± 3.4
+ PIH	21.4 ± 2.9	12.0[A] ± 6.4	49.2 ± 2.33	21.5[A] ± 1.20	36.8[A] ± 11.1	32.7[A] ± 7.4	30.5[A] ± 14.2	57.7 ± 1.3
+ o-108	21.6 ± 2.8	14.7 ± 7.3	49.2 ± 1.47	21.3[A] ± 1.07	28.5 ± 9.7	29.8 ± 8.3	41.7 ± 17.4	60.1 ± 0.9

Data shown as mean ± SD for each group. Control ($n = 6$), Untreated β-Thal. ($n = 6$), β-Thal. + chelator ($n = 5$/group). All differences between control and untreated β-thalassemic mice were statistically significant, $p < 0.001$. [A] Denotes statistically significant difference between untreated and chelator-treated β-thalassemic mice, $p < 0.05$. Hct: hematocrit, Retic: reticulocyte count, MCV: mean cell volume, MCHC: mean cell hemoglobin concentration, MCVr: mean cell volume reticulocyte index. Reticulocyte parameters L, M, and H refer to low, medium, and heavy staining-intensity reticulocytes, respectively.

Table 4. Effects of Iron Chelators on Organ Pathology and Tissue Iron in β-Thalassemic Mice

Mice	Spleen/Body Weight Ratio %	Non-Heme Iron (Liver) nmoles/mg wet weight	Perls' Iron Staining^C % Liver	% Spleen
Control	0.26 ± 0.04	0.78 ± 0.23	nd	1.39 ± 0.38
β-Thal.				
Untreated	1.55 ± 0.32	1.65 ± 0.03	0.23 ± 0.21	5.45 ± 1.03
+ DFO	1.40 ± 0.21	1.54 ± 0.15	0.11 ± 0.11	4.42 ± 0.70
+ L1	1.40 ± 0.14	1.56 ± 0.19	0.07 ± 0.09	2.96^A ± 1.83
+ PIH	1.37 ± 0.27	1.59 ± 0.15	0.04 ± 0.05	3.82^A ± 1.08
+ o-108	1.44 ± 0.22	1.19^A ± 0.47	0.02^A ± 0.02	2.36^B ± 0.61

Data shown as mean ± SD for each group. All differences between control and untreated β-thalassemic mice were statistically significant, $p < 0.001$. ^{A} Denotes statistically significant difference between untreated and chelator-treated β-thalassemic mice, $p < 0.05$; ^{B} denotes $p < 0.001$. ^{C} Areas staining positive for iron using Perls' Prussian blue dye expressed as a percentage of total area examined. nd: non-detectable iron as per Perls' staining technique (described in the Methods, section 2.3.7.3.).
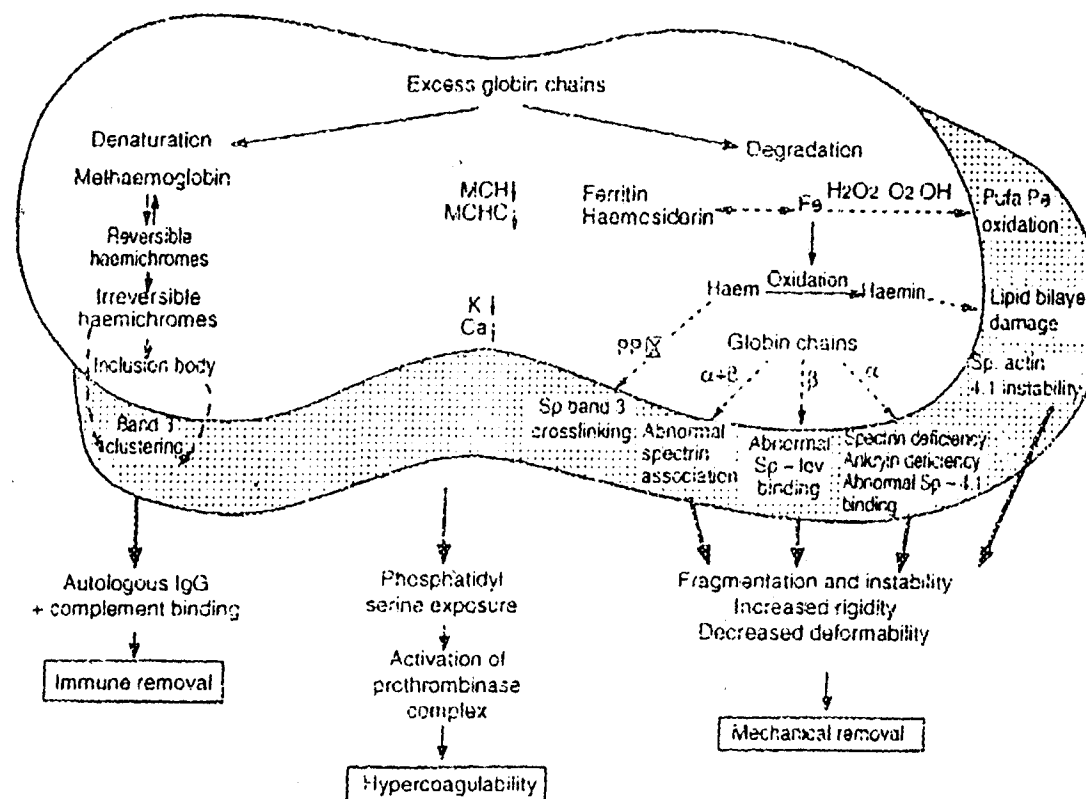
Figure 1. Pathways Involved in Membrane Damage and Shortened RBC Lifespan in β-Thalassemia.
Sp: spectrin, Pufa: polyunsaturated fatty acid, Pe: phosphatidyl ethanolamine, Iov: inside-out vesicles, MCH: mean cell hemoglobin, MCHC: mean cell hemoglobin concentration. From Weatherall (1998, *Bailliere's Clinical Haematology* 11:127-46).
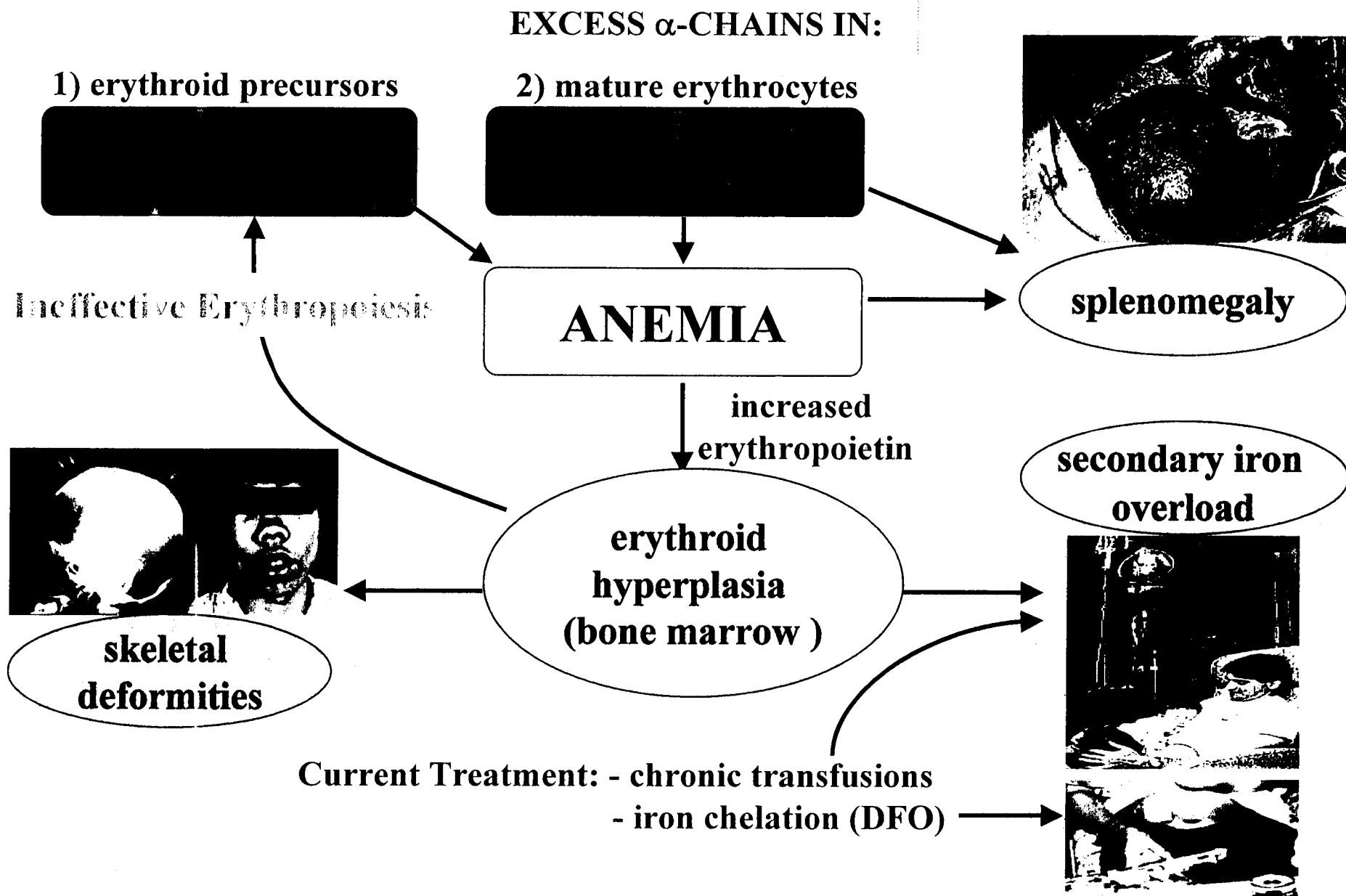
EXCESS α-CHAINS IN:

1) erythroid precursors

2) mature erythrocytes

Ineffective Erythropoiesis

ANEMIA

splenomegaly

increased
erythropoietin

skeletal
deformities

erythroid
hyperplasia
(bone marrow)

secondary iron
overload

Current Treatment: - chronic transfusions
- iron chelation (DFO)

Figure 2. Clinical Consequences of α-Chain Accumulation in β-Thalassemia

Normal Human Erythrocyte

α-chains

HYPOSMOTIC LYSIS
4°C, 45 minutes

1) Normal erythrocytes mix with exogenous purified α-chains (with heme moieties attached)

2) Cells regurgitate contents into medium

3) Cell contents mix with α-chains

Human Model β-Thalassemic Erythrocyte

5) Cells reseal

4) Cells swell, incorporate regurgitated Hb and added α-chains

ISOTONIC RESEALING
37°C, 45 minutes

Figure 3. Preparation of Human Model β-Thalassemic Erythrocytes

β-Thalassemic Donors
poor breeding efficiency
$n = 2$

Myeloablated Recipients
control mice, readily available
$n = 26$

10-12 wk engraftment

Recipients Expressing
β-Thalassemic Phenotype
$n = 26$

Figure 4. **Generation of a β-Thalassemic Mouse Population.** Bone marrow transplants were performed, transferring the bone marrow from a small number of β-thalassemic mice to a relatively large number of control recipients. C57BL/6J[GPI-1a] mice were lethally irradiated and injected intravenously with 1.8 million bone marrow cells in 350 μL volume (as described in the Methods, section 2.3.3.1.). The chimeric mice were monitored for hematopoietic engraftment at 4, 7, and 10 wk post-transplant before commencing the iron chelator regimen on wk 12. All recipients were found to have adopted a β-thalassemic phenotype identical to donor mice.
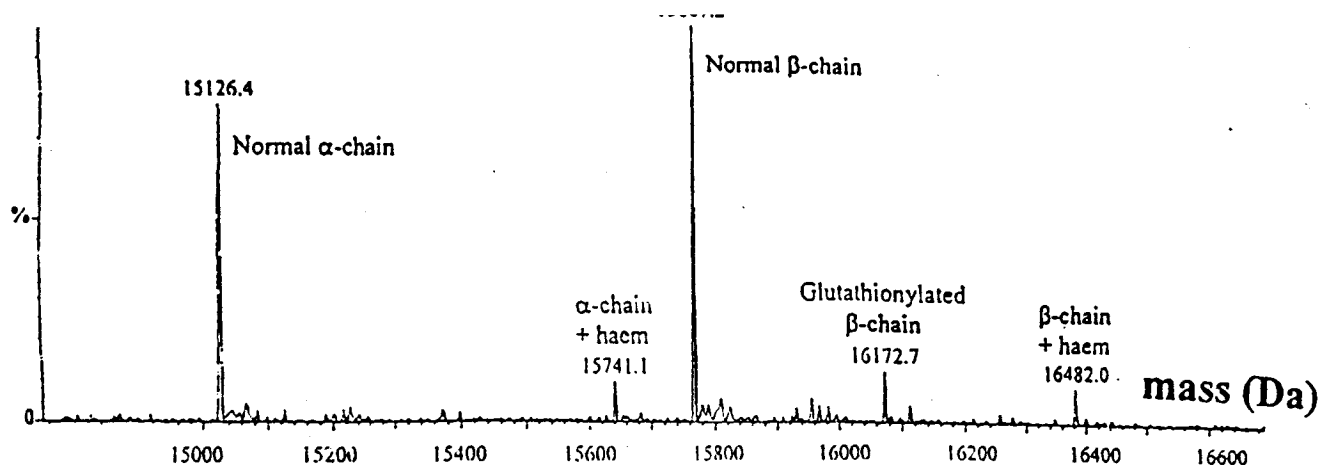
Figure 5 A. Standard deconvoluted ESI mass spectra of blood from a healthy adult subject diluted 500-fold in ddH$_2$O. Normal α-hemoglobin chains display a characteristic peak at 15126.4 Da, while the α-chain + heme group displays a peak at 15741.1 Da.

From: Wild BJ, Green BN, Cooper EK. *et al.* Rapid identification of haemoglobin variants by electrospray ionization mass spectrometry. Blood Cells, Molecules, and Diseases. 27:691-704, 2001.
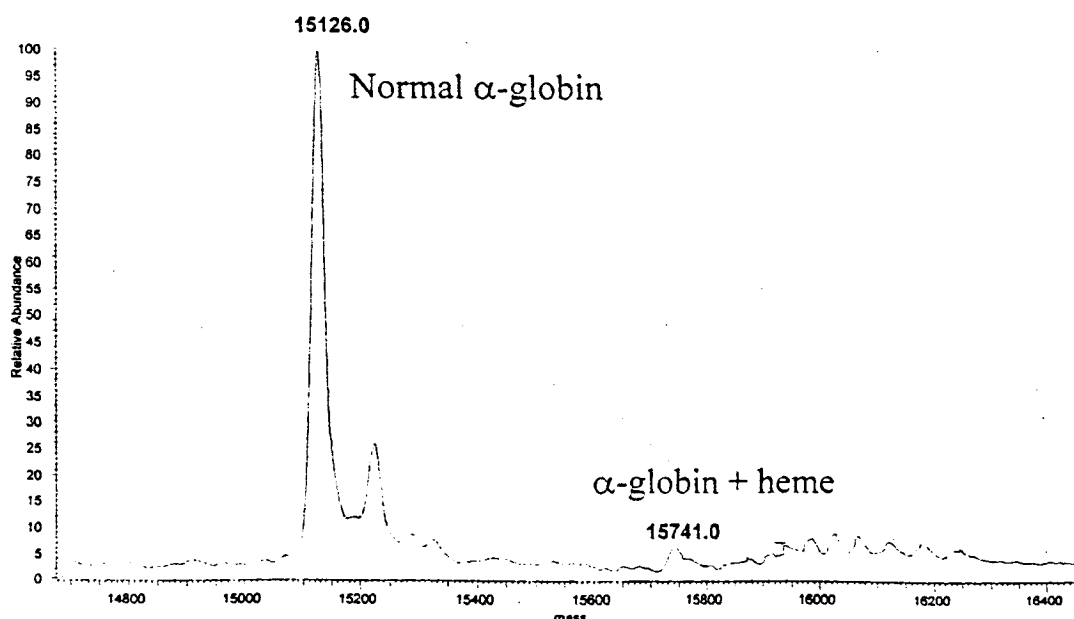
Figure 5 B. Deconvoluted ESI mass spectra of 0.8 mg/mL purified α-hemoglobin. Subunits were isolated from normal adult whole blood and diluted 1:150 with ddH$_2$O to obtain characteristic peaks and associated molecular mass values.
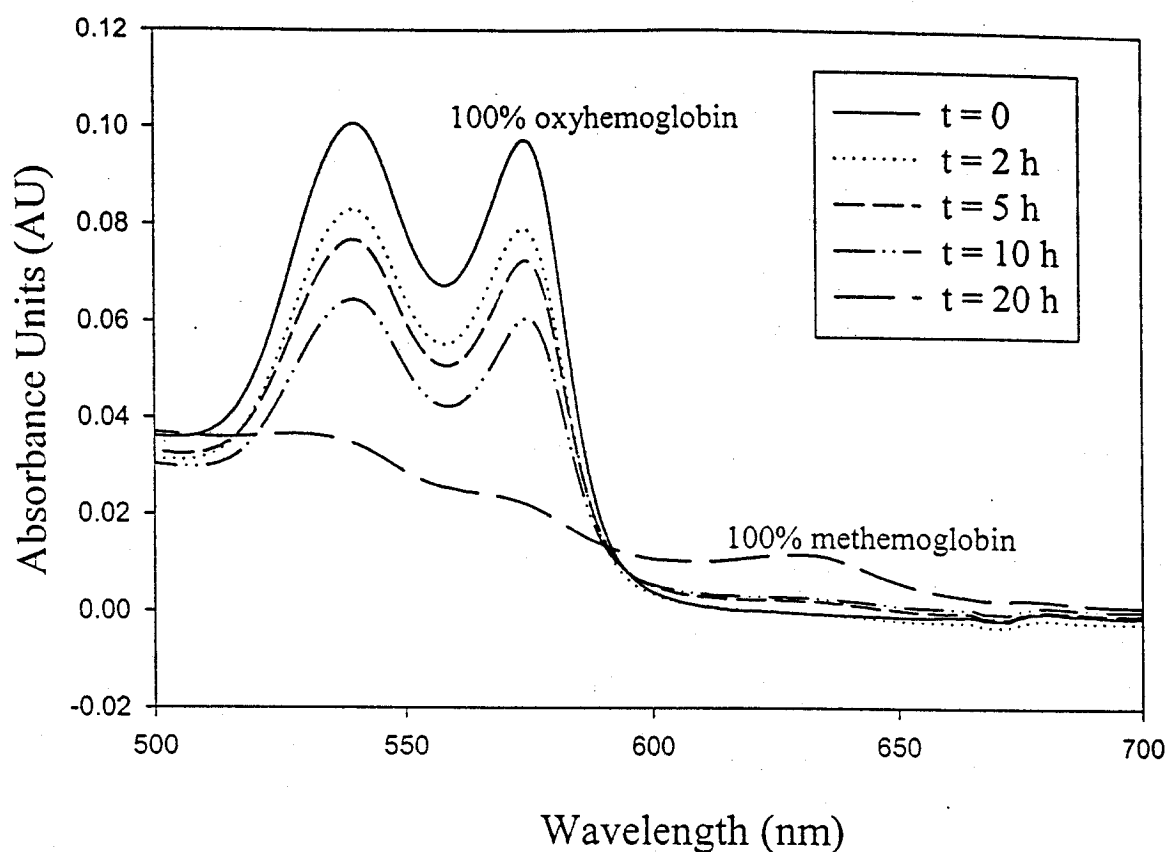
Figure 6. **Sequential scans of hemoglobin undergoing oxidation.** Whole blood was incubated over 20 h at 37°C; aliquots were removed at intervals and packed erythrocytes were diluted 1:500 in double distilled water and examined spectrophotometrically. The initial sample (solid line) contained 100% oxyhemoglobin; subsequent lines represent hemoglobin in its progressive stages of oxidative denaturation with the final scan depicting lysate containing solely methemoglobin.
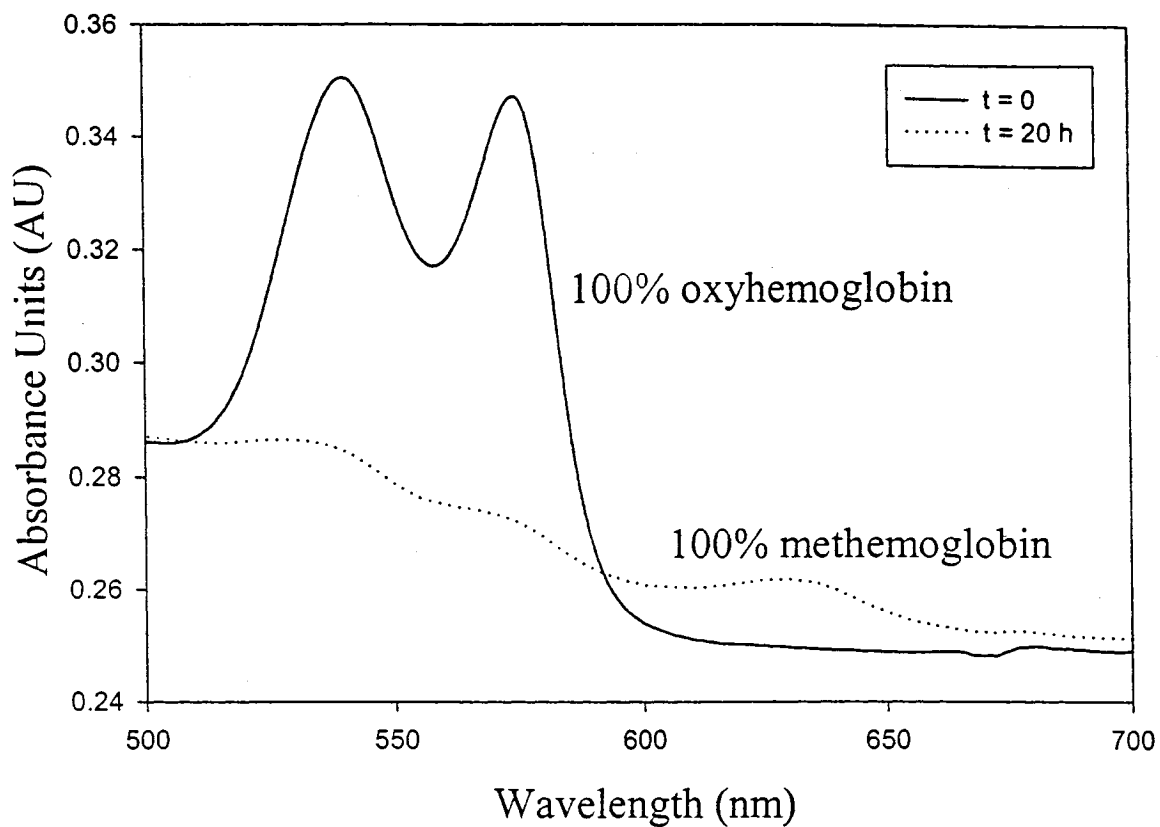
Figure 7. **Initial Spectrum of Purified α-Hemoglobin Chains and Spectrum Taken Following 20 h Incubation.** Subunits were diluted 1:100 in double distilled water and analyzed spectrophotometrically for functional denaturation response over time. Initial composition of lysate was 100% oxyhemoglobin (solid line); following overnight incubation at 25°C, progressive oxidative denaturation of α-chains took place, yielding 100% methemoglobin (dotted line) in final lysate.
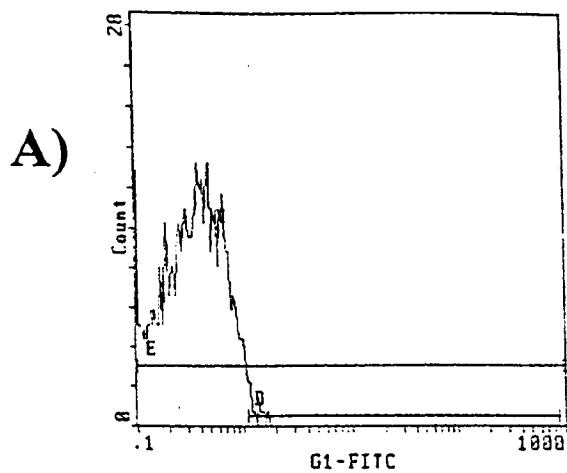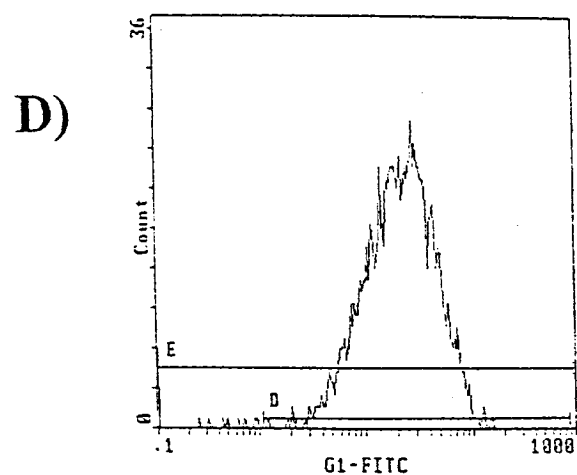
Relative Intensity
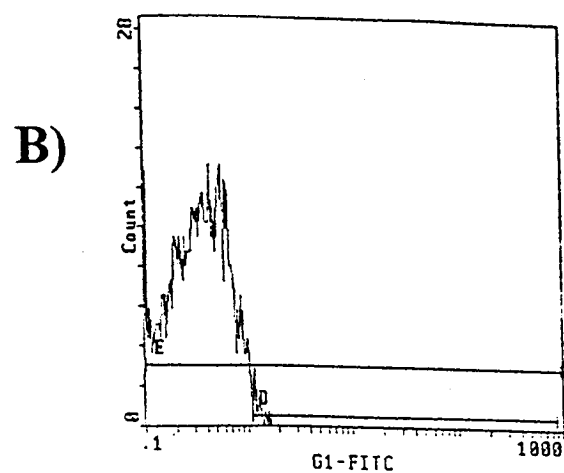
Relative Intensity
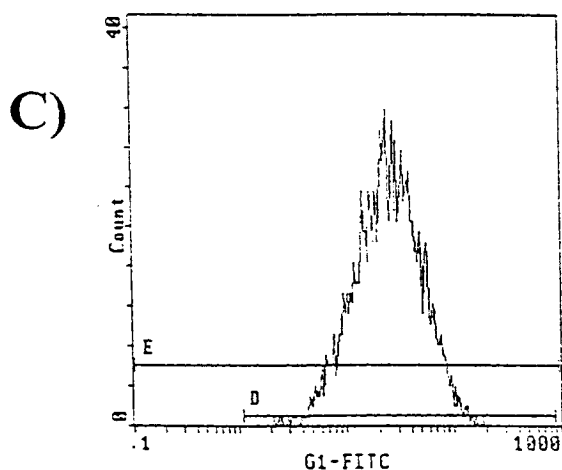
Relative Intensity

Relative Intensity

Figure 8. **Encapsulation of purified α-hemoglobin chains into human erythrocytes.** FACScan data depicting the fluorescence of erythrocytes loaded with FITC-Dextran alone or admixed with purified α-hemoglobin chains. Cells exhibiting relative fluorescence intensities greater than 1 (within region "D"), were considered to have incorporated FITC-Dex while values below 1 reflected typical low-level inherent cellular fluorescence. Background cellular fluorescence was measured in control (A) and control-resealed cells (B), yielding 1.18% and 0.9% respectively. The fluorescence intensities of cells lysed and resealed in the presence of either 5 mg FITC-Dex/mL pRBC alone or FITC-Dex in suspension with α-subunits (13.5 mg α-chains/mL pRBC) are seen in panels C and D, respectively. In both cases, when fluorescent RBC were expressed as a percentage of the total counted (5000 cells), more than 98.5% of red cells were found to have incorporated the exogenous material. Samples were prepared in triplicate and representative histograms for each condition are shown.
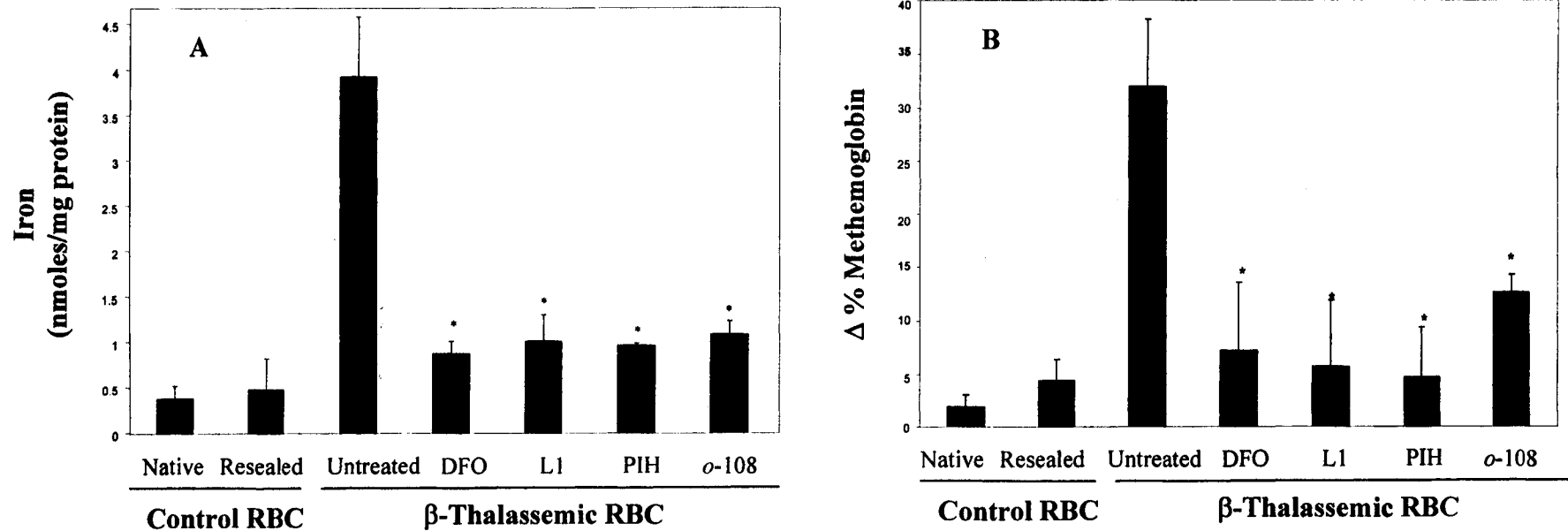
Figure 9. Effects of Iron Chelators On Membrane-Associated Non-Heme Iron (A), and Iron-Mediated Hemoglobin Oxidation (B), in Human Control and Model β-Thalassemic RBC.

Native cells and cells having undergone osmotic lysis and resealing in absence of α-chains (Resealed), as well as model β-thalassemic RBC untreated or treated with 50 μM chelator, were incubated over 20 h at 37°C. (A) Membrane iron measured after 20 h as described in the Methods (2.3.2.3.) was significantly reduced in chelator-treated RBC compared to untreated (* $p < 0.002$). (B) Aliquots were removed at 0 and 20 h and the increase in methemoglobin, reported as a percentage of total hemoglobin, was determined as described in the Methods (2.3.2.4.). Corresponding to their decrease in membrane iron, chelator-treated RBC generated significantly less methemoglobin over the 20 h period compared to untreated (* $p < 0.01$), suggesting protection against oxidative damage. Shown are the mean ± SD of three independent experiments.

Weeks post-transplant:

4 wk

Gpi Gpi 1 2 3 4 5 6 7 8 9 10
 a   b

7 wk

Gpi Gpi 1 2 3 4 5 6 7 8 9 10
 a   b

10 wk

Gpi Gpi 1 2 3 4 5 6 7 8 9 10
 a   b

Control Recipient ᵃ ᵇ β-Thalassemic
Isoform   Donor Isoform

Figure 10. Glucose Phosphate Isomerase (Gpi) Phenotyping of Recipient Mice 4, 7, and 10 Weeks Following Murine β-Thalassemic Bone Marrow Transplant.

Peripheral blood of transplanted mice was analyzed at the protein level to determine the proportion of endogenous RBC remaining, and the proportion contributed by the donor (Gpi-1b) at different stages following BMT. Gpi-1 isoforms "a" and "b" were derived from C57BL/6J[GPI-1a] (recipient) and C57BL/6J[GPI-1b] (donor) mice, respectively. Lanes 1-10 reveal the Gpi-1 isotypes of ten representative transplanted mice. At 4 weeks, the majority of recipient RBC were of endogenous origin, as Gpi-1a was the principal form of the enzyme detected. After 7 weeks, however, over 50% of recipient RBC expressed Gpi-1b. By week 10, all recipients produced strictly isoform "b", indicating a switch to β-thalassemic RBC production exclusively, and therefore, complete hematopoietic engraftment.
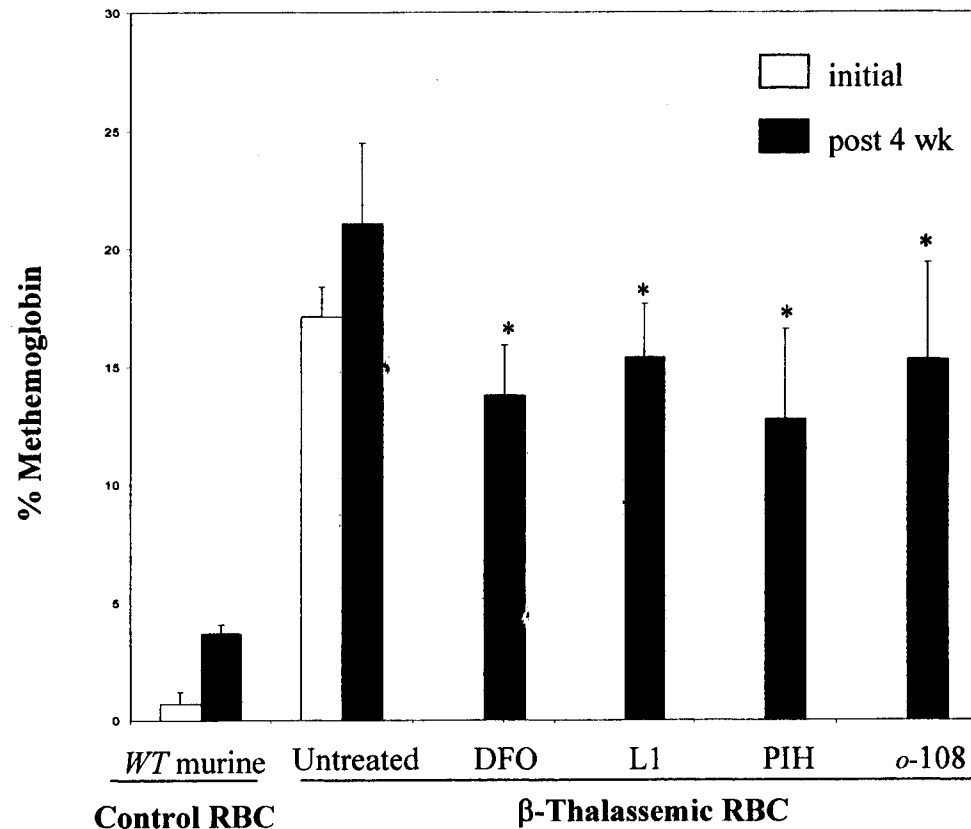
Figure 11. **Effects of Iron Chelators on Iron-Mediated Hemoglobin Oxidation in Murine β-Thalassemic RBC.**

Methemoglobin production, corresponding to cellular oxidative stress, was measured as described in the Methods (2.3.6.2.) and expressed as a percentage of total hemoglobin. Levels were evaluated before commencing treatment and following 4 wk at 50 mg chelator/kg/day.

Initial methemoglobin levels in chelator-treated β-thalassemic mice were indistinguishable from those in untreated mice (initial values presented for untreated only). RBC from chelator-treated β-thalassemic mice generated significantly less methemoglobin subsequent to the iron removal regime compared to those from untreated mice (* $p < 0.03$). Shown are the mean $\pm$ SD for each group.
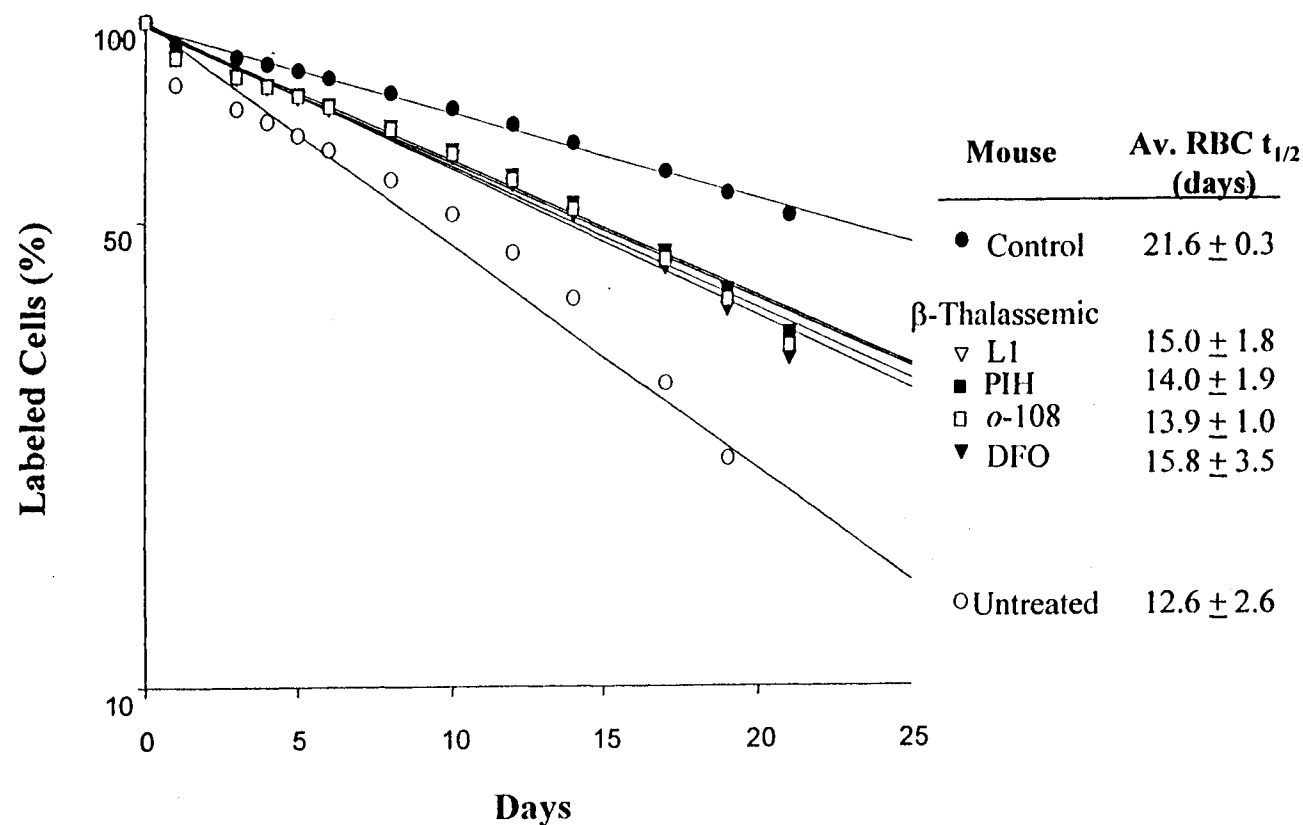
Figure 12. Representative RBC Survival Curves from Untreated and Iron Chelator-Treated β-Thalassemic Mice. Lifespan studies began one week after commencing the iron chelator regime of 50 mg chelator/kg/day. The decay of biotinylated RBC was monitored over 21 days and plotted as a percentage of labeled cells (log scale) over the number of days. Data is from individual animals representative of their treatment groups.
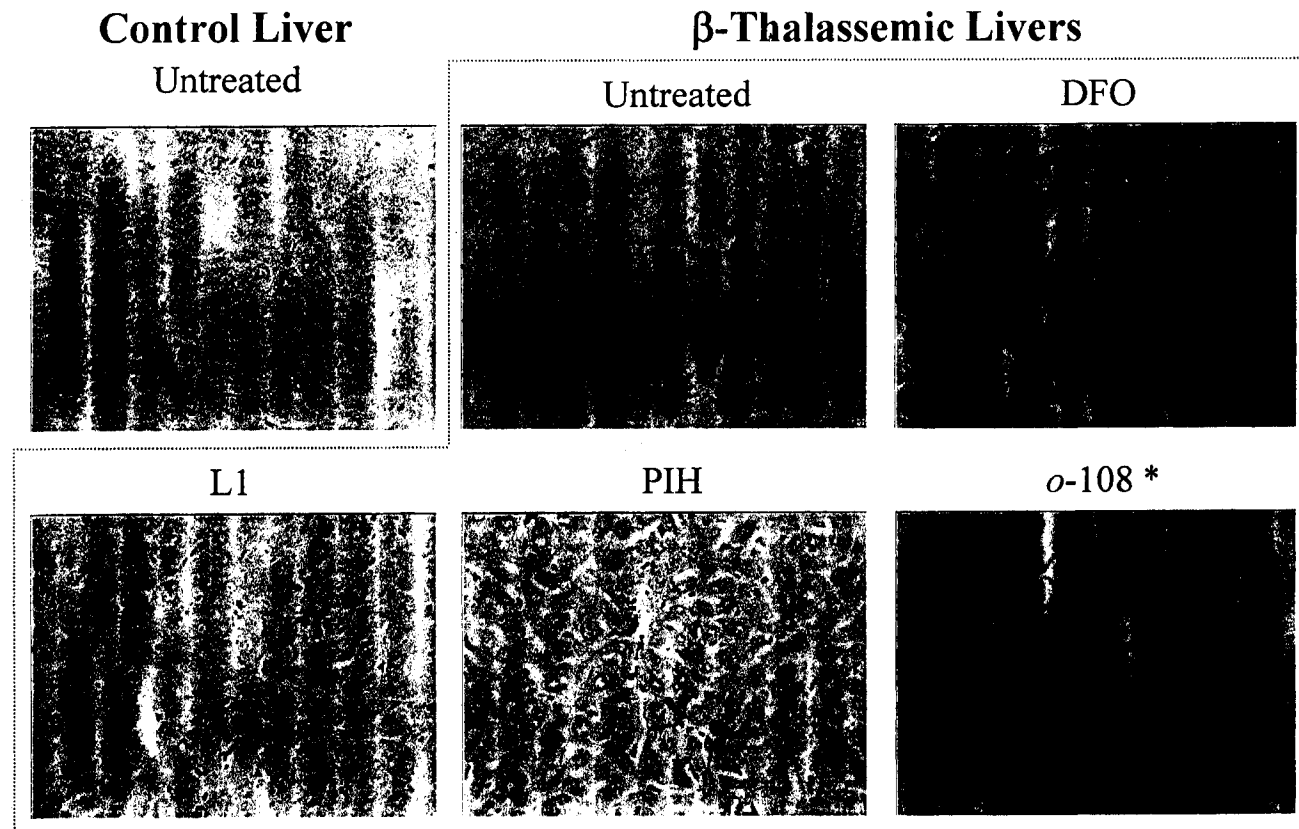
Figure 13. Iron Chelators Reduce Liver Iron Accumulation in β-Thalassemic Mice.

Following 4 wk of iron chelator treatment, liver sections were stained for iron using Perls' Prussian blue dye and a hematoxylin and eosin counterstain as described in the Methods. The percentage of stainable iron was averaged for each treatment group and representative tissue sections from individual animals are depicted (20 X). * $p < 0.05$ compared to untreated β-thalassemic group.
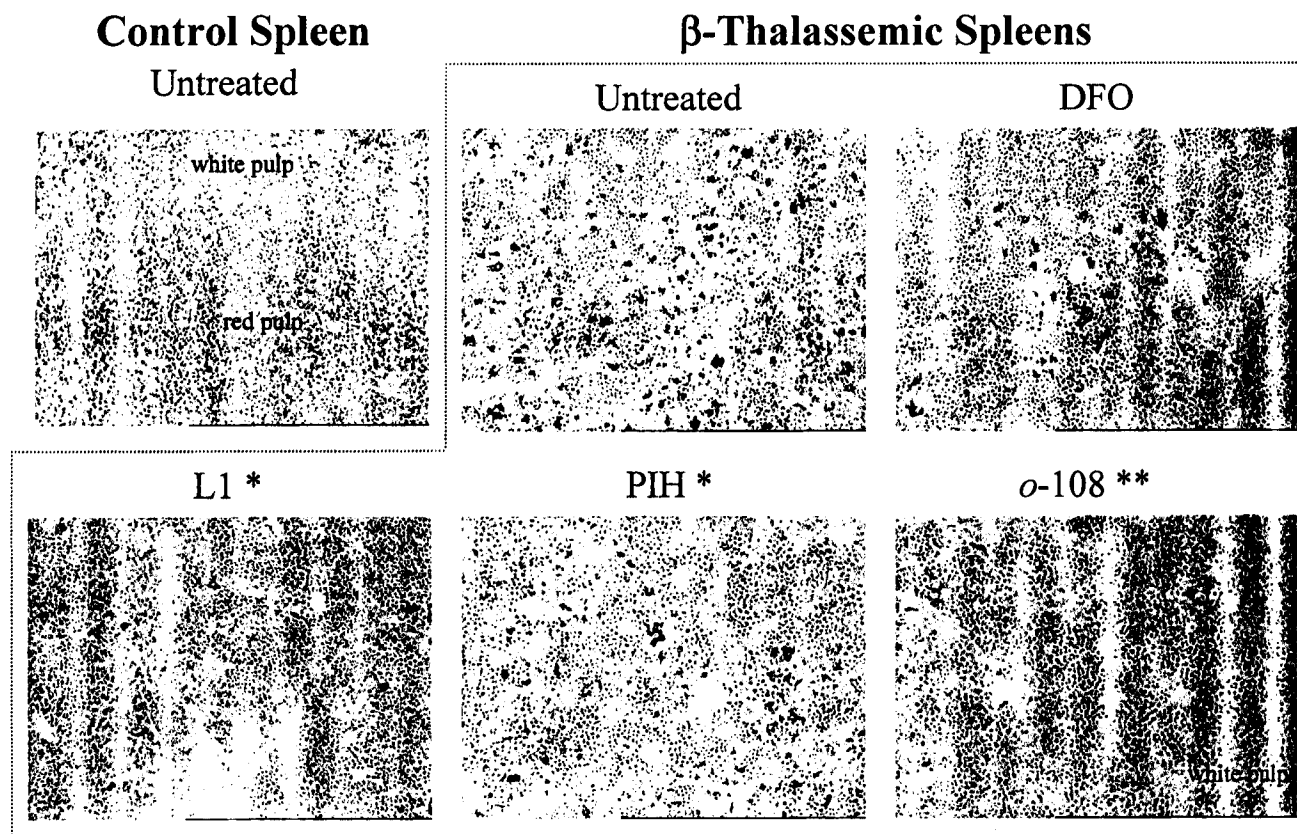
Control Spleen **β-Thalassemic Spleens**

Untreated

Figure 14. Iron Chelators Reduce Splenic Iron Accumulation in β-Thalassemic Mice.

Spleen sections were stained for iron using Perls' Prussian blue dye and a hematoxylin and eosin counterstain, as in *Fig. 13* (described in the Methods). The percentage of stainable iron was averaged for each treatment group and representative tissue sections are depicted (20 X).

* p < 0.05, ** p < 0.001 compared to untreated β-thalassemic group.